University of Alberta

Differential $^{15}N_2$-/$^{14}N_2$-isotope Dansylhydrazine Labeling and LC-MS for Quantification of the Human Carbonyl Metabolome

by

Margot Renée Dawe

A thesis submitted to the Faculty of Graduate Studies and Research
in partial fulfillment of the requirements for the degree of

Master of Science

Department of Chemistry

Fall 2011
Edmonton, Alberta

Abstract

The objective of this work was the design and use of paired labeling reagents that are chemically identical but isotopically different to provide a simple and robust means of quantitative mass spectrometry (MS) based metabolome profiling. Herein is presented the differential $^{15}N_2$-/$^{14}N_2$-isotope dansylhydrazine (DH) derivatization strategy for the quantitative profiling of carbonyl compounds in the human metabolome with sensitive analysis by liquid chromatography electrospray ionization Fourier Transform ion cyclotron resonance mass spectrometry (LC-ESI FT-ICR-MS). This is a universal technique for the identification and quantification of ketones, aldehydes, keto-acids, and sugars in biofluids by the formation of a relatively hydrophobic dansylhydrazone derivative that has shown significant improvement of reversed phase LC properties and enhancement of ESI-MS signals in LC-MS. There is no observed isotope effect using reversed phase LC and the isoforms of the light- and heavy-chain labeled metabolites are co-eluted and simultaneously detected by MS, allowing for precise quantification and confident metabolite identification. Applications of this technique are presented for the analysis of the human urinary and plasma metabolomes.

Acknowledgement

I would like to thank my supervisor, Dr. Liang Li, for his guidance, support, and encouragement. He is a wonderful teacher, and it has been a pleasure and an honour learning more about mass spectrometry under his direction. I have found his enthusiasm and passion for analytical chemistry to be very inspirational.

I would also like to thank my supervisory committee for reviewing my thesis and for their helpful suggestions.

Dr. Randy Whittle and the entire staff of the University of Alberta's Mass Spectrometry Laboratory are gratefully acknowledged for their instruction and advice for my FT-ICR-MS experiments.

I would like to thank the members of the Li research group that I have worked with during my graduate program: Lu Chen, Melisa Clements, Dr. Andrea De Souza, Dr. Yan Gong, Dr. Kevin Guo, Avalyn Lewis, Dr. Andy Lo, Jun Peng, Difei Sun, Yanan Tang, Chiao-Li Tseng, Dr. Nan Wang, Dr. Peng Wang, Dr. Fang Wu, Yiman Wu, Dan Xu, Mingguo Xu, Xiaoxia Ye, Dr. Bryce Young, Jiamin Zheng, Ruokun Zhou, and Azeret Zuniga. Working with all of these individuals made for a very enjoyable and enriching graduate experience. I would especially like to thank Dr. Andrea De Souza for her mentorship in the beginning of my research and for her patience, insight and support. I am very grateful to have shared in this learning experience with Andrea.

I would like to thank Dr. David Wishart and all the members of the Human Metabolome Project for providing many of the standards used in my studies and for valuable comments, support, and opportunities they have provided to me throughout the completion of my program.

The University Of Alberta Department Of Chemistry, School Of Graduate Studies, Genome Canada, Genome Alberta, CRC program, and the Alberta Heritage Foundation for Medical Research Studentship are acknowledged for financial support.

Finally, thank you to my parents, Ken and Marian, and to my brother, Tony, for their love and support, and to my sister, Louise, for being my best

friend, always listening to me, and for many helpful discussions. Thank you to my good friends and fellow chemists Dr. Peter Blanchard and Nicole Oro for all of their support and encouragement. Finally, thank you to my partner, Jonathan Murphy, for his extraordinary patience, understanding and love.

Table of Contents

List of Tables

List of Figures

List of Abbreviations

AC	Alternating current
ACN	Acetonitrile
APCI	Atmospheric pressure chemical ionization
B	Homogenous magnetic field
Biofluid	Biological fluid
Biosystem	Biological system
BIRD	Blackbody infrared dissociation
BPC	Base peak ion chromatogram
CAD	Collisionally activated dissociation
capLC	Capillary liquid chromatography
CI	Chemical ionization
CEM	Channel electron multiplier
CRM	Charge residue model
CSF	Cerebrospinal fluid
Da	Dalton
dc	Direct current
DCM	Dichloromethane
DH	Dansylhydrazine
DmPA	p-dimethylaminophenacyl
DNPH	2,4-dinitrophenylhydrazine
Dns	Dansyl, $C_{12}H_{12}NO_2S$
DnsCl	Dansyl chloride
d_p	Particle size
EI	Electron impact ionization
EIC	Extracted ion chromatogram
ESI	Electrospray ionization
EtAc	Ethyl acetate
EtOH	Ethanol
FA	Formic acid

FAB	Fast atom bombardment
FT-ICR-MS	Fourier Transform ion cyclotron resonance mass spectrometry
GC	Gas chromatography
GC-MS	Gas chromatography mass spectrometry
HILIC	Hydrophilic interaction chromatography
HLB	Hydrophilic-liphophilic balance
HMDB	Human Metabolome Database
HML	Human Metabolome Library
HPLC	High performance liquid chromatography
ICAT	Isotope-coded affinity tags
i.d.	Internal diameter
IEM	Ion evaporation model
iPA	Isopropanol
IRMPD	Multiphoton infrared photodissociation
IS	Internal standard
iTRAQ	Isobaric tag for relative and absolute quantitation
LC	Liquid chromatography
LC-MS	Liquid chromatography mass spectrometry
m/z	Mass-to-charge ratio
MALDI	Matrix-assisted laser desorption/ionization
MeOH	Methanol
min	Minute
MS	Mass spectrometry
ms	Millisecond
MS^n	Tandem mass spectrometry
MS/MS	Tandem mass spectrometry
nESI	Nano electrospray (nanospray)
nLC	Nano liquid chromatography
NMR	Nuclear magnetic resonance
n.o.	Not observed
o.d.	Outer diameter

ppm	Parts per million
PVDF	Polyvinylidene fluoride
R	Resolving power
rf	Radio-frequency
R_f	Retention factor
RP	Reversed phase
RPLC	Reversed phase liquid chromatography
s	Second
SDS	Sodium dodecyl sulfate
SID	Surface-induced dissociation
SIDT	Single ion in droplet theory
SIFT-MS	Selected ion flow tube mass spectrometry
SIL	Stable isotope-labeled
SPE	Solid phase extraction
SPME	Solid phase microextraction
TCA	Trichloroacetic acid
TFA	Trifluoroacetic acid
TFMSA	Trifluoromethanesulfonic acid
THF	Tetrahydrofuran
TIC	Total ion chromatogram
TOF	Time-of-flight
t	Time
t_R	Retention time
UPLC	Ultra performance liquid chromatography
UVPD	Ultraviolet photodissociation
UV-Vis	Ultraviolet-visible spectroscopy

Chapter 1: Introduction

1. General Introduction

Metabolomics is the comprehensive analysis of endogenous small molecules (metabolites) of biological systems (biosystems). Liquid chromatography mass spectrometry (LC-MS) has become an important analytical tool for the characterization of the metabolome. Mass spectrometry, when combined with effective sample preparation and chromatographic separation, offers the ability for quantitative analyses with high selectivity and sensitivity and the potential to identify previously unknown metabolites. Recent advances in MS instrumentation have allowed for tremendous progress in the growing field of metabolomics. An ideal metabolomics study would provide a complete qualitative and quantitative profile of an organism's metabolome. However, due to the vast complexity of metabolites which compose a biosystem, the development of methods tailored to the analysis of a class of metabolites sharing similar structural moieties is desirable. Using this targeted approach, a large number of metabolites can potentially be identified, thereby increasing the overall metabolome coverage.

The analyses of human carbonyl metabolites have been of recent interest for disease biomarker discovery and biological functional studies. Global analysis of carbonyl compounds by LC-MS is challenging as a result of great diversity of chemical structures and properties, and matrix and ion suppression effects. The work presented in this thesis was directed towards the development of a quantitative method for profiling the endogenous human carbonyl metabolome based on differential $^{15}N_2$-/$^{14}N_2$-isotope dansylhydrazine labeling with sensitive analysis by liquid chromatography electrospray ionization Fourier transform ion cyclotron resonance mass spectrometry (LC-ESI FT-ICR-MS).

1.1. Mass Spectrometry: Principles and Instrumentation

Mass spectrometry is the art of measuring the mass of an ion. Using a mass spectrometer, the mass of a molecule is determined from the measurement

of the mass-to-charge ratio (m/z) of its ion. J.J. Thomson is credited for inventing the first primitive mass spectrometer, following his studies on electrical discharges which led to his discovery of the electron in 1897.[1] The parabola spectrograph he developed in the early 1900s was used for the determination of the m/z of ions. This experimental instrument used discharge tubes to generate ions, which moved through parabolic trajectories upon passing into electric and magnetic fields, and which were detected as rays at a fluorescent screen or photographic plate. Thomson's experiments in 1912 with neon, using his spectrograph, lead to the observation of a double parabola on the photographic plate, which he concluded to result from two different atomic forms of neon. This observation was the first evidence of the existence of elemental isotopes. The separation of the isotopes of neon by mass using the parabola spectrograph was the first example of what we now consider to be mass spectrometry.

F. W. Aston worked with Thomson on these experiments at the University of Cambridge and went on to further develop the mass spectrometer and improve the resolution achieved by having the ions separate by mass and focus by velocity.[2] A. J. Dempster at the University of Chicago further developed the instrument model into a form that is still in use commercially.[3] This model uses magnetic deflection with directional focusing of the ions into an electrical collector. Since the 1930s a wide range of mass spectrometers has been developed varying in the form of ionization, ion transport, ion detection and with greatly enhanced resolving power.

In general, the mass spectrometer consists of four main components; a sample inlet, an ionization source, a mass analyzer and an ion detector. Molecules are introduced into the system via the sample inlet and then converted into ions by the ionization source. The ions are then electrostatically guided into a mass analyzer and separated according to their m/z. At the detector, the current signal/energy of the incident ions is recorded and transmitted to a computer which generates a mass spectrum from the data. A variety of inlets, sources, analyzers and detectors are available. The choice of instrumentation is dependent on the sample to be analyzed, the analyte of interest, and the desired outcome.

1.1.1. Electrospray Ionization

The role of the ionization source is to transform sample molecules from solution into gas phase ions for introduction into the low vacuum region of the mass analyzer. There are several types of ionization sources available including electron impact ionization (EI), chemical ionization (CI), atmospheric pressure chemical ionization (APCI), fast atom bombardment (FAB), matrix-assisted laser desorption/ionization (MALDI), and electrospray ionization (ESI). It is A. J. Dempster that is also credited with developing the first EI source.[3] For the EI process, the analyte of interest must be volatile as the sample is vaporized into the source and impacted by a beam of electrons of sufficient energy to result in ionization of the molecules. This was the original source created for MS instruments and is still the most widely used. However, EI limits the analysis to volatile small molecules. The analysis of larger biological macromolecules required the development of a different type of ionization source which led to a new generation of ionization techniques. Such ionization techniques as MALDI and ESI, coupled with MS, developed in the 1980s have revolutionized the field of biomolecular analysis. The Nobel Prize in Chemistry 2002 was awarded one half jointly to John B. Fenn and Koichi Tanaka "for their development of soft desorption ionization methods for mass spectrometric analyses of biological macromolecules" for ESI and MALDI, respectively.[4, 5]

In this research, focused on the analyses of human metabolites, ESI was chosen as the ionization technique for its high sensitivity of detecting small molecules and readiness to interface with liquid chromatography (LC) (see Figure 1.1 for a schematic of ESI-MS). ESI is a technique which is well suited towards such samples of extreme molecular complexity and has become an important tool for quantitative metabolome profiling. The phenomenon of electrospray was first reported by J. Zeleny in 1914.[6] In 1968, Dole, et al. applied ESI to the production of gas-phase ions,[7] and in 1984, the coupling of ESI to MS was reported independently by Yamashita and Fenn[8], and Aleksandrov, et al[9].

ESI is capable of ionizing large, non-volatile and labile molecules. The sample is introduced to the source at low concentrations in a solution which flows

through a capillary tube to which a high voltage (2 - 4 kV) is applied at the tip. In positive ion mode, a positive potential charge is applied to the tip. Briefly, when a high voltage is applied to the tube of solution, this solution becomes charged. Charged liquid exiting the ESI capillary tip forms what is known as a Taylor cone. The Taylor cone gives way to a fine filament and then breaks into a fine spray of positively charged droplets. Solvent evaporation of the charged droplets produces progeny charged droplets and so-on until gas-phase ions are finally produced and guided into the mass analyzer.

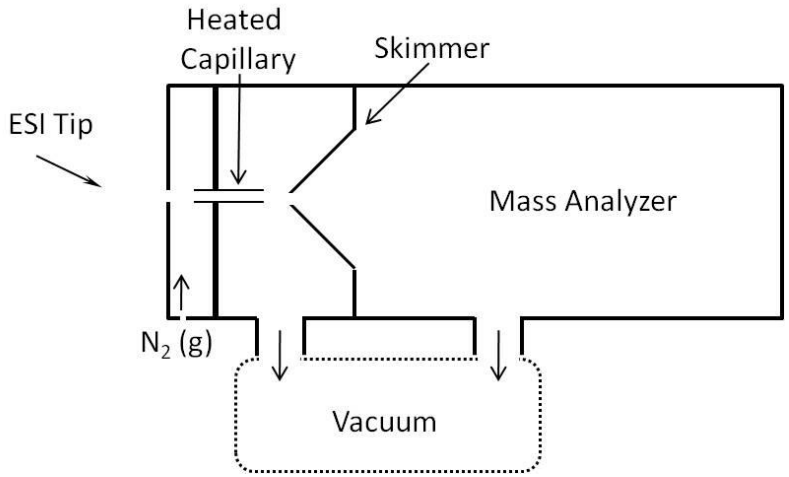

Figure 1.1. General schematic of the interfacing of ESI to a mass analyzer (adapted from Kebarle, et al., 2009[10]).

This process has been described by Kebarle and Tang as taking place in four major steps.[10, 11] The first step of the process is the production of charged droplets at the ESI capillary tip, in the atmospheric region of the instrument. This takes place by the induction of an electric field at the end of the capillary, (E_c) given by:

$$E_c = \frac{2V_c}{r_c \ln(\frac{4d}{r_c})} \approx 1.6 \times 10^6 Vm^{-1} \qquad (Eq.\ 1.1.)$$

where: V_c = applied capillary potential (2-3 kV)

r_c = capillary outer radius (typically 1 mm o.d.)

d = distance from the counter electrode (1-3 cm)

When E_c is on, the solution flowing through the ESI capillary will be penetrated resulting in a polarization of the solution and an enrichment of positive ions near the meniscus of the liquid. A destabilization of the meniscus results from the downfield forces due to the polarization. This leads to the formation of the cone known as the Taylor cone. The surface tension of the liquid, which is typically a polar solvent, resists the increased surface that is generated by the formation of the cone. When E_c is sufficiently high, the cone gives way to a fine jet or liquid filament which emerges from the tip of the cone. In positive ion mode, there is an excess of positive ions which charge the surface of the jet. Downstream, jet destabilization resulting from charge repulsion leads to the formation of separate charged droplets which appears as a spray (see Figure 1.2).

In the second step of the process, shrinkage of the charged droplets occurs due to solvent evaporation of the charged droplets accomplished by flowing a dry gas, typically nitrogen, in the first outer-chamber. The charged droplets continue to travel downfield towards the opposing electrode. Repeated charge-induced droplet disintegrations mark the third step of the process followed by the generation of gas phase ions from the small highly charged droplets in the final step. [10, 12]

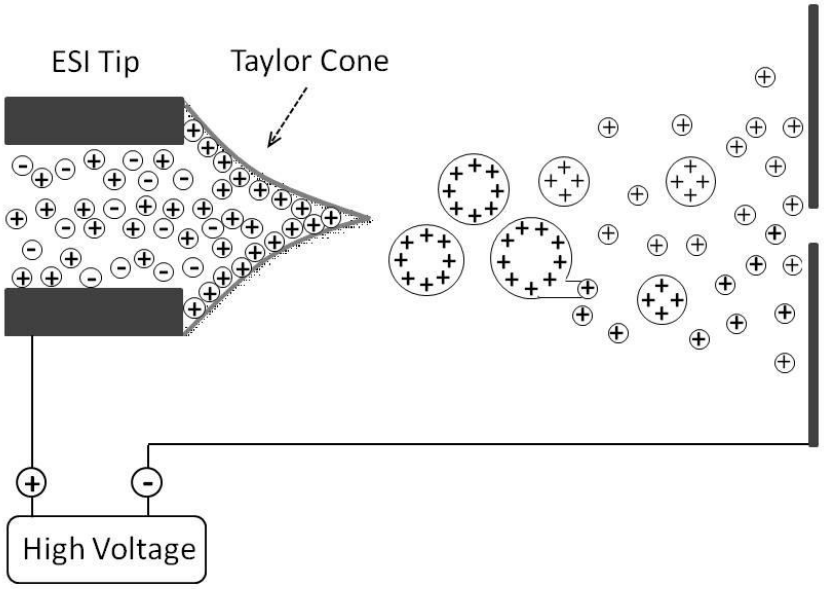

Figure 1.2. Illustration of the four major processes which lead to the production of gas-phase ions by an ESI source in positive ion mode (adapted from Kebarle, et al., 2009[10]).

Currently there are two main theories for the mechanism by which gas-phase ions are formed from charged droplets. The single ion in droplet theory (SIDT), also known as the charge residue model (CRM), was first introduced by Dole and co-workers. They proposed that solvent evaporation from a charged droplet would increase the surface-charge density until the point at which surface tension and the Coulombic repulsion forces become comparable; that is, the Rayleigh limit. Once this point was exceeded, a series of 'Coulomb explosions' or Rayleigh instabilities would produce extremely small droplets containing only one molecule of solute *via* a fission process. As the last of the solvent evaporates, they suggest a free gas-phase ion is produced by the single molecule retaining some of its droplet's charge.[7] This theory has been criticized for not giving enough detail into how a droplet containing only one charge is formed.

The ion evaporation model (IEM) developed by Irbane and Thomson is well supported, and is the more widely accepted theory for the formation of gas-phase ions. The IEM, similar to the CRM, assumes that solvent evaporation leads

to droplet shrinkage and a resulting increase of the electric field normal at the droplet surface which causes the series of Coulomb explosions. The IEM was developed from transition state theory which implies that there is an energy barrier which must be exceeded for an ion to evaporate out of solvent. This energy barrier is a result of the opposing electrostatic forces. At a given decreased droplet radius, the increasing repulsion between like charges overcomes the surface tension at the droplet surface and elastic deformation of the droplet occurs where a charged site on a protonated molecule that has approached the droplet surface is moved a distance outside the droplet and then finally the repulsion force lifts the solute ion from the droplet surface allowing the escape of the ion into the gas-phase.[10, 12-14] These ions are then guided by an electrostatic gradient and pressure difference to travel through a heated capillary and enter into the first low pressure chamber where a further electrostatic gradient between the capillary and the skimmer allows the ions to be cleaned up and directed into the orifice of the mass analyzer.

1.1.2. Mass Analyzer

The mass analyzer is the heart of the mass spectrometer. Once guided into the mass analyzer, the ions are separated according to their m/z. A variety of mass analyzers are available. Widely used analyzers for small molecule analysis include: quadrupole, quadruple ion trap, linear ion trap, time-of-flight (TOF), reflectron TOF, quadupole TOF, Fourier transform ion cyclotron resonance (FT-ICR), and orbitrap. The choice of an appropriate mass analyzer requires the consideration of a number of factors including desired mass range, resolving power/resolution, mass measurement accuracy, ion transmission, and spectral recording speed. In this work, preliminary studies were carried out using a quadrupole ion trap MS instrument and further qualitative and quantitative studies were performed using an FT-ICR-MS.

1.1.2.1. Quadrupole Ion Trap MS

The creation of the quadrupole and the quadrupole ion trap, often referred to as the Paul Trap or the Paul Ion Trap, is credited to Wolfgang Paul in 1953 and are still the most widely used mass analyzers today.[15] Paul was jointly awarded the Nobel Prize in Physics in 1989 for his work in "developing the ion trap technique."[16] The quadrupole ion trap mass analyzer is the three-dimensional analogue of the two-dimensional linear quadrupole mass analyzer. The operation of these types of analyzers is based on ion motion in rf electric fields. The linear quadrupole mass analyzer, often referred to as the quadrupole mass filter, consists of a linear array of four cylindrical rods to which rf and dc voltages are applied creating a hyperbolic field. Forces inside the quadrupole are exerted along the z-axis in which the ions travel on their way from the source to the detector. Ions oscillate in the x,y-plane with frequencies depending on the m/z value of the ion and with excursions dependent on the amplitude of the applied potentials. Ion trajectories and stabilities inside the quadrupole mass filter are ultimately directly dependent on the applied rf and dc voltages, as defined by the Mathieu equations and as given by the a-q stability diagram (see Figure 1.3). The canonical form of the Mathieu differential equation has both bound and unbound solutions, where the bounded corresponds to stable ion trajectory in the quadrupole and the motion of the ion in the z-direction can be summarized by a stability diagram given in terms of the Mathieu coordinates a and q. The m/z range of stable ion motion can be made large, as in a broad bandpass mass filter, by decreasing the slope ($a/q \sim zU/V$, where U ~ dc component and V ~ rf component) or be made narrow, as in a narrow bandpass mass filter, by increasing the slope such that only the tip of the a-q diagram is intersected by the mass scan line (dc dominates). If both the U and the V (the rf and dc components) are kept constant, then a/q or the slope of the mass scan line is kept constant. In this situation, U and V can then be increased simultaneously or swept and ions within the certain defined mass window will be brought to the tip of a-q diagram and in the order of increasing mass, ions will pass the mass filter achieving mass scanning.[16, 17]

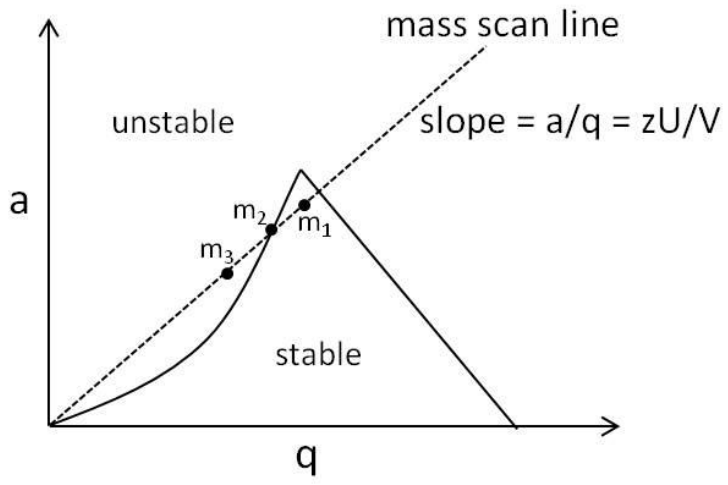

Figure 1.3. The a-q stability diagram, where ($m_3 > m_2 > m_1$). (Adapted from Chemistry 423 class notes, Fall 2007, Prof Liang Li, University of Alberta).

In the ion trap mass analyzer, ion motion is again influenced by forces generated by the application of an rf field. However, in this case, these forces occur in all three, rather than just two dimensions. The ion trap mass analyzer consists of three electrodes with hyperbolic surfaces: two adjacent end-cap electrodes and one central ring electrode, as shown in Figure 1.4. In the quadrupole, stable ion motion was allowed one dimension of freedom in the z-direction, however, in the ion trap, no degrees of freedom are available for stable motion and hence the ions are trapped. Again, the ion's ability to be trapped in the applied electric field depends on the ion's stability which relies on the applied rf and dc voltages applied to the trap and governed by the Mathieu equations and the a-q stability diagram, where in the case of the ion trap, both stability in the z-direction and radial stability must be maintained for stable ion motion.

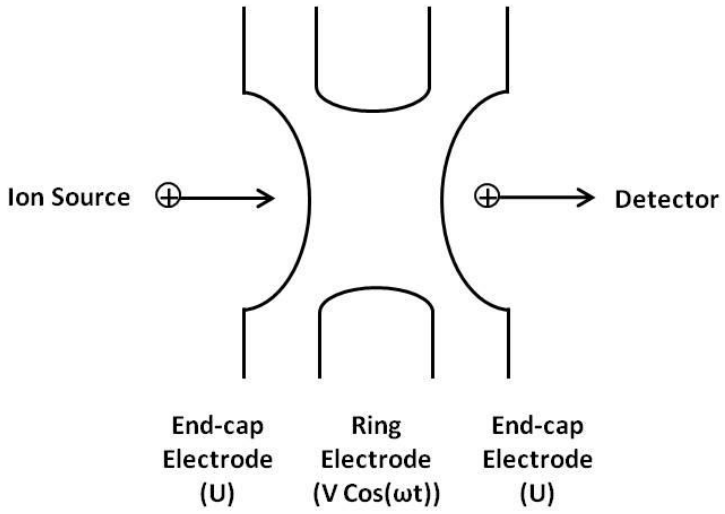

Figure 1.4. Ion trap mass analyzer consisting of a ring electrode and two end-cap electrodes. Where U = applied dc potential to the end-caps with respect to the ring electrode, V = rf applied to the ring electrode, ω = angular frequency, and t = time (adapted from Chemistry 423 class notes, Fall 2007, Prof Liang Li, University of Alberta).

Ions enter into the trap following clean-up from an octopole ion guide. An octople focusing lens functions similar to an rf-only quadrupole mass filter, however there are eight rods instead of four, and is essentially a very broad and efficient bandpass mass filter. In an octopole focusing lens there is no dc component which means the slope of the mass scan line (a/q) is zero. Therefore ions of a wide range of m/z are allowed past the filter and are focused into the ion trap. Once inside the trap, the U and the V (the rf and dc voltages) can be varied to confine the ions within the trapping zone. Again by fixing the U and the V, ions of varying masses can be simultaneously trapped, but at different placements in the zone. It is the oscillating rf potential applied to the ring electrode that maintains the ions as a focused packet at the center of the trap. Focusing of the ions in the zone can be further optimized using helium gas, ~ 1 mTorr, as a collision gas inside the trap to lessen the kinetic energy of the ions which then allows for improved occupation of the central trapping region by the ions.[17]

Inside the ion trap, the potentials can again be adjusted to allow for a broad or narrow mass range of ions, or a single ion mass to be isolated and ejected from the trap to the detector. Ions have a characteristic frequency of oscillation depending on their mass and move in resonance with the applied rf field. In order to eject ions from the trap to the detector, a supplementary rf field is ramped to the end-cap electrodes to match the motion of the ions in the z-direction such that ions moving in resonance with the main rf will pick up some additional energy from the supplementary field. At the point where an ion gains too much energy, the motion will become unstable and the ion will be ejected from the trap exiting through the aperture of the latter end-cap electrode and entering the detector.[16, 17]

Commonly the detector for a quadrupole ion trap mass analyzer is an electron multiplier. Specifically it is the channel electron multiplier (CEM) which is a continuous dynode multiplier which is made of a semi-conducting material and is curved in order to prevent positive-ion feedback. An incoming ion hits the surface of the electron multiplier with very high velocity inducing the emission of electrons which continue on in the CEM striking the surface and emitting further electrons resulting in an avalanche of electrons which are collected at an amplifier, or anode. The collected signal is used to produce the mass spectrum.

In this work, the ion trap was not used to perform tandem MS experiments (MS^n). However these studies would have been possible using the ion trap as its ability to perform MS^n experiments is one of the main advantages of this type of mass analyzer. Here, all ions are ejected from the trap except for the ion(s) of interest. These parent ions are then subjected to a supplementary rf voltage that will excite the ions but not cause them to gain sufficient energy to become unstable. This results in a wider oscillation trajectory and collision-induced dissociation of the ions *via* energetic collisions with the helium gas. These product-ions are then ejected to the detector by scanning the rf supplementary voltage.[17]

The ion trap typically has a mass range from m/z 10 to 3000, with resolving power of $R < 3000$ and mass measurement accuracy of 0.1 - 0.2 Da. It has good ion transmission with all trapped ions being scanned to the detector and

a typical spectral recording speed of 1-10 spectra/s. The ion trap is relatively inexpensive, easily combined with LC or gas chromatography (GC) and has unique MS^n capabilities. However, the trap can only hold ~10^5 - 10^6 ions before Coulombic repulsions or space-charge effects significantly reduce the mass resolution.

1.1.2.2. Fourier Transform Ion Cyclotron Resonance MS

Fourier Transform Ion Cyclotron Resonance MS (FT-ICR-MS) is a type of trapping mass analyzer and provides the highest resolving power and mass accuracy available among MS instruments. The operation of the FT-ICR mass analyzer is based on ion cyclotron motion derived from the cyclotron principles first described by Lawrence in 1932.[18] The advantages of applying FT-ICR to mass spectrometry were demonstrated by Comisarow and Marshall in 1974.[19] Unlike other traps, the motion of ions in this analyzer is governed by both electric and magnetic fields. Also, the ICR cell is essentially able to collect an entire spectrum all at once rather than having to scan one frequency at a time in order to collect the spectrum as performed by other traps.

In an FT-ICR-MS instrument, ions can be introduced to the system by ESI. Once ions have entered through the source they are carried through a number of pumping stages under increasingly high vacuum. Skimmers, a hexapole, a quadrupole and further ion transfer optics are in place to focus the ions and steer them through the system at specific times during a scanning event prior to introduction to the ICR cell. Once inside the core of the mass analyzer, the ICR cell, ions become influenced by a spatially uniform static magnetic induction field and undergo cyclotron motion at a frequency characteristic of their m/z. It is given that ions traveling in the z-direction inside a homogeneous magnetic field, B, will face an opposing force, the Lorentz force, as described by *Eq. 1.2*.

$$Force = (mass)(acceleration) = m\left(\frac{dv}{dt}\right) = q(\vec{v} \times \vec{B}) \qquad (Eq.\ 1.2.)$$

Where, m = ionic mass, q = charge, *v* = velocity, and x B = the vector cross product indicating that the Lorentz force is perpendicular to the plane established by the ion velocity and the encompassing magnetic field.[20-22]

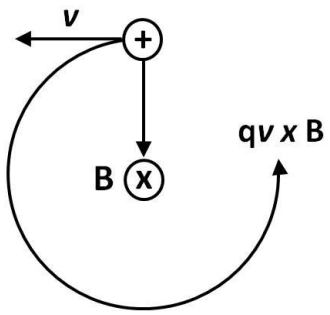

Figure 1.5. Ion cyclotron motion is shown in the plane perpendicular to the magnetic field lines, where the magnetic field, B, is pointing into the plane of the page. An ion of mass m and charge q is constrained to a circular orbit by the homogeneous magnetic field, B. The orbit has a characteristic angular frequency, ω_c, called the cyclotron frequency (adapted from Marshall, et al., 1998 [22]).

With angular acceleration in the plane perpendicular to B expressed as $dv/dt = v_{xy}^2/r$, where r is the radius of the cyclotron orbital, and angular frequency expressed as $\omega_c = v_{xy}/r$, then *Eq. 1.2* can be simplified to give,

$$\omega_c = \frac{qB}{m} \qquad (Eq.\ 1.3.)$$

This equation gives the "unperturbed" cyclotron frequency of an ion. From this equation it is shown that ICR frequency is independent of velocity for ions of the same m/z (here shown as m/q). Hence the m/z of an ion is inversely related to the cyclotron frequency which is fundamental to how this analyzer is capable of producing such high quality MS data.[23]

In general, the ICR cell consists of a cubic geometry, as shown in Figure 1.6, with two trapping electrodes, two excitation plates on the front and back, and two detection plates on the top and bottom. The trapping plates are positioned perpendicular to the magnetic field, B, such that a potential well is created by the application of a small symmetric electric field which traps the ions inside the cell. This applied voltage causes the ions to undergo simple harmonic oscillation along the z-axis of the magnetic field between the two trapping plates which confines them axially while the spatially uniform static magnetic field confines the ions radially in the x,y-plane. Together, the magnetic and electric fields create the three-dimensional Penning Trap and operate on the ions independently to give rise to magnetron motion. This results in the precession of the guiding center of the ion cyclotron motion about the center of the ICR cell.[22]

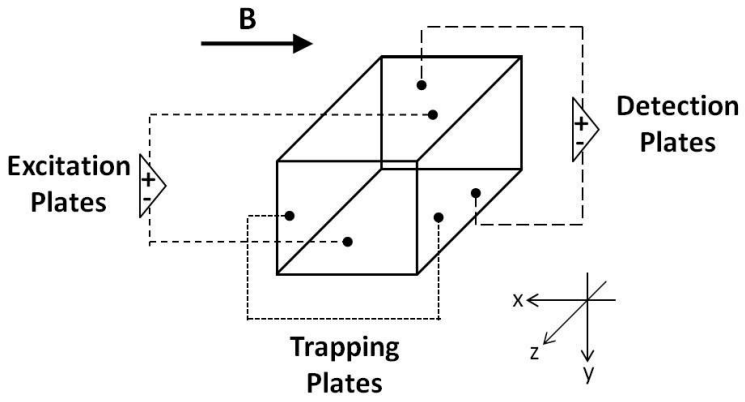

Figure 1.6. Simplified depiction of an ICR cell showing the positions of the two excitation plates on the front and back, the two trapping plates on both sides, and the two detection plates on the top and bottom (adapted from Marshall, et al., 1998 [22]).

The sequence of events that occur for ion detection inside an FT-ICR-MS is unique from other types of analyzers as the main events leading to detection for this MS occur all within the analyzer cell but are spread out in time; for other analyzers, the events occur at different locations in the instrument but occur continuously at the same time. The four main events composing the experimental

sequence for an FT-ICR-MS include a quench, which ejects leftover ions from a previous experiment from the ICR cell, then ion formation, in which ions are transferred into the cell or, in certain cases, ions are formed within the cell, followed by ion excitation and detection.

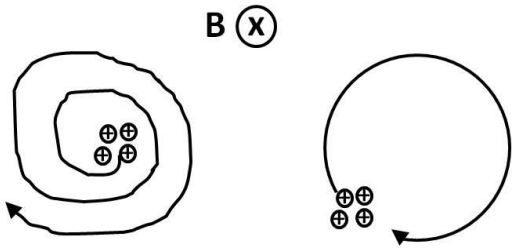

Figure 1.7. Ion excitation and detection.

Ion excitation within the ICR cell is accomplished by the application of an AC electric field to the two excitation plates which are parallel to the axis of the magnetic field. An ion undergoing cyclotron motion in the field will absorb the kinetic energy from the applied voltage and expand its orbit steadily when the frequency of the applied electric field is in resonance with that of the cyclotron frequency of the particular ion of mass m, as depicted in the first panel of Figure 1.7. Ions of the same m/z will be excited simultaneously. As they absorb energy from the applied electric field, the velocity of their cyclotron motion increases and the ions of a given mass are accelerated together forming a tightly grouped packet following a spiral path of increasing radius. Once excited to the larger orbital, as shown in the second panel of Figure 1.7, the coherently orbiting ion packet induces a differential current between the two opposing detection plates known as the image current. The current amplitude is proportional to the orbiting ion population of the particular m/z packet. This image signal is then amplified, digitized, and the time-domain analog signal is stored for processing by a computer where fast Fourier transformation, magnitude computation, and frequency to m/z conversion is carried out to give the mass spectrum as a plot of m/z versus signal intensity. Using FT-ICR-MS, ions of a wide range of masses can be detected simultaneously by the application of broadband excitation and

detection using an rf chirp. This is a rapid sweep (2 - 5 ms) of applied electric potentials exciting all ions with a cyclotron frequency in the range of the sweep frequency. Nearly simultaneously all the ions are excited and reach the larger cyclotron orbit together. This results in a composite image current at the detection plates which is transformed to give the mass spectrum.[22, 23]

Tandem mass spectrometry experiments are possible with the FT-ICR-MS by the addition of events to the sequence. Manipulation of excitation waveforms can be performed in order to excite ions in the cell in a mass-selective fashion. Popular forms of MS/MS experiments include collisionally activated dissociation (CAD), surface-induced dissociation (SID), ultraviolet photodissociation (UVPD), infrared multiphoton photodissociation (IRMPD), and blackbody infrared dissociation (BIRD).[22]

FT-ICR-MS typically has a wide mass range of m/z (up to 5,000). It has the best resolving power of all mass analyzers, with a resolution of 1,000,000 being possible, and routinely achieved resolution of 10,000. Mass measurement accuracy is < 0.0005 % or < 5 ppm, with a routinely observed mass measurement accuracy of < 2 ppm. All ions in the cell are detected but when used with ESI, where ions are produced outside the cell, all ions may not be transmitted due to the various stages of vacuums at increasingly low pressure that the ions must travel through to gain entrance to the analyzer, which can result in ion loss or reduced sensitivity. The spectral recording speed is considered slow compared to other analyzers, typically 1 s or more, as a long decay signal is essential for the generation of high resolution spectra. The analyzer is the least versatile due to the high vacuum requirements and it is very expensive, requiring both helium and liquid nitrogen. This mass analyzer can also have undesirable space-charge effects when the ICR cell is populated in excess of ~ 10^4 ions, leading to reduced mass resolution.[22] The limitations of FT-ICR-MS are outweighed by its ability to produce high resolution and high mass accuracy data which are key in the identification and quantification of small molecules. The FT-ICR-MS used in this study was the Bruker 9.4 T Apex-Qe FT-ICR-MS. A schematic overview of this instrument is shown in Figure 1.8.

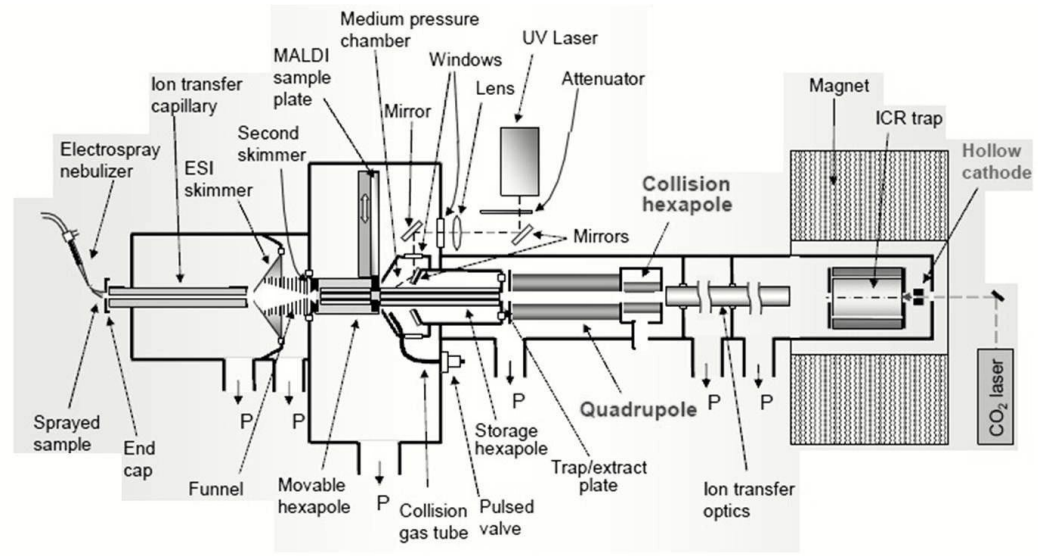

Figure 1.8. Schematic of the Bruker Apex-Qe FT-ICR-MS. P indicates pressure, as in a region which is under vacuum created by a pump (mechanical pump, turbo pumps, and cryo pumps are in use). This figure was reproduced with permission from Bruker Daltonics.[24]

1.1.3. Liquid Chromatography

Liquid chromatography (LC) is a technique that can be used in combination with mass spectrometry to achieve separation of the analytes in a mixture prior to ionization and detection, such that individual sample components may be identified and quantified. This is important for metabolomics as a single sample may contain thousands of analytes. Identification of these metabolites using MS would be far too complex if a separation technique such as LC was not used in line with the mass analyzer in order to achieve individual analyte detection. The most commonly used form of LC for metabolomics is reversed phase LC (RPLC) and this is done using high performance liquid chromatography, also referred to as high pressure liquid chromatography (HPLC). RPLC uses a non-polar stationary phase packed inside of a column and a polar mobile phase composed of water with an organic solvent, typically acetonitrile, which is pumped through the column. The sample is injected into the flow of mobile phase and carried into the column where the sample components interact

with the stationary phase as they travel along the length of the column carried by the mobile phase. The column is a cylindrical tube filled with small, spherical particles (1.5 - 5 μm in diameter), often porous silica (typically 10 nm pore size for use in small molecule studies). The inside of each silica pore is covered with the stationary phase which is usually C18 groups for RPLC. As the sample is carried through the column by the mobile phase, the different analytes will enter the particle pores by diffusion and interact with the C18 phase. The separation of analytes in the column is achieved by differential migration. Based on the polarity of the analyte, it will interact more with the stationary phase or the mobile phase. Relatively polar analytes will migrate through the column with a higher average velocity than less polar components as they will have less interaction with the stationary phase and therefore will be less retained and will elute from the column earlier. As a sample migrates through the column, its components will become further spread out along the column. Analytes of the same polarity will encompass a certain volume or zone on the column as migration occurs, known as a band. When a band is eluted from the column and goes on to reach the detector it gives what is called a peak. If good separation of sample components on the column was achieved then each peak is representative of a unique analyte. The time at which the analyte leaves the column, the retention time t_R, is indicative of the analyte identity and the peak area is representative of the analyte concentration in the sample.[25] Hence analyte identification and quantification is greatly simplified using LC in combination with MS.

Combination of LC with MS is amenable as LC is easily interfaced to ESI, where the column eluent is fed into the ESI spray needle. This is achieved using LC flow rates of 1 mL/min or less. In gradient elution LC, the mobile phase composition is gradually made less polar throughout the experiment by increasing the percentage of acetonitrile present to help elute less polar analytes. The presence of acetonitrile in the mobile phase allows for decreased surface tension of the ESI spray droplets than experienced with water allowing for improved spray and therefore increased sensitivity.[10] The combination of LC with MS helps to reduce laborious sample preparation steps and improve sample throughput as,

frequently with the use of LC, samples can be analyzed directly. Another important advantage of combining LC with MS is that LC separation reduces the complexity of the sample introduced to ESI at any point in time, which helps to reduce ion suppression effects commonly observed with ESI and thereby helps to increase the sensitivity of the analysis by increasing ionization efficiency. Ion suppression is still an issue even with the use of LC; the effects are just minimized in comparison to other sample introduction methods such as direct infusion.

Ion suppression arises in LC-MS as a result of matrix effects which result from the complexity of the sample matrix in samples such as biofluids. Ion suppression refers to the negative influence which matrix complexity can have on analyte ionization in electrospray. Ion suppression occurs when a co-eluted sample component influences the ionization of a co-eluted analyte. This in turn affects the detection capability as suppressed ionization will result in species not being fully ionized nor transmitted to the mass analyzer for detection. Precision and accuracy of the analysis are subsequently impacted.[11]

Many studies have reported ion suppression to be a serious issue for the electrospray process.[10, 26-28] During ESI, analytes are in competition for occupation of sites at the droplet surface. Easily ionized species are generated preferentially and then dominate the spectra causing the detection of other species to be suppressed. The effects of ion suppression can be reduced by using an optimized LC separation in order to reduce co-elution of analytes, by keeping the LC system (such as tubing and mobile phase) and sample preparation steps (such as vials and pipette tips) stringently clean to reduce the introduction of impurities such as polymers, and by implementing sample preparation clean-up procedures such as solid phase extraction (SPE) to help reduce the sample complexity and thereby reduce matrix effects and ion suppression. The use of surfactants, such as sodium dodecyl sulfate (SDS), and ion-pairing reagents, such as trifluoroacetic acid (TFA), should be avoided as well. The content of non-volatile species in the sample such as salts can also have deleterious effects on ionization efficiency. Sample concentrations should be kept at less than 10^{-5} M as above this concentration the detection linearity is often lost and is believed to be a result of

saturation of the ESI droplets which causes inhibition of ionization due to the competition for space and/or charge. The addition of a bit of acid to the sample and mobile phase can help to improve the ionization of analytes as often species in a biological matrix are quite basic and therefore inhibit the competition for charge or are difficult to charge.[26] Care must be taken in the choice of acid as certain acids such as trifluoroacetic acid (TFA), which is an ion-pairing agent, have been found to cause an increase in ion suppression while other acids, such as acetic acid, interfere with the quality of LC separation. Formic acid (FA) has been found to be a good additive for performing metabolomics studies *via* LC-MS. The use of an internal standard with the LC-MS analysis can help to correct for the effects of ion suppression on the quantitative performance, especially where the analyte and internal standard co-elute as they are exposed to the same extent of ion suppression.[27]

Other theories on the mechanism of ion suppression indicate that a high concentration of co-eluting species results in an increase in the surface tension of formed droplets and therefore solvent evaporation is reduced and species encounter more difficulty in escaping the droplet and entering the gas-phase.[29] It has also been shown that analytes of a higher mass can suppress the ionization of analytes of lower mass and that more polar analytes are generally more susceptible to ion suppression.[27, 30] It is evident that the key to minimizing ion suppression effects relies on achieving good separation of sample components prior to introduction to ESI using chromatography.

1.1.3.1. Low Flow Liquid Chromatography Nanoelectrospray Ionization MS

Conventionally LC is performed at flow rates of 10 μL/min - 3 mL/min using a standard LC instrument with a column of internal diameter (i.d.) 1.0, 2.1, 3.0, or 4.6 mm. Miniaturization of LC techniques has lead to the development of the low flow LC techniques, capillary LC and nano LC, where capillary LC (capLC) loosely refers to LC performed at a reduced flow rate of 1 – 100 μL/min using a column of internal diameter (i.d.) 100 - 500 μm and where nano LC (nLC)

loosely refers to LC performed at flow rates of 200 - 1000 nL/min using a capillary column of i.d. 10 - 100 μm. In 1988, Karlsson and Novotny's studies provided insight into the development of nLC as an alternate technique to regular flow LC allowing for higher efficiencies and peak capacities (resulting from the use of smaller column particle sizes (d_p) of 3 - 5 μm), capability of working with smaller sample sizes, lower mobile phase consumption, and improved compatibility with MS.[31, 32] These advantages have allowed for the use of nLC to become widely popular, particularly in the fields of proteomics and small molecule analyses such as metabolomics.

Similarly, electrospray also has been miniaturized. Initially nanospray, or nano electrospray (nESI), was developed by Wilm and Mann during the 90's so that smaller sample sizes could be analyzed which would be useful again for the analyses of biological samples where often available sample sizes are limited.[33, 34] In conventional ESI, the spray tip typically has an outer diameter (o.d.) of 1 mm and is located 1 - 3 cm from the orifice. Due to the relatively large ESI tip diameter, droplets produced are large and therefore require the fairly large distance between the tip and the orifice in order to evolve gas phase ions. As a consequence of the large distance, only about 30 % of ions produced are converted to the gas phase and make it to the orifice for entrance into the mass analyzer, therefore the majority of the sample is wasted. With nESI, the spray tip is in fact a capillary which can be pulled to a very fine tip of o.d. 1 - 2 μm (typically larger, 10 - 100 μm, o.d. tips are in use).[34, 35] With a finer spray tip, smaller droplets are produced which result in higher ionization efficiency. As a result, the emitter tip is positioned much closer to the orifice resulting in significantly improved efficiency of ion transmission to the mass analyzer. When combined with a low flow rate produced by a nLC, the low effusion rate allows for high electrospray sensitivity. Less solvent evaporation is required for the production of gas phase ions when the initially formed droplets are relatively small. Consequently, impurities such as salts are better tolerated by nESI as less evaporation results in less concentration of any impurities that may be present. The use of a sheath gas and thermal heating to aid in droplet evaporation is not

required in nESI due to the formation of smaller droplets. Also since the droplets are small, sample components will see a greater surface area charge density on the droplet, allowing for improved formation of gas phase ions and therefore significantly decreased ion suppression. Lower abundance ions and ions suppressed in regular ESI will hence see improved detection with nESI.[10]

In summary, benefits of nLC-nESI MS for the analysis of small molecules in complex matrices include improved separation efficiency, greater sensitivity, enhanced dynamic range, reduced competition for gas-phase ion formation, minimized ion suppression, and smaller sample size required for analysis. Nano LC and nanospray have been very important in the fields of biochemical analysis, particularly for proteomics[36] and increasingly for metabolomics[37].

1.2. Metabolomics

Metabolomics is the comprehensive analysis of endogenous small molecules (metabolites) of biosystems. Metabolites are the end products of cellular processes, and their concentrations can be regarded as the definitive response of a biosystem to genetic or environmental influences.[38, 39] The detection, identification, and quantification of metabolites are key for a thorough understanding of living systems. The set of metabolites produced by an organism defines its metabolome. Together with genomics, transcriptomics, and proteomics, metabolomics is playing an integral role in the characterization of metabolomes *via* in depth biological studies, as well as serving as a powerful new tool in disease biomarker discovery.[38, 40-42]

The fundamentals of metabolomics have been in practice for many years, for example, relating that bodily fluids could be used to determine a state of disease or the identification of a high concentration of glucose in diabetic urine (1700s). In the early 1970s small molecule analysis performed using GC-MS based approaches was the debut of mass spectrometry based metabolomics.[43] The first 'omics' experiments of this type are credited to be performed by Dalgliesh, et al. in 1966, describing GC-MS profiling of urine and tissue extracts for a wide range of metabolites.[43] Mamer, et al.[44] and Horning, et al.[45] expanded on these

experiments by performing further urine metabolite profiling using GC-MS reported in 1971. These initial experiments lead to an entire field of metabolomics experiments being carried out using GC-MS. It is still in use today for global profiling approaches[46] but has for the most part been surpassed by other techniques such as nuclear magnetic resonance (NMR) and LC-MS.

It is only in the past decade that the field of metabolomics has really flourished and been defined as an important field of 'omics' research. The term metabolome was first coined by Oliver in 1998 [47] and Fiehn first defined metabolomics in 2001 as the comprehensive and quantitative analysis of all metabolites that could help in the understanding of biosystems and revealing of their metabolome[40]. Metabolomics has rapidly evolved over the past few years, from being a low key area of research to a mainstream field widely recognized and practiced in labs throughout the world. This boom in the field can be attributed to the recent improvements in analytical techniques for small molecule analysis including both mass spectrometry and nuclear magnetic resonance spectroscopy.

For metabolomics studies it is desirable for one method to allow for the generation of a global profile of the metabolome. Key research in the area of untargeted, unbiased metabolomics studies have been reported by Siuzdak and co-workers, focusing mainly on comprehensive LC-MS based techniques.[48-50] LC-MS has become the analytical technique of choice for metabolome profiling as improved separation and ion production has helped to extend the dynamic range which can be achieved using MS detection and thereby has lead to increased coverage of the metabolome.

Another approach to achieving comprehensive metabolome coverage is to study the different constituent biofluids composing a metabolome of a particular biosystem, such as human urine, plasma, or cerebrospinal fluid (CSF), and then use several analytical platforms to provide a comprehensive view of the biofluid. Different analytical techniques have different strengths in the type of metabolites that can be accurately quantified and identified. In this type of study it is the aim to compile the results of several analytical platforms to give a global overview of

the particular biofluid metabolome. This approach was taken by Wishart, et al. in the profiling of the human CSF metabolome by compiling the results obtained by NMR, GC-MS, and LC-ESI FT-ICR-MS analyses. They were able to identify three-hundred and eight metabolites in this manner.[51]

An ideal metabolomic study would provide a comprehensive, qualitative and quantitative overview of the metabolic state of an organism. However, as a result of the great diversity in chemophysical properties of metabolites, the presence of metabolites over extended dynamic ranges, and the sheer number of metabolites (~ 4,000 - > 20,000) which are present in a biosystem, the universal detection of all metabolites is extremely challenging.[49, 52, 53]

1.2.1. Targeted Metabolomics

Alternatively, the metabolome of a biosystem can be viewed as the combination of many sub-metabolomes, each consisting of the metabolites that share a common functional group (for example all carbonyl-containing metabolites or carbonyl metabolome). A 'targeted' metabolomics approach can thus be applied, which is the directed study of a smaller class of metabolites within the biosystem using a tailored method of analysis.[54, 55] A more complete and accurate profile of the metabolome may be obtained by breaking down the task into several targeted studies of the sub-metabolomes and then compiling the results to provide a comprehensive view of the metabolome as a whole.

As of yet, there is no single analytical platform that is suited to the precise and accurate identification and quantification of all the metabolites composing a metabolome. A single all-inclusive platform for comprehensive metabolomics analysis is unlikely due to the vast array of metabolites that make up a metabolome. Therefore, targeted analyses have become popular among metabolomics researchers, with the most developed targeted class or sub-metabolome being lipids, sometimes referred to as 'lipidomics' or the 'lipidome'. A rapid expansion in the field of targeted lipid metabolite profiling has resulted from advances in analytical technology as well as an interest in the central role that lipid metabolism has been found to play in metabolic and inflammatory

disorders.[56] Disease biomarker discovery research is a main source of motivation for a majority of targeted metabolomics studies. Advances in technology, such as the introduction of MS/MS experiments and improvements in LC separations, has allowed for greatly improved limits of detection and the ability to distinguish between isomers allowing for improved quantitation of low abundance diagnostic metabolites. Applications of such analytical platforms to targeted metabolomics studies has allowed for disease screening and identification. For example, the profiling of biofluids for acylcarnitine metabolites has lead to the development and wide use of neonatal screening tests for inborn errors of metabolism.[57] In fact, neonatal screening for a range of diseases by MS is now widely established, including more than thirty metabolic disorders that can be identified by monitoring the concentrations of organic acids, amino acids, fatty acids, and steroid hormones and about two-hundred inherited enzymatic disorders which can be monitored *via* targeted metabolic profiling.[48, 54]

In our research group, we are currently pursuing an analytical approach of selectively labeling the metabolites of sub-metabolomes which consist of specific functional groups, followed by LC-MS analysis for identification and quantification. Our research goal is to develop new isotope reagents that would not only provide an isotope tag to the metabolites, but also improve the performance of LC separation and MS detection. Our work includes the quantitative profiling of amine-containing metabolites with ^{13}C-/^{12}C-formaldehyde[58], amine- and phenol-containing metabolites with $^{13}C_2$-/$^{12}C_2$-dansyl chloride (DnsCl)[59], and carboxylic acid-containing metabolites with $^{13}C_2$-/$^{12}C_2$-p-dimethylaminophenacyl (DmPA) bromide[60]. Studies are on-going for the isotopic labeling of the acylcarnitine and acylglycine sub-metabolomes. And the studies of the quantitative isotopic profiling of the human carbonyl sub-metabolome with $^{15}N_2$-/$^{14}N_2$-dansylhydrazine (DH) using LC-MS are presented in this thesis.

Mass spectrometry has become increasingly popular in endogenous metabolite research and has emerged as a leading detection technique for both comprehensive and targeted metabolome analyses.[48] NMR is also a popular technique in the field of metabolomics given its speed and accuracy; however

NMR suffers from overlapping spectral signals, poor sensitivity and poor dynamic range. Gas chromatography mass spectrometry (GC-MS) has traditionally been a method of choice for metabolite profiling for its high resolution and reproducibility, and also for the advantage of having access to widely available EI spectral libraries.[48, 61] Unfortunately GC-MS is limited to nonpolar and volatile molecules. Derivatization can be used to partially overcome this disadvantage, however since GC-MS is also restricted in mass range it does not provide complete profiling of derivatized samples.

Biofluids such as urine and plasma contain a wide range of metabolites of varying chemophysical properties from small, simple molecules to polar, macromolecules. LC-MS is a technique well suited for such samples of extreme molecular complexity and has become an important tool for metabolome profiling as a result of its sensitivity, selectivity, quantitative reproducibility, and wide dynamic range and mass range.[41, 48, 49, 62-65] Additionally, nLC-nESI MS has become increasingly popular for metabolomics as it further enhances the sensitivity and dynamic range of the analysis. [49, 66] nLC-nESI MS was employed in this work in order to enhance the detection sensitivity of low abundance carbonyl metabolites present in biofluids. There are a variety of mass analyzers in use for metabolite profiling. FT-ICR-MS has become increasingly popular for metabolomics research and was an attractive choice for this study due to its ultrahigh resolving power in m/z, mass accuracy, limits of detection and dynamic range.[67-69] In profiling the human metabolome for carbonyl metabolites, both known and unknown metabolites were expected and the resolving power of the FT-ICR-MS was advantageous in the determination of these structures.

Quantitative profiling of carbonyl-containing metabolites in complex biological samples is important for disease biomarker discovery. Targeted studies of select carbonyls performed on the biofluids of humans with conditions such as cancer, diabetes and specific inherited metabolomic diseases have shown elevated concentrations of certain ketones and aldehydes.[70-76] Studies indicate that carbonyls have the potential to be biomarkers of such conditions and therefore the

development of sensitive techniques for the global quantitative profiling of the carbonyl metabolome is essential.

1.2.2. Carbonyl Labeling

Chemical derivatization of carbonyl compounds is desirable for analysis by LC-ESI MS in order to improve the chromatographic behavior, ionization efficiency, and detection sensitivity. Without derivatization, matrix effects can suppress the ionization of carbonyls. Also, carbonyls are usually relatively polar compounds and therefore they are not retained well by RPLC columns, often eluting in the column void volume with many other polar components. A number of analytical methods exist for the analysis of ketones and aldehydes in complex matrices.[77-82] The analysis of carbonyls in the past has generally been performed in solution by acid catalyzed pre-column reaction of the keto group with a hydrazine-based labeling reagent. The most common derivatizing agent for ketones and aldehydes is 2,4-dinitrophenylhydrazine (DNPH) which is the classical reagent first introduced by Allen[83] and Brady[84] in the early 1930s. This widely employed derivatizing agent is in use for several international standard procedures and is compatible with both LC and GC based analyses, as well as being an important component of qualitative analysis in organic labs for the confirmation of carbonyls. DNPH and the class of hydrazine-based derivatizing agents that it represents are popular for their rapid reaction rates with carbonyl analytes, crystallization of the hydrazone products, simple synthesis of the reagent, and ultraviolet-visible (UV-Vis) spectroscopic properties.[85]

Another promising hydrazine-based carbonyl labeling reagent is dansylhydrazine (5-dimethylaminonaphthalene-1-sulfohydrazide), first introduced in the 1970s.[86-88] It is used in the acid catalyzed derivatization of ketones and aldehydes yielding the corresponding dansylhydrazone which has been commonly separated using LC and sensitively and selectively detected using UV-Vis, fluorescence, and chemiluminescence detection.[89-92] This labeling agent has been widely used in the derivatization of steroids,[93-95] carbohydrates,[96-98] and ketones and aldehydes in the environment.[89, 99] Solution phase and solid phase pre-column

derivatization of carbonyls using DH have been studied.[93, 100-103] Many previous uses of the labeling technique have taken advantage of the chromophoric properties of DH for detection. However we found the DH tag appealing for the hydrophobic properties it introduces to labeled analytes making them more amenable to separation by RPLC and for its easily ionized dimethylamino moiety on the dansyl group which is advantageous for the ESI-MS detection of the dansylhydrazones, enhancing the MS detection sensitivity by at least one to three orders of magnitude. As a result, a much greater number of metabolites can be profiled using RPLC-MS and there is no need to switch the columns or change the polarity of the ionization source for analyzing a sample. Few previous uses of DH for the quantitative detection of a metabolite by MS have been reported. This was the use of DH labeling for targeted detection of succinylacetone in dried blood spots using ESI tandem MS detection (ESI-MS/MS),[75, 104] the use of MS for the identification of mono- and bis-derivatives of progesterone with DH,[103] and the use of MS for the detection of DH labeled malondialdehyde in plasma.[102]

1.2.3. Quantitative Differential Isotope Labeling

Usually, to achieve precise quantitation of a small number of analytes, the isotope-labeled internal standard method is deemed most accurate and requires the use of an isotope-labeled internal standard for each targeted analyte, which helps to overcome the matrix and ion suppression effects encountered in LC-ESI MS. However this can be impractical where the isotope-labeled standards required are unavailable, expensive, difficult to synthesize, the target analytes are unknown or where there are many target analytes, as is the case for metabolome analysis.

To overcome these effects, we have developed a methodology for analyzing sub-metabolomes based on differential isotope labeling. This method uses a chemical reaction to introduce an isotope tag to the analyte(s) of interest and a mass-difference isotope tag to the same analyte(s) in a comparative sample or standard(s). The labeled samples are then combined for analysis and metabolite isoforms are co-eluted by RPLC and detected using MS. Where a biofluid sample is labeled light and a set of standards of known concentrations are labeled heavy,

the peak intensity ratio of the isoform pairs can be used for absolute quantitation of the metabolites in the biofluid sample. This methodology can also be used for relative quantitation of metabolites where two biofluid samples are being compared.

This type of derivatization technique originated and gained popularity in the field of proteomics in the form of isotope-coded affinity tags (ICAT),[105] however there are few reports of this methodology being used in the field of metabolomics. The iTRAQ (isobaric tag for relative and absolute quantitation) reagent, widely popular for quantitative proteomics, has been used for metabolic labeling of amino acids in urine and blood.[106] O'Maille, et al. have used $^{13}C_4$-labeled succinic anyhydride and deuterated butanol for the labeling of hydroxyl- and carboxyl-containing metabolites, respectively.[107] Yang et al. has described a method using a deuterium based differential labeling tag for fatty acids, a tag for estrogens, and another tag for tocopherol metabolites.[108-110] Tsukamoto, et al. also presents a deuterium based differential isotope labeling reagent for fatty acids, as well as have Lamos, et al.[111-113] Fukusaki, et al. have used a ^{13}C-methylation tag for flavonoid quantitation.[114] Shortreed, et al. and Abello, et al. have used ^{13}C-based tags for the differential labeling of amine-containing metabolites.[115, 116] Guo, et al. (from our research group) has reported a variety of differential isotope labeling methods based on ^{13}C-reagents for amine-, phenol-, and carboxyl-containing metabolites.[58-60] GC-MS has also been used for analysis of metabolites with the differential labeling technique by Huang, et al. for the quantitation of amino acids, fatty acids, and organic acids.[117] MALDI-MS has even been applied for the profiling of carboxylic acid metabolites using the differential isotope labeling approach.[118] Note that a related method involves the use of isotope enriched media for cell culturing[70, 119-122] and isotope enriched environments/feeds for plant harvesting.[123-125] Another related method has been used in NMR-based targeted metabolomic profiling, with a ^{15}N-ethanolamine tag to create enhanced signal for carboxyl containing metabolites.[126]

The beauty of the differential isotope labeling method that we have developed is that the isotope label has been incorporated into the tag and therefore

by combining a biofluid sample or standard set with the differential isotope labeling reagent all of the metabolites containing the functional group of interest are labeled generating in one reaction an isotope labeled internal standard for every target metabolite.

1.3. Overview of Thesis

This thesis presents mass spectrometry-based metabolomics for quantitative carbonyl metabolome profiling. An optimized method for the determination of carbonyl-containing metabolites in human biological fluids (biofluids) was developed using dansylhydrazine labeling. The conversion of these carbonyls to their dansylhydrazone derivatives has shown significant improvement of RPLC chromatographic properties and enhancement of ESI-MS signals making them readily amenable for analysis by LC-MS. Further enhancement of sensitivity and reduction of sample size was achieved using nLC-nESI MS. Nano flow LC methods appropriate for the analysis of derivatized biological samples were developed which were suitable for the interface with nESI-MS in a 9.4 Tesla FT-ICR-MS. With the mass accuracy offered by FT-ICR-MS in combination with the analysis of labeled standards, it was possible to compose a carbonyl metabolite library that could be used in profiling DH labeled biofluids. This work is presented in Chapter 2.

A robust, quantitative carbonyl metabolome profiling technique was developed using differential $^{15}N_2$-/$^{14}N_2$-isotope dansylhydrazine labeling with analysis by LC-MS. This method of derivatization was used to generate a $^{15}N_2$-stable isotope labeled internal standard for each corresponding $^{14}N_2$-labeled analyte. The dansylhydrazine isoforms were co-eluted and simultaneously detected and hence no isotopic effect was observed, as is common when using deuterium labeled standards for RPLC, allowing for reliable, absolute quantitation of metabolites. A scheme for the synthesis of $^{15}N_2$-isotope dansylhydrazine *via* a one-step reaction was developed and performed. Application of the differential $^{15}N_2$-/$^{14}N_2$-DH labeling method with analysis by nLC-nESI FT-ICR-MS to the absolute quantitation of carbonyl metabolites in a human urine and plasma sample

was performed and results are presented. It was found that carbohydrates in biofluids could also be derivatized using DH. The derivatization protocol was optimized for carbohydrate labeling and quantitation of identified sugars in the biofluid samples was performed as well. Finally, a larger carbonyl metabolome profiling study was carried out to determine the range in which the identified carbonyls and carbohydrates are found in urine. Relative quantitation of carbonyl metabolites present in the urine of samples collected from ten female and ten male volunteers over a three day period was performed using the differential isotope DH labeling technique. This quantitative work is presented in Chapter 3. Conclusions and future directions are presented in Chapter 4.

1.4. Literature Cited

(1) Thomson, J. J. *Philos. Mag.* **1897**, *44*.
(2) Aston, F. W. *Philos. Mag.* **1919**, *XXXVIII*.
(3) Dempster, A. J. *Phys. Rev.* **1918**, *11*, 316-325.
(4) Fenn, J. B. *Nobel Lecture, Decemeber 8, 2002*.
(5) Tanaka, K. *Nobel Lecture, Decemeber 8, 2002*.
(6) Zeleny, J. *Phys. Rev.* **1914**, *3*, 69-91.
(7) Dole, M.; Mack, L. L.; Hines, R. L. *J. Chem. Phys.* **1968**, *49*, 2240-2249.
(8) Yamashita, M.; Fenn, J. B. *J. Phys. Chem.* **1984**, *88*, 4451-4459.
(9) Aleksandrov, M. L.; Gall, L. N.; Krasnov, N. V.; Nikolayev, V.; Pavlenko, V. A.; Shkurov, V. A. *Doklady Akademii Nauk SSR.* **1984**, *277*, 379-383.
(10) Kebarle, P.; Verkerk, U. H. *Mass Spectrom. Rev.* **2009**, *28*, 898-917.
(11) Kebarle, P.; Tang, L. *Anal. Chem.* **1993**, *65*, A972-A986.
(12) Kebarle, P.; Peschke, M. *Anal. Chim. Acta.* **2000**, *406*, 11-35.
(13) Iribarne, J. V.; Thomson, B. A. *J. Chem. Phys.* **1976**, *64*, 2287-2294.
(14) Kebarle, P. *J. Mass Spectrom.* **2000**, *35*, 804-817.
(15) Paul, W.; Steinwedel, H. *Z. Naturfors. Sect. A-J. Phys. Sci.* **1953**, *8*, 448-450.
(16) Paul, W. *Nobel Lecture, Decemeber 8, 1989*, 22.
(17) Jonscher, K. R.; Yates, J. R. *Anal. Biochem.* **1997**, *244*, 1-15.
(18) Lawrence, E. Q.; Livingston, M. S. *Phys. Rev.* **1932**, *40*, 19-35.
(19) Comisarow, M. B.; Marshall, A. G. *Chem. Phys. Lett.* **1974**, *25*, 282-283.
(20) Comisarow, M. B. *Hyperfine Interact.* **1993**, *81*, 171-178.
(21) Zhang, L. K.; Rempel, D.; Pramanik, B. N.; Gross, M. L. *Mass Spectrom. Rev.* **2005**, *24*, 286-309.
(22) Marshall, A. G.; Hendrickson, C. L.; Jackson, G. S. *Mass Spectrom. Rev.* **1998**, *17*, 1-35.
(23) Marshall, A. G.; Hendrickson, C. L. *Int. J. Mass Spectrom.* **2002**, *215*, 59-75.

(24) Fourier Transform Mass Spectrometry A Training Course: FT-ICR MS APEX IV and APEX IV-Q. *Bruker Daltonik GmbH, Bremen, Germany*, **2006**.
(25) Snyder, L. R.; Kirkland, J. J.; Dolan, J. W. *Introduction to Modern Liquid Chromatography, Third Edition*; John Wiley & Sons, Inc.: Hoboken, New Jersey, 2010.
(26) Jessome, L. L.; Volmer, D. A. *LC-GC North America.* **2006**, *24*, 498-510.
(27) Annesley, T. M. *Clin Chem* **2003**, *49*, 1041-1044.
(28) Antignac, J. P.; de Wasch, K.; Monteau, F.; De Brabander, H.; Andre, F.; Le Bizec, B. *Anal. Chim. Acta.* **2005**, *529*, 129-136.
(29) Beaudry, F.; Vachon, P. *Biomed. Chromatogr.* **2006**, *20*, 200-205.
(30) Sterner, J. L.; Johnston, M. V.; Nicol, G. R.; Ridge, D. P. *J. Mass Spectrom.* **2000**, *35*, 385-391.
(31) Karlsson, K. E.; Novotny, M. *Anal. Chem.* **1988**, *60*, 1662-1665.
(32) Hernandez-Borges, J.; Aturki, Z.; Rocco, A.; Fanali, S. *J. Sep. Sci.* **2007**, *30*, 1589-1610.
(33) Wilm, M. S.; Mann, M. *Int. J. Mass Spectrom.* **1994**, *136*, 167-180.
(34) Wilm, M.; Mann, M. *Anal. Chem.* **1996**, *68*, 1-8.
(35) Wickremsinhe, E. R.; Singh, G.; Ackermann, B. L.; Gillespie, T. A.; Chaudhary, A. K. *Curr. Drug Metab.* **2006**, *7*, 913-928.
(36) Wilm, M.; Shevchenko, A.; Houthaeve, T.; Breit, S.; Schweigerer, L.; Fotsis, T.; Mann, M. *Nature.* **1996**, *379*, 466-469.
(37) Metz, T. O.; Page, J. S.; Baker, E. S.; Tang, K. Q.; Ding, J.; Shen, Y. F.; Smith, R. D. *Trac-Trends Anal. Chem.* **2008**, *27*, 205-214.
(38) Fiehn, O. *Plant Mol.Biol.* **2002**, *48*, 155-171.
(39) Rochfort, S. *J. Nat. Prod.* **2005**, *68*, 1813-1820.
(40) Fiehn, O. *Compar. Funct. Genom.* **2001**, *2*, 155-168.
(41) Villas-Boas, S. G.; Mas, S.; Akesson, M.; Smedsgaard, J.; Nielsen, J. *Mass Spectrom. Rev.* **2005**, *24*, 613-646.
(42) Kim, Y. S.; Maruvada, P.; Milner, J. A. *Future Oncol.* **2008**, *4*, 93-102.
(43) Dalgliesh .C. E.; Horning, E. C.; Horning, M. G.; Knox, K. L.; Yarger, K. *Biochem. J.* **1966**, *101*, 792-810.
(44) Mamer, O. A.; Crawhall, J. C.; Santjoa, S. *Clin. Chim. Acta.* **1971**, *32*, 171-184.
(45) Horning, E. C.; Horning, M. G. *Clin. Chem.* **1971**, *17*, 802-809.
(46) Pasikanti, K. K.; Ho, P. C.; Chan, E. C. Y. *Rapid Commun. Mass Spectrom.* **2008**, *22*, 2984-2992.
(47) Oliver, S. G.; Winson, M. K.; Kell, D. B.; Baganz, F. *Trends Biotechnol.* **1998**, *16*, 373-378.
(48) Want, E. J.; Cravatt, B. F.; Siuzdak, G. *Chembiochem.* **2005**, *6*, 1941-1951.
(49) Want, E. J.; Nordstrom, A.; Morita, H.; Siuzdak, G. *J. Proteome Res.* **2007**, *6*, 459-468.
(50) Cravatt, B. F.; Prosperogarcia, O.; Siuzdak, G.; Gilula, N. B.; Henriksen, S. J.; Boger, D. L.; Lerner, R. A. *Science.* **1995**, *268*, 1506-1509.

(51) Wishart, D. S.; Lewis, M. J.; Morrissey, J. A.; Flegel, M. D.; Jeroncic, K.; Xiong, Y. P.; Cheng, D.; Eisner, R.; Gautam, B.; Tzur, D.; Sawhney, S.; Bamforth, F.; Greiner, R.; Li, L. *J. Chromatogr. B* **2008**, *871*, 164-173.
(52) Fernie, A. R.; Trethewey, R. N.; Krotzky, A. J.; Willmitzer, L. *Nat. Rev. Mol. Cell Biol.* **2004**, *5*, 763-769.
(53) Lu, W.; Bennett, B. D.; Rabinowitz, J. D. *J. Chromatogr. B* **2008**, *871*, 236-242.
(54) Griffiths, W. J.; Koal, T.; Wang, Y. Q.; Kohl, M.; Enot, D. P.; Deigner, H. P. *Angew. Chem.-Int. Edit.* **2010**, *49*, 5426-5445.
(55) Carlson, E. E.; Cravatt, B. F. *Nat. Methods.* **2007**, *4*, 429-435.
(56) Morris, M.; Watkins, S. M. *Curr. Opin. Chem. Biol.* **2005**, *9*, 407-412.
(57) Millington, D. S.; Kodo, N.; Norwood, D. L.; Roe, C. R. *J. Inherit. Metab. Dis.* **1990**, *13*, 321-324.
(58) Guo, K.; Ji, C.; Li, L. *Anal. Chem.* **2007**, *79*, 8631-8638.
(59) Guo, K.; Li, L. *Anal. Chem.* **2009**, *81*, 3919-3932.
(60) Guo, K.; Li, L. *Anal. Chem.* **2010**, *82*, 8789-8793.
(61) Fiehn, O. *Trac-Trends Anal. Chem.* **2008**, *27*, 261-269.
(62) Dunn, W. B.; Bailey, N. J. C.; Johnson, H. E. *Analyst* **2005**, *130*, 606-625.
(63) Dettmer, K.; Aronov, P. A.; Hammock, B. D. *Mass Spectrom. Rev.* **2007**, *26*, 51-78.
(64) Scalbert, A.; Brennan, L.; Fiehn, O.; Hankemeier, T.; Kristal, B. S.; van Ommen, B.; Pujos-Guillot, E.; Verheij, E.; Wishart, D.; Wopereis, S. *Metabolomics.* **2009**, *5*, 435-458.
(65) Theodoridis, G.; Gika, H. G.; Wilson, I. D. *Trac-Trends Anal. Chem.* **2008**, *27*, 251-260.
(66) Lanckmans, K.; Van Eeckhaut, A.; Sarre, S.; Smolders, I.; Michotte, Y. *J. Chromatogr. A* **2006**, *1131*, 166-175.
(67) Ohta, D.; Kanaya, S.; Suzuki, H. *Curr. Opin. Biotechnol.* **2010**, *21*, 35-44.
(68) Han, J.; Danell, R. M.; Patel, J. R.; Gumerov, D. R.; Scarlett, C. O.; Speir, J. P.; Parker, C. E.; Rusyn, I.; Zeisel, S.; Borchers, C. H. *Metabolomics.* **2008**, *4*, 128-140.
(69) Brown, S. C.; Kruppa, G.; Dasseux, J. L. *Mass Spectrom. Rev.* **2005**, *24*, 223-231.
(70) Bennett, B. D.; Yuan, J.; Kimball, E. H.; Rabinowitz, J. D. *Nat. Protoc.* **2008**, *3*, 1299-1311.
(71) Li, N.; Deng, C. H.; Yao, N.; Shen, X. Z.; Zhang, X. M. *Anal. Chim. Acta.* **2005**, *540*, 317-323.
(72) Zimmermann, D.; Hartmann, M.; Moyer, M. P.; Nolte, J.; Baumbach, J. I. *Metabolomics.* **2007**, *3*, 13-17.
(73) Zhang, H. J.; Huang, J. F.; Lin, B.; Feng, Y. Q. *J. Chromatogr. A* **2007**, *1160*, 114-119.
(74) Xue, R. Y.; Dong, L.; Zhang, S.; Deng, C. H.; Liu, T. T.; Wang, J. Y.; Shen, X. Z. *Rapid Commun. in Mass Spectrom.* **2008**, *22*, 1181-1186.
(75) Al-Dirbashi, O. Y.; Rashed, M. S.; Jacob, M.; Al-Ahaideb, L. Y.; Al-Amoudi, M.; Rahbeeni, Z.; Al-Sayed, M. M.; Al-Hassnan, Z.; Al-Owain, M.; Al-Zeidan, H. *Biomed. Chromatogr.* **2008**, *22*, 1181-1185.

(76) Lv, L. L.; Xu, H.; Song, D. D.; Cui, Y. F.; Hu, S.; Zhang, G. B. *J. Chromatogr. A* **2010**, *1217*, 2365-2370.
(77) O'Brien-Coker, I. C.; Mallet, G. P. A. I. *Rapid Commun. Mass Spectrom.* **2001**, *15*, 920-928.
(78) Johnson, D. W. *Rapid Commun. Mass Spectrom.* **2007**, *21*, 2926-2932.
(79) Santa, T.; Al-Dirbashi, O. Y.; Ichibangase, T.; Rashed, M. S.; Fukushima, T.; Imai, K. *Biomed. Chromatogr.* **2008**, *22*, 115-118.
(80) Eggink, M.; Wijtmans, M.; Ekkebus, R.; Lingeman, H.; de Esch, I. J. P.; Kool, J.; Niessen, W. M. A.; Irth, H. *Anal. Chem.* **2008**, *80*, 9042-9051.
(81) Banos, C. E.; Silva, M. *J. Chromatogr. B.* **2010**, *878*, 653-658.
(82) Eggink, M.; Wijtmans, M.; Kretschmer, A.; Kool, J.; Lingeman, H.; de Esch, I. J. P.; Niessen, W. M. A.; Irth, H. *Anal. Bioanal. Chem.* **2010**, *397*, 665-675.
(83) Allen, C. F. H. *J. Am. Chem. Soc.* **1930**, *52*, 2955-2959.
(84) Brady, O. L. *J. Chem. Soc.* **1931**, 756-759.
(85) Vogel, M.; Buldt, A.; Karst, U. *Fresenius J. Anal. Chem.* **2000**, *366*, 781-791.
(86) Graef, V. Z. Klin. Chem. Klin. Biochem. **1970**, *8*, 320.
(87) Chayen, R.; Dvir, R.; Gould, S.; Harell, A. *Anal. Biochem.* **1971**, *42*, 283-286.
(88) Seiler, N.; Wiechmann, M. *Progress in Thin-Layer Chromatography and Related Methods*; Humphrey Science: Ann Arbor, 1970.
(89) Banos, C. E.; Silva, M. *Anal. Lett.* **2009**, *42*, 1352-1367.
(90) Mainka, A.; Bachmann, K. *J. Chromatogr. A* **1997**, *767*, 241-247.
(91) Bachmann, K.; Haag, I.; Han, K. Y.; Schmitzer, R. Q. *Fresenius J. Anal. Chem.* **1993**, *346*, 786-788.
(92) Lord, H. L.; Rosenfeld, J.; Raha, S.; Hamadeh, M. J. *J. Sep. Sci.* **2008**, *31*, 387-401.
(93) Appelblad, P.; Ponten, E.; Jaegfeldt, L. H.; Backstrom, T.; Irgum, K. *Anal. Chem.* **1997**, *69*, 4905-4911.
(94) Visser, S. A. G.; Smulders, C. G. M. A.; Gladdines, W. W. F. T.; Irth, H.; van der Graaf, P. H.; Danhof, M. *J. Chromatogr. B.* **2000**, *745*, 357-363.
(95) Peng, X. D.; Xua, D. H.; Jin, J.; Meia, X. T.; Lv, J. Y.; Xua, S. B. *Int. J. Pharm.* **2007**, *337*, 25-30.
(96) Avigad, G. *J. Chromatogr.* **1977**, *139*, 343-347.
(97) Mopper, K.; Johnson, L. *J. Chromatogr.* **1983**, *256*, 27-38.
(98) Perez, S. A.; Colon, L. A. *Electrophoresis.* **1996**, *17*, 352-358.
(99) Herrington, J.; Zhang, L.; Whitaker, D.; Sheldon, L.; Zhang, J. *J. Environ. Monit.* **2005**, *7*, 969-976.
(100) Binding, N.; Kläning, H.; Karst, U.; Pötter, W.; Czeschinski, P.; Witting, U. *Fresenius J. Anal. Chem.* **1998**, *362*, 270-273.
(101) Herrington, J. S.; Zhang, J. J. *Atmos. Environ.* **2008**, *42*, 2429-2436.
(102) Lord, H. L.; Rosenfeld, J.; Volovich, V.; Kumbhare, D.; Parkinson, B. *J. Chromatogr. B.* **2009**, *877*, 1292-1298.
(103) Appelblad, P.; Ahmed, A.; Ponten, E.; Backstrom, T.; Irgum, K. *Anal. Chem.* **2001**, *73*, 3701-3708.

(104) Al-Dirbashi, O. Y.; Rashed, M. S.; Ten Brink, H. J.; Jakobs, C.; Filimban, N.; Al-Ahaidib, L. Y.; Jacob, M.; Al-Sayed, M. M.; Al-Hassnan, Z.; Faqeih, E. *J. Chromatogr. B.* **2006**, *831*, 274-280.
(105) Gygi, S. P.; Rist, B.; Gerber, S. A.; Turecek, F.; Gelb, M. H.; Aebersold, R. *Nat. Biotechnol.* **1999**, *17*, 994-999.
(106) Casetta, B.; Daniels, S.; Stanick, W. A.; Cox, D.; Nimkar, S.; Cardenas, J.; Gamble, T. N. *Clin. Biochem.* **2006**, *39*, 1099-1099.
(107) O'Maille, G.; Go, E. P.; Hoang, L.; Want, E. J.; Smith, C.; O'Maille, P.; Nordstrom, A.; Morita, H.; Qin, C.; Uritboonthai, W.; Apon, J.; Moore, R.; Garrett, J.; Siuzdak, G. *Spectr.-Int. J.* **2008**, *22*, 327-343.
(108) Yang, W. C.; Adamec, J.; Regnier, F. E. *Anal. Chem.* **2007**, *79*, 5150-5157.
(109) Yang, W. C.; Regnier, F. E.; Sliva, D.; Adamec, J. *J. Chromatogr. B.* **2008**, *870*, 233-240.
(110) Yang, W. C.; Regnier, F. E.; Jiang, Q.; Adamec, J. *J. Chromatogr. A.* **2010**, *1217*, 667-675.
(111) Tsukamoto, Y.; Santa, T.; Yoshida, H.; Miyano, H.; Fukushima, T.; Hirayama, K.; Imai, K.; Funatsu, T. *Biomed. Chromatogr.* **2006**, *20*, 358-364.
(112) Tsukamoto, Y.; Santa, T.; Yoshida, H.; Miyano, H.; Fukushima, T.; Hirayama, K.; Imai, K.; Funatsu, T. *Biomed. Chromatogr.* **2006**, *20*, 1049-1055.
(113) Lamos, S. M.; Shortreed, M. R.; Frey, B. L.; Belshaw, P. J.; Smith, L. M. *Anal. Chem.* **2007**, *79*, 5143-5149.
(114) Fukusaki, E. I.; Harada, K.; Bamba, T.; Kobayashi, A. *J. Biosci. Bioeng.* **2005**, *99*, 75-77.
(115) Shortreed, M. R.; Lamos, S. M.; Frey, B. L.; Phillips, M. F.; Patel, M.; Belshaw, P. J.; Smith, L. M. *Anal. Chem.* **2006**, *78*, 6398-6403.
(116) Abello, N.; Geurink, P. P.; van der Toorn, M.; van Oosterhout, A. J. M.; Lugtenburg, J.; van der Marel, G. A.; Kerstjens, H. A. M.; Postma, D. S.; Overkleeft, H. S.; Bischoff, R. *Anal. Chem.* **2008**, *80*, 9171-9180.
(117) Huang, X.; Regnier, F. E. *Anal. Chem.* **2008**, *80*, 107-114.
(118) Koulman, A.; Petras, D.; Narayana, V. K.; Wang, L.; Volmer, D. A. *Anal. Chem.* **2009**, *81*, 7544-7551.
(119) Mashego, M. R.; Wu, L.; Van Dam, J. C.; Ras, C.; Vinke, J. L.; Van Winden, W. A.; Van Gulik, W. M.; Heijnen, J. J. *Biotechnol. Bioeng.* **2004**, *85*, 620-628.
(120) Kim, J. K.; Harada, K.; Bamba, T.; Fukusaki, E.; Kobayashi, A. *Biosci. Biotechnol. Biochem.* **2005**, *69*, 1331-1340.
(121) Hegeman, A. D.; Schulte, C. F.; Cui, Q.; Lewis, I. A.; Huttlin, E. L.; Eghbalnia, H.; Harms, A. C.; Ulrich, E. L.; Markley, J. L.; Sussman, M. R. *Anal. Chem.* **2007**, *79*, 6912-6921.
(122) Buscher, J. M.; Czernik, D.; Ewald, J. C.; Sauer, U.; Zamboni, N. *Anal. Chem.* **2009**, *81*, 2135-2143.
(123) Giavalisco, P.; Hummel, J.; Lisec, J.; Inostroza, A. C.; Catchpole, G.; Willmitzer, L. *Anal. Chem.* **2008**, *80*, 9417-9425.

(124) Giavalisco, P.; Kohl, K.; Hummel, J.; Seiwert, B.; Willmitzer, L. *Analytical Chemistry* **2009**, *81*, 6546-6551.
(125) Feldberg, L.; Venger, I.; Malitsky, S.; Rogachev, I.; Aharoni, A. *Anal. Chem.* **2009**, *81*, 9257-9266.
(126) Ye, T.; Mo, H.; Shanaiah, N.; Gowda, G. A. N.; Zhang, S.; Raftery, D. *Anal. Chem.* **2009**, *81*, 4882-4888.

Chapter 2: Development of a Method for the Profiling of the Carbonyl Metabolome by LC-MS.

2.1. Introduction

Metabolomics is a field of research concentrated on the comprehensive analysis of low molecular weight (< 1500 Da) endogenous small molecules (metabolites) in tissues and biofluids. The complete set of metabolites produced by an organism defines its metabolome. Metabolomics is playing an important role in defining complex biosystems, as well as providing a new approach for disease biomarker discovery and diagnosis. An ideal metabolomic study would provide a comprehensive and quantitative overview of the metabolic state of an organism.[1-3] However, due to the great diversity in physiochemical properties of metabolites, the presence of metabolites over extended concentration dynamic ranges, and the sheer number of metabolites which are present in a biosystem, a universal detection of all metabolites is extremely challenging. Mass spectrometry (MS) has emerged as the foremost technology for comprehensive endogenous metabolite profiling. MS-based metabolomics has become popular for the wide dynamic range that can be achieved, the ability to detect a diverse number of metabolites of varying molecular complexities, and the ability to perform highly reproducible quantitative analysis. In combination with liquid chromatography (LC) separation and electrospray ionization (ESI), thousands of metabolites can be separated and then ionized with minimal ion suppression, as a result of the decrease in analytes competing for gas phase ion production and entrance into the MS. LC-MS based platforms have become an increasingly important tool for metabolome profiling.[4, 5]

However, despite the analytical power of LC-MS for comprehensive metabolomics, the extreme complexity and dynamics of a metabolome results in challenges in the detection and quantitation of all of the metabolites. A strategy that can be used to overcome the issue of metabolite diversity is to fractionate a metabolome into many sub-metabolomes with each consisting of the metabolites

which share a common functional group (e.g., all carbonyl-containing metabolites or carbonyl metabolome). Then each sub-metabolome can be profiled using a reagent to selectively react with the metabolites containing specific functional groups, followed by optimized LC-MS analysis tailored for the identification and quantification of the targeted metabolites. By compiling the results from the analyses of these sub-metabolomes a more complete profile of a whole metabolome may be obtained. Our research goal uses this analytical strategy of selectively labeling the metabolites of sub-metabolomes which contain specific chemical moieties, followed by LC-MS analysis for identification and quantification. The reagents developed are not only highly specific to the targeted classes of metabolites but also developed to vastly improve the performance of LC separation and MS detection for the labeled metabolites. Sub-metabolomes currently profiled in our research group include the amine metabolome[6], the amine and phenol metabolome[7], the carboxyl metabolome[8], and on-going research into the profiling of the acylcarnitine and acylglycine[9] sub-metabolomes. This chapter presents the development and application of a technique for the selective labeling and profiling of the carbonyl metabolome via LC-MS.

A metabolome is identified to be the complete set of metabolites in an organism.[10] In terms of metabolomics, an organism or biosystem is composed of sub-sets of tissues and biofluids. For comprehensive metabolome coverage, the biosystem must be broken down into its constituent tissues and biofluids and each be profiled individually. Human urine and blood are clinically important biofluids and have been the most commonly used biofluids for diagnostic testing. Both urine and blood are highly complex and their comprehensive quantitative profiling is important for defining the human metabolome and for expanding biological and clinical studies and tests. Urine is popular for metabolomic studies and was chosen for this study as its collection is non-invasive, presents the ability to collect multiple samples over time, and it is quite complex in molecular composition as revealed by previous studies. Sample preparation is relatively simple compared to other biofluids, such as plasma or serum, but many considerations must be taken into account as previous studies show that there is

much variability between samples in the diversity of the metabolites present as well as the dynamic range (> 9 orders of magnitude).[11] These factors, among others, present a challenge in the complete characterization of the human urinary metabolome. A recent study by Want, et al. presents considerations and a protocol for the global profiling of the urinary metabolome via ultra performance-LC-MS (UPLC-MS).[11] The conditions chosen for their study balance metabolome coverage but do not provide full coverage of the complex urinary metabolome. A recent review by Ryan, et al. further highlights challenges and progress made in measuring the complete human urinary metabolome.[12]

Blood is another popular biofluid for metabolomic studies as a result of its clinical importance and its metabolite-rich composition. Blood consists of a cellular component, the blood cells and platelets, and a liquid carrier, plasma, which accounts for ~ 50 % of the volume of this biofluid. Metabolomic studies profile the metabolites found in the plasma or the serum. Plasma is the liquid supernatant obtained from blood following treatment with an anti-coagulant and centrifugation. Serum is obtained as the supernatant liquid where an anti-coagulant is not used and blood is allowed to clot and then is centrifuged. Plasma and serum are believed to be similar at the molecular level, however plasma lacks the proteins involved in clotting, such as fibrinogen and prothrombin. Comprehensive profiling of the human serum metabolome has been of interest and Wishart, et al. have recently published the results of a quantitative study in which they were able to identify 4229 metabolites in human serum which displays the vast complexity of this biofluid; but many of them identified were lipids and lipid metabolites.[13]

Full coverage of the human carbonyl metabolome in tissues and biofluids has not been achieved and presents a challenge analytically as these small molecules are often quite polar and often thought to be present at very low concentrations making them difficult to detect sensitively and quantify accurately. Analytical derivatization has been a requirement for the analysis of ketones and aldehydes in biofluids both by GC-MS and LC-MS. Previously published studies often target only one or a few specific carbonyls in the urine or plasma for

monitoring as indicators of a disease state. Targeted studies of a few ketones in urine and blood have been performed using techniques such as selected ion flow tube MS (SIFT-MS)[14], solid phase microextraction (SPME) GC-MS[15, 16], and LC-MS/MS[17], in combination with analyte derivatization. The majority of the interest in the quantitative profiling of ketones is for disease biomarker discovery or detection. Acetone has been regarded as a biomarker of diabetes[18], and there is interest to correlate high concentrations of other ketones with the disease states or other physiological conditions. Aldehydes are of interest as they are found in the metabolome as by-products of the oxidation of various macromolecules such as proteins, DNA, and lipids. Radical induced oxidative stress in injured or dying cells is associated with various pathological conditions, such as cancer. Therefore the study of aldehydes in human biofluids has become popular and important for disease biomarker discovery. A widely accepted lipid peroxidation index is the measurement of the concentrations of malondialdehyde (MDA) in the urine or blood. Lipid peroxidation also produces a great variety of other aldehydes species such as alkanals, alkenals, hydroxyl-alkenals, and alkadienals. Previous studies of select derivatized aldehydes in biofluids have been performed using techniques based on variations of GC-MS[19], LC-UV[20], and LC-MS/MS[21, 22].

In our studies we have developed a method for the profiling of carbonyl-containing metabolites in human urine and plasma. This was based on the derivatization of these targeted metabolites with dansylhydrazine (DH). Significant improvement of RPLC properties and enhancement of LC-MS signals of carbonyl containing metabolites have been achieved using this method. Further enhancement of sensitivity and high resolution and accuracy was obtained by analyzing the derivatized biofluids using nLC-nESI FT-ICR-MS.

Another challenge involved in comprehensive metabolome profiling is the data analysis. Metabolomics has greatly lacked in the electronic database equivalents to other "omics" fields, such as GenBank[23] for genomics or for example UniProt[24] for proteomics. This limitation makes dealing with the large amounts of data produced from comprehensive analyses of such complex samples very challenging and indeed places a bottle-neck in throughput and accuracy of

metabolome profiling experiments. With the release of the Human Metabolome Database (HMDB)[25, 26] and other related compound databases such as KEGG[27], LipidMaps[28], PubChem[29], ChEBI[30], MMCD[31], Metlin[32] and MassBank[33], metabolomics is evolving to become more quantitative and more complete in terms of human metabolome coverage. By specifically profiling the human carbonyl metabolome we had envisioned developing a metabolite database that could help in our own studies of human biofluids as well as to be made public as part of the HMDB in order to aid others in their data analysis and to enhance the overall coverage of the human metabolome. Of course, the technique developed herein should be applicable to the profiling of the metabolome of other biological systems such as mouse, plant, food, etc.

2.2. Experimental

2.2.1. Materials and Reagents

All chemicals, standards, and reagents were purchased from Sigma-Aldrich Canada (Markham, ON) except those otherwise noted. The following standards, given by HMDB accession number, were obtained from the Human Metabolite Library (HML): 00005, 00019, 00031, 00044, 00060, 00098, 00127, 00169, 00174, 00194, 00201, 00205, 00208, 00223, 00243, 00283, 00289, 00300, 00310, 00357, 00374, 00398, 00408, 00422, 00462, 00467, 00474, 00491, 00501, 00503, 00562, 00635, 00646, 00695, 00699, 00707, 00714, 00720, 00753, 00821, 00840, 00849, 00859, 00990, 01015, 01051, 01140, 01167, 01184, 01259, 01358, 01864, 01867, 01882, 01892, 01975, 02939, 03269, 03312, 03315, 03366, 03407, 03543, 03543, 04461, 05842, 05846, 05994, 06115, 06236, 11603, and 11623. LC-MS grade water, methanol (MeOH), and acetonitrile (ACN) were purchased from Fisher Scientific (Edmonton, AB, Canada). LC-MS grade formic acid (FA) and trifluroroacetic acid (TFA) was purchased from Sigma-Aldrich Canada (Markham, ON). Oasis hydrophilic-lipophilic balance (HLB) solid phase extraction (SPE) cartridges (30 mg, 1 mL) were purchased from Waters

Corporation (Milford, MA). Urine and blood samples were provided by a healthy individual.

2.2.2. Sample Pre-treatment and Dansylhydrazine Labeling Conditions

Stock solutions of standards were prepared in MeOH and stored at -20 ^{o}C prior to derivatization with DH. Urine was provided by a healthy individual that fasted for 12 consecutive hours overnight and during the morning. Urine collected was the second void volume of the day and during the fast only water was permitted to be consumed. Urine was cooled on ice for 20 min and was then mixed 1:1 with MeOH and centrifuged for 10 min at 4,000 rpm. Using a SpeedVac the volume of supernatant obtained was reduced back to the original volume of urine collected. Then 100 μL aliquots of this concentrated urine supernatant were taken to dryness using a SpeedVac and then stored at -80 ^{o}C prior to reconstitution in MeOH and derivatization with DH.

Blood was provided by a healthy individual that fasted (no food or water) for 12 consecutive hours overnight and during the morning. The blood was collected in tubes containing EDTA as the anti-coagulant (1.8 mg K_2EDTA per mL of blood) and was transported on ice. The blood was transferred from the EDTA tubes into 50 mL Falcon tubes that had been pre-cleaned with LC-MS grade MeOH and H_2O. In total ~ 200 mL blood had been collected. It was then centrifuged for one hour at 4,000 rpm resulting in ~ 100 mL of supernatant (plasma). 1 mL aliquots of plasma were then transferred to pre-cleaned 15 mL Falcon tubes. To each 1 mL aliquot, 0.5 mL of cold 0.1 % FA in ACN (-20 ^{o}C) was added and then kept at 4 ^{o}C for 30 min. This was repeated until a final volume of 4 mL of cold 0.1 % FA in ACN had been added. The tubes were then centrifuged for 10 min at 4,000 rpm. ~ 4.5 mL of supernantant was obtained from each tube and was diluted with LC-MS grade water to obtain a mixture that was ~ 20 % ACN. This mixture was then passed through Microcon molecular weight cut-off (MWCO) filters of 3,000 Da using a centrifuge at 10,500 rpm, 4 ^{o}C until complete. The filters had been pre-cleaned with LC-MS grade H_2O and the collection vials had been pre-cleaned with LC-MS grade MeOH and H_2O. The

filtrate was combined and then 1 mL aliquots of the filtrate were reduced to dryness using the SpeedVac and then stored at -80 ^{o}C prior to reconstitution in MeOH and derivatization with DH.

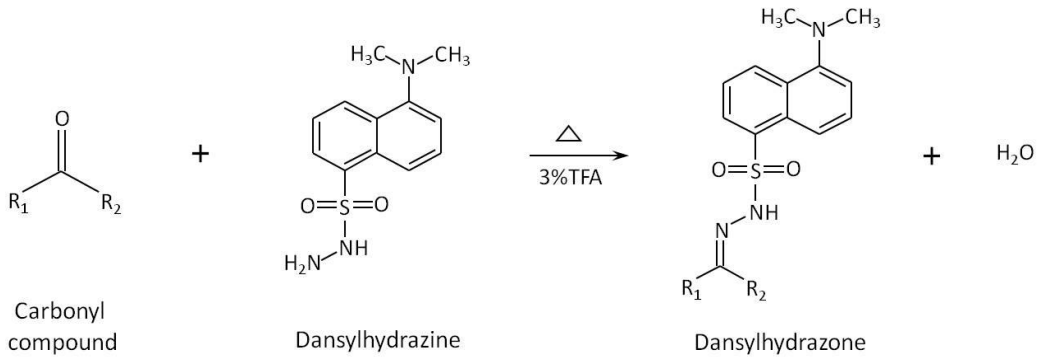

Figure 2.1. Dansylhydrazine labeling scheme.

Shown in Figure 2.1 is the reaction scheme for the labeling of carbonyl-containing compounds using dansylhydrazine (DH). This labeling protocol was applied to both standards and biofluids (i.e., urine and plasma). For derivatization, carbonyl standards solutions were prepared in MeOH and urine and plasma were reconstituted in 1 mL MeOH using sonication at room temperature and combined with 125 µL 3 % (v/v) TFA in MeOH and 125 µL 20 mM DH. The reaction mixtures were vortexed for 1 min and then centrifuged for 1 min at 14,000 rpm. The reaction was then allowed to proceed for one hour at 60 ^{o}C at 300 rpm in an Innova-4000 benchtop incubator shaker. After which, the mixture was again vortexed and centrifuged and then the reaction was quenched by cooling it at -20 ^{o}C, followed by evaporation of acid and solvent using a SpeedVac concentrator system. SPE using HLB Oasis cartridges was then performed separately on the DH labeled standards, urine, and plasma. The cartridges were conditioned with 5 mL MeOH, 1 mL H_2O and equilibrated with 1 mL of 10 % MeOH/H_2O. Labeled urine was reconstituted in 1.2 mL 10 % MeOH and loaded onto the SPE cartridge, the reaction vial was rinsed with 50 µL 10 % MeOH and loaded with the sample. The cartridge was then washed with 1 mL 40 % MeOH/H_2O and the dansylhydrazones were eluted with 1.2 mL MeOH. The labeled standards, urine

or plasma collected eluate was reduced to dryness using the SpeedVac concentrator system and stored at -80 ^{o}C overnight (or up to a week) if the analysis could not be performed immediately. The mixture was then diluted in the initial LC gradient mobile phase for injection and analysis by LC-MS. Figure 2.2 shows a summary of this labeling protocol for biofluids, urine and plasma.

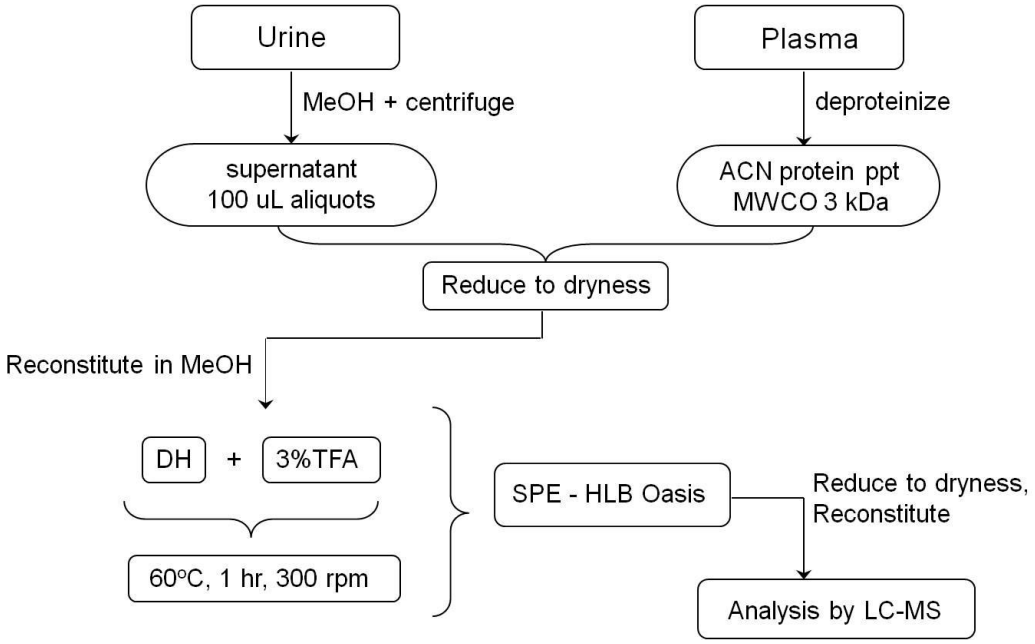

Figure 2.2. Overview of DH labeling procedure for biofluids.

2.2.3. LC Ion Trap MS Conditions

The HPLC system used was an Agilent 1100 series equipped with an auto sampler, binary pump, and degasser. The column used was an ACE C18 3 μm, 50 mm x 2.1 mm, 100 Å, column (Aberdeen, Scotland). The LC system was interfaced to the ESI source of a Bruker Esquire 3000plus quadrupole ion trap MS (Bruker, Bremen, Germany). LC mobile phase A was 0.1 % (v/v) LC-MS grade FA in LC-MS grade H_2O, and mobile phase B was 0.1 % (v/v) LC-MS grade FA in LC-MS grade ACN. The main binary gradient elution profile used for confirming DH derivatized standards was as follows: t = 0 min, 15 % B; t = 1 min, 15 % B; t = 5 min, 55 % B; t = 18 min, 100 % B; t = 22 min, 100 % B; t =

22.1 min, 15 % B; t = 26 min, 15 % B. The flow rate was 0.2 mL/min and the injection volume was 20 μL. The auto sampler was set at 4 ^{o}C and the column was at room temperature.

Using the Esquire 3000plus MS, all spectra were acquired in positive ion mode. MS source parameters include: capillary voltage 3500 V, end plate offset -500 V, nebulizer gas 20.0 psi, dry gas flow 6.0 L/min, and dry temperature 300 ^{o}C. Further MS settings include: skimmer voltage 40.0 V, capillary exit 118.0 V, octopole (1) DC 12.00 V, octopole (2) DC 1.70 V, octopole RF 125.0 Vpp, lens (1) -5.0 V, lens (2) -60.0 V, and trap drive 53.9. The scan range was set at 50 to 1000 m/z.

2.2.4. nLC-nESI FT-ICR-MS Conditions

The HPLC system used was an Agilent 1100 series capillary LC system with modified flow rate of 1.0 μL/min and equipped with manual injector, binary pump, and degasser. The column used was a Waters Xterra MS C18 3.5 μm, 150 μm x 150 mm, 125 Å, NanoEase column (Milford, MA). The LC system was interfaced to the nESI source of a Bruker 9.4 T Apex-Qe FT-ICR-MS (Bruker, Billerica, MA). The nESI tip used in the interface of the NanoEase column to the nESI source of the FT-ICR-MS was a New Objective PicoTip Emitter Silica Tip 30 ± 2 μm (Woburn, MA). LC mobile phase A was 0.1 % (v/v) LC-MS grade FA in LC-MS grade H_2O, and mobile phase B was 0.1 % (v/v) LC-MS grade FA in LC-MS grade ACN. The binary gradient elution profile was as follows: t = 0 min, 15 % B; t = 5 min, 15 % B; t = 12 min, 55 % B; t = 50 min, 100 % B; t = 65 min, 100 % B. The flow rate was 1.0 μL/min and the sample loop injection volume was 2.0 μL. nLC separation on column was performed at room temperature (which was monitored).

Using the FT-ICR-MS, all spectra were acquired in positive ion mode; the negative ion mode was found to be much less sensitive for the detection of the DH labeled metabolites. FT-ICR-MS spray chamber (nESI) parameters used include: capillary voltage 1800 V (typically), dry temperature 120 ^{o}C, and dry gas flow 2.0 L/min. Accumulation settings include: TD (Fid Size) 256 k, average spectra 2,

source accumulation time 0.0010 s, ion accumulation time 0.1 s, TOF (AQS) 0.0007 s, and DC extract bias voltage 0.7 V. Source optics settings include: capillary exit 240 V, deflector plate 250.0 V, funnel (1) 180 V, skimmer (1) 18.0 V, funnel (2) 6.1 V, skimmer (2) 5.0 V, hexapole DC 4.0 V, trap 20 V, and extract -10 V. Qh settings include: focus lens -100 V, entrance lens 1.8 V, entrance lens trap 4.7 V, entrance lens extract 20 V, DC extract bias 0.7 V, exit lens trap 22.0 V, and exit lens extract -12.0 V. Transfer optics settings include: accelerator (1) 45 V, high voltage -3000 V, vertical beam steer (1) 0.5 V, horizontal beam steer (1) 17.5 V, focusing lens (1) -160 V, focusing lens (2) -20 V, and focusing lens (3) -100 V. Analyzer settings include: side kick -12.7 V, side kick offset -1.8 V, excitation amplitude 4.00 dB, front trap plate 1.0 V, back trap plate 1.2 V, and analyzer entrance -4.0 V. The scan range was set at 86.62 to 800.00 m/z using broadband detection and spectra were acquired in chromatography mode with a run time of 65.0 min. The maximum resolution and transient length varied per instrument calibration but were typically 28000 (at m/z 400) and 0.0786 s, respectively.

2.3. Results and Discussion

2.3.1. Dansylhydrazine Derivatization

Detection of ketones and aldehydes in biological fluids by LC-MS is a challenging task as these analytes are not ionized efficiently in ESI and suffer from ion suppression effects resulting from the complexity of the sample. In this work, labeling chemistry was developed to overcome these effects, allowing for reliable quantification of the carbonyl metabolome using LC-MS. The choice of DH as the labeling reagent was based on well-studied derivatization chemistry, which was found to be both simple and robust.

DH derivatization is an acid catalyzed reaction which converts carbonyls into dansylhydrazones (shown in Figure 2.1 and 2.3). Careful optimization of the reaction conditions was carried out. Since DH labeling is an equilibrium reaction, an excess of reagent was used in order to help force the reaction to completion.

Optimal product formation was obtained in the presence 1 – 5 times molar excess of DH reagent. Also, since water is a reaction by-product, and both DH and the derivatives are susceptible to hydrolysis in the presence of water yielding dansylsulfonic acid (see Figure 2.3), the elimination of water from the reaction was desirable in order to help drive the labeling reaction to completion.

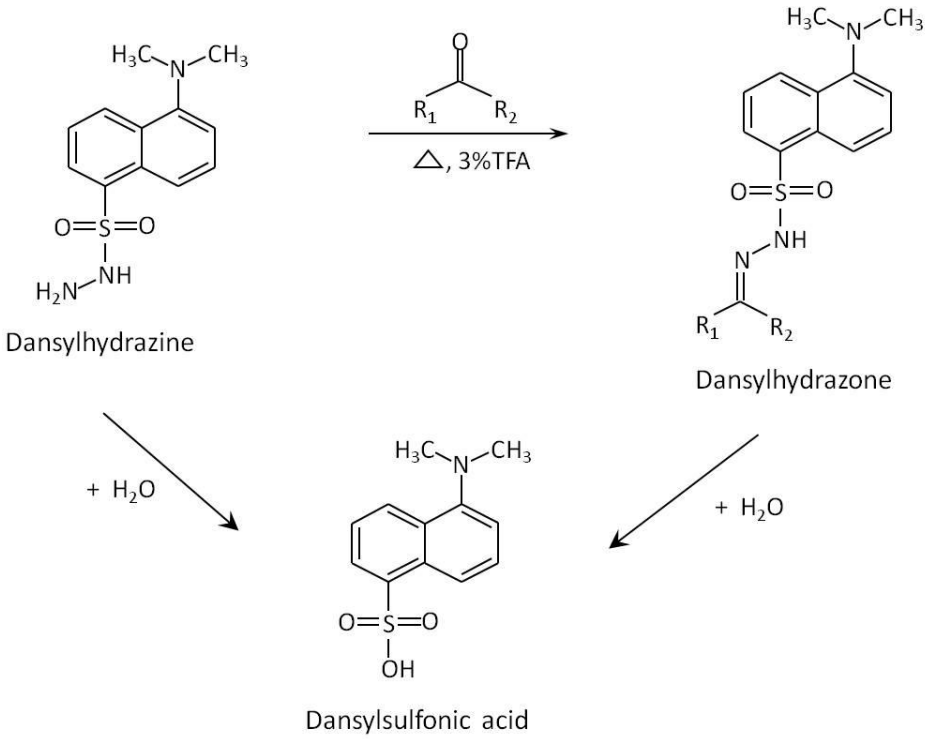

Figure 2.3. Reaction scheme for DH derivatization of carbonyls and the formation of hydrolysis degradation products.

The DH derivatization has been previously reported as being sensitive to water, as the reagent and product can undergo hydrolysis as outlined in Figure 2.3. Therefore, in this study it was chosen to perform the reaction in non-aqueous solvent phase.[34-36] A variety of organic solvents were tested with the reaction to determine which solvent would allow for the greatest amount of product formation. These included acetone, acetonitrile, methanol, ethanol and isopropanol. Since biofluids are aqueous, considerations had to be made for the removal of water from samples in order to allow for optimal product formation.

Urine was chosen as the example biofluid and aliquots of urine were reduced to dryness and the solvents were also tested based on their ability to reconstitute dried urine concentrates. Dansylhydrazone formation follows the mechanism of imine derivative formation and therefore it is expected that a protic solvent such as an alcohol would be preferred over the use of an aprotic reaction solvent such as acetone and acetonitrile, as was observed. Note that acetone reacts with the labeling reagent, thus consuming the reagent during the label reaction; which is another reason that acetone is not a good solvent. The alcohols performed comparably as the reaction solvent, with methanol giving only a slightly higher product yield. Methanol has the highest dielectric constant of the alcohols tested (ε = 33, at 25 ^{o}C) and therefore has the greatest ability to solvate (insulate) charges during the reaction which helps to stabilize the charged species formed as reaction intermediates and aids in the completion of the reaction. Methanol was also preferable for urine reconstitution and therefore was the solvent of choice for performing the carbonyl labeling. Methanol seems to be the most highly reported solvent used by others who have previously performed this reaction on carbonyl compounds in solution phase.[34, 37]

The stability of DH in different compositions of aqueous and organic solvent (MeOH) was also evaluated in order to judge the solvent's suitability, for instance to judge if aqueous mobile phase during RPLC or wash steps during SPE would have a significant effect on the samples. The tested compositions were 1 mM DH in 10 %, 30 %, 50 %, and 70 % MeOH in water. By LC-MS, measured peak area deviation of DH was less than 10 % for the compositions tested (see Figure 2.4.). The samples were stored in a -20 ^{o}C freezer and then re-analyzed on a third day. The peak area deviations were less than 6 % of those measured on the first day indicating sufficient reagent stability for aqueous LC conditions. Note that the deviations observed did show a trend of increasing slightly with increasing aqueous composition and with storage showing slight susceptibility towards hydrolysis, however minimal. It was also observed that if DH was stored at -20 ^{o}C in a solution of the initial gradient composition, 15 % ACN in H_2O + 0.1 % FA, ready for injection for LC-MS analysis, for a period of two weeks, that the

DH would completely react with the FA forming the respective dansylhydrazone. No shift in retention time was observed for DH and DH labeled FA; however, the MS shows the conversion of DH (m/z 266) to yield this by-product (m/z 294). Therefore derivatized samples were either analyzed directly following the derivatization procedure or stored in a -80 ^{o}C freezer in the concentrated, neutral form and were then reconstituted immediately before LC-MS analysis in order to keep product degradation and by-product formation at an absolute minimum.

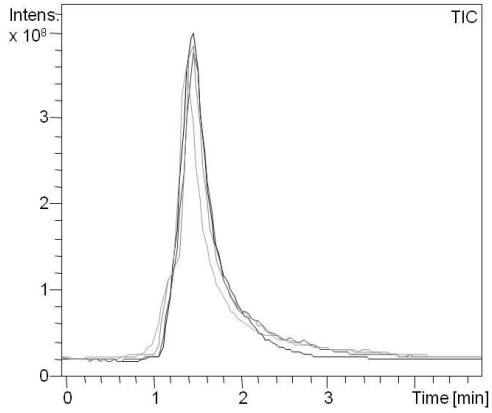

Figure 2.4. Overlaid total ion chromatograms (TICs) of DH prepared in 10, 30, 50 and 70 % MeOH, showing a peak area deviation < 10 %.

Since the labeling reaction is acid-catalyzed, the reaction conditions were also optimized for choice of acid. Acids tested include hydrochloric acid, acetic acid, trichloroacetic acid (TCA), trifluoroacetic acid (TFA) and trifluoromethanesulfonic acid (TFMSA). Different concentrations and ratios of acid prepared in methanol were evaluated for product formation such as 4 % acetic acid, 65 % HCl, 3 % TCA, 3 % TFA, 9 % TFA, 3 % TFMSA, and 9 % TFMSA. It was found that 3 % TFA and 3 % TFMSA resulted in the greatest dansylhydrazone formation as evaluated by peak area comparison from LC-MS analyses performed on each of the labeled standard test samples. TFMSA was found to be impractical for use and storage due to the exothermic reaction it undergoes when added to polar solvents, as well as for the formation of triflates and other by-products that occur in the presence of methanol and the high

reactivity displayed in the presence of atmospheric moisture. Therefore, TFA was chosen as the acid catalyst for the derivatization.

Reaction time and temperature were tested and 60 min at 60 ^{o}C was found to be optimal. In order to test the reaction time required, a test sample was prepared by forming a mixture of ten aldehyde standards, 0.2 mM (CH_2O – $C_{10}H_{20}O$) in MeOH and then monitored for product formation by LC-MS at 0, 20, 40, 60, and 80 min following the addition of the acid catalyst, 3 % TFA, and the reagent, DH, in triplicate. As shown in Figure 2.5 optimal product formation was observed at a reaction time of 60 min. Note that the reduced yield observed at 80 min is most likely due to the degradation of the reagent and derivatized products as a result of side reactions, such as hydrolysis as shown in Figure 2.3. At a reaction temperature of 60 ^{o}C, product formation as a measure of peak area was, on average, observed to be at least 5 % greater than the same reaction performed at room temperature. Therefore it was determined that the greatest yield of dansylhydrazones was obtained when the reaction was carried out for one hour at 60 ^{o}C.

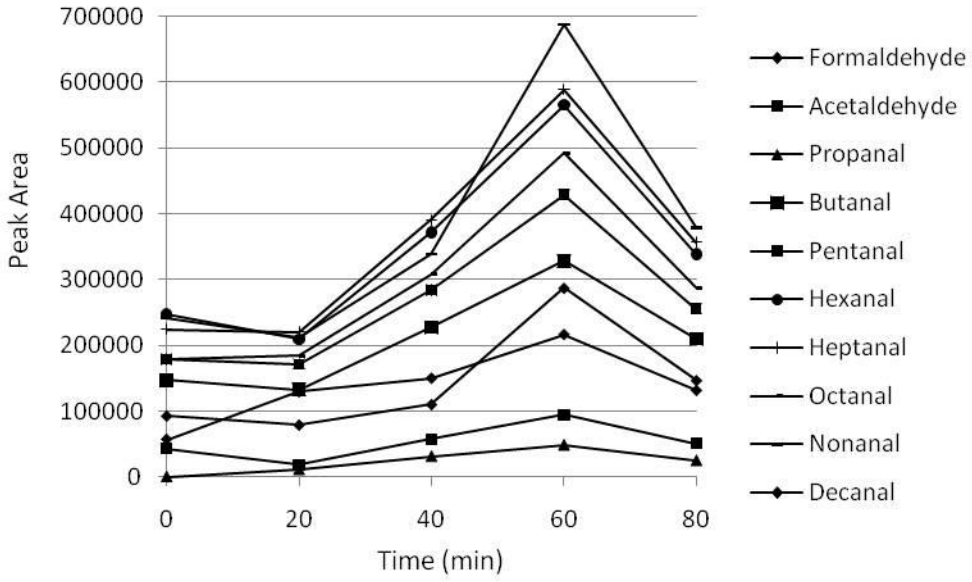

Figure 2.5. LC-MS peak area of DH derivatized aldehyde standards monitored during the course of the reaction to show the effect of reaction time on yield.

Following derivatization, the reaction must be quenched. This is usually preferred to be achieved by the addition of a chemical to consume the remaining excess of reagent. This was sought to be done by using an exogenous carbonyl as the quencher which would elute from the column in a region where it would not interfere or co-elute with labeled sample analytes. However, due to the wide range of endogenous metabolites expected and observed in the biofluid samples such a quencher could not be found. Therefore, the reaction was quenched by cooling at -20 ^{o}C and acid catalyst was removed by reducing the reaction mixture to dryness and then complete TFA removal was accomplished during the solid phase extraction (SPE) clean-up of the labeled samples.

Removal of the acid from the labeled samples also seems to be key in the prevention of product isomer formation.[38] The dansylhydrazone product is an imine (Schiff base) derivative which is obtained from the reaction of a carbonyl compound with a primary amine, DH. Formation of the dansylhydrazone proceeds by the protonation of the carbonyl group of the analyte, followed by nucleophilic addition of the hydrazine N to the C=O bond of the carbonyl analyte resulting in an alcohol intermediate (a hemiaminal). Further protonation of the intermediate results in a 1,2-elimination dehydration forming the C=N bond to yield the dansylhydrazone product. The proposed mechanism for the acid-catalyzed dansylhydrazone formation is shown in Figure 2.6. Isomerization can occur about the C=N bond of the hydrazone, with the E-isomer being formed predominantly over the Z-isomer. When both E- and Z- geometric stereoisomers are observed chromatographically, the E-isomer is later eluting as it is able to interact more freely with the stationary phase.[35, 39] Formation of the Z-isomer was reduced or eliminated by removal of traces of strong acid and water from the samples and by the use of a C18 RPLC column for analysis.[38]

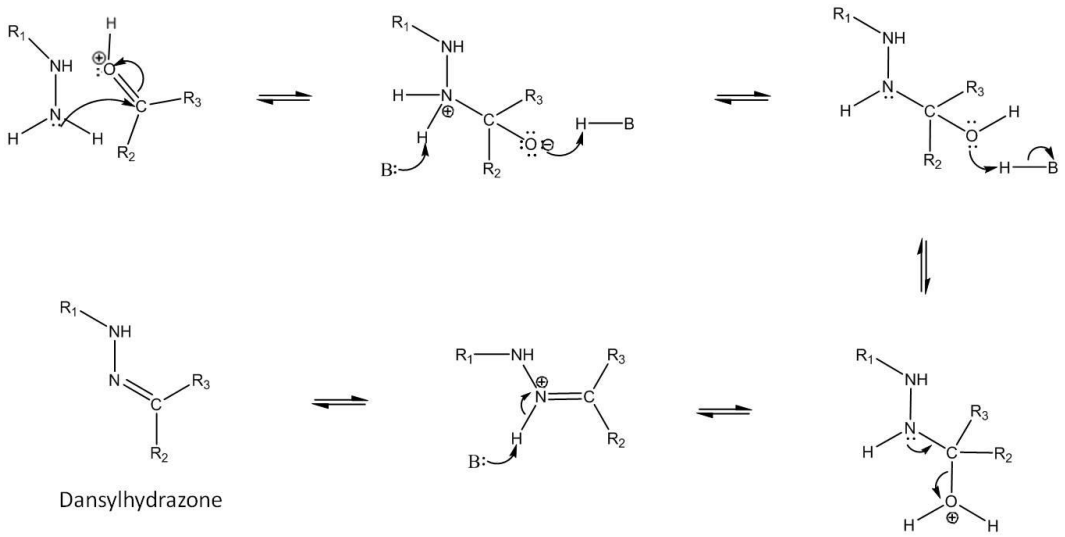

Figure 2.6. Proposed mechanism for acid-catalyzed dansylhydrazone formation. Where R_1 = dansyl group ($C_{12}H_{12}NO_2S$), R_2 and R_3 = any alkyl group, B: = base or any species in the solution that is capable of removing a proton, and H-B = acid or any species in the solution that is capable of donating a proton.

Intra-day and inter-day repeatability of the labeling method was evaluated on a set of standards and a urine sample; deviation was found to be less than 7 %. A mixture of nine aldehyde standards were derivatized with DH in the presence of 3 % TFA in triplicate. LC-MS was used to analyze the derivatized standard mixtures by peak area on the first day (intra-day) and then for three consecutive days (inter-day). The labeling reproducibility as a measure of the percent relative standard deviation (% RSD) is given in Table 2.1.

Table 2.1. Overall DH labeling reproducibility calculated based on three intra-day repeated labeling experiments and three inter-day repeated labeling experiments using peak area from LC-MS analyses.

Labeled Standard	Reproducibility (% RSD)
Formaldehyde	6.0
Butanal	3.9
Pentanal	4.6
Hexanal	3.2
Heptanal	5.5
Octanal	6.6
Nonanal	6.4
Decanal	5.1
Undecanal	2.7

Solid phase extraction (SPE) was used to help achieve labeled sample clean-up and concentration. SPE was found to be useful in the enrichment of the labeled analytes in complex biofluid samples without concentrating the interfering matrix components, such as salts in the case of urine, and lipids in the case of plasma. Signal response and sensitivity are improved by the minimization of ion suppression resulting from the matrix and the reduction of co-elution of interferants and tagged analytes. Also with the use of the nLC column chosen for the DH labeling studies, an appropriate guard column was unavailable and therefore the use of SPE to clean-up the samples prior to nLC-MS analysis was desirable in order to help extend the column lifetime.

Two different reversed phase (RP) SPE chemistries were investigated for their ability to retain, recover, and improve the detection of labeled biofluid carbonyls. The two SPE cartridges tested were the 1 cc Agilent AccuBOND ODS C18, a traditional silica-based C18 sorbent, and the 1 cc Waters Oasis HLB, a new class of RP sorbent. The Agilent AccuBOND ODS C18 is packed with reversed phase, octadecylsilane, bonded silica sorbent suitable for both polar and non-polar neutral, weakly acidic, and weakly basic analytes. The Waters Oasis HLB consists of a hydrophilic-lipophilic balanced RP hydrophobic, polymeric sorbent made of

poly(divinylbenzene-co-N-vinylpyrrolidone) suitable for a broad chromatographic polarity range of acids, bases, and neutrals.

To develop an optimized SPE protocol for the labeled samples, the load and washes were examined for breakthrough and premature elution of analytes of interest. Careful optimization of the load and wash solvents was performed. With the conditions set as 5 mL MeOH followed by 1 mL H_2O as cartridge conditioner, 1 mL 10 % MeOH/H_2O for equilibration, then loading of the sample in 1.2 mL 10 % MeOH/H_2O and washing with 1 mL 40 % MeOH/H_2O, no labeled analytes of interest were found in the collected load or wash from labeled standards, urine, and plasma as monitored by LC-MS (see Figure 2.7). Note that unlabeled and labeled urine and plasma loads and washes were compared and no components of interest were lost. When reconstituting derivatized samples for SPE loading, it is best to first add the 120 μL of MeOH and vortex/sonicate the sample well prior to the addition of the 1080 μL of H_2O immediately before sample loading in order to ensure complete reconstitution of the sample and minimize sample loss and degradation. This is important for the more hydrophobic carbonyls as it was observed during optimization experiments that with increasing carbon chain length there was an decrease in the reproducibility, which was improved by reconstituting the samples as described rather than just immediately vortexing in 10 % MeOH/H_2O. This reproducibility was also improved by reconstituting the concentrated SPE elute for LC-MS analysis in ACN rather than MeOH, as ACN is a stronger solvent.

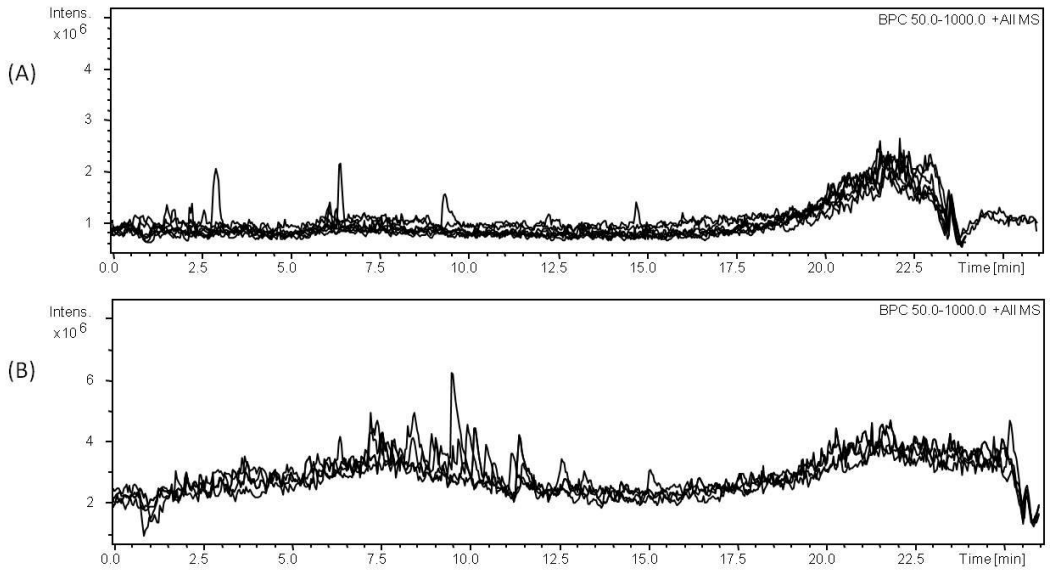

Figure 2.7. (A) Overlaid base peak ion chromatograms (BPCs) of the SPE load and wash collections of a sample blank (MeOH + 3 % TFA), an SPE blank (H_2O), and a set of ten DH derivatized carbonyl standards. The three low intensity peaks observed were identified in the load collections of the sample and SPE blanks, m/z 475, and is believed to be a minor SPE contaminant. (B) Overlaid BPCs of the SPE load and wash collections of DH derivatized urine and plasma. There is high background noise in parts of the chromatograms and no real peaks observed. A blank injection of 15 % ACN in H2O + 0.1 % FA was also included to show LC-MS background in both (A) and (B).

Performance of the ODS C18 cartridge and the Oasis HLB SPE cartridges were compared by analyzing a mixture of labeled carbonyl standards that differed in their sample preparation only by the type of SPE cartridge used, either ODS or HLB. It was found that SPE performed using the Oasis HLB cartridge most often yielded higher recovery of the derivatized analytes than observed with the AccuBOND ODS C18 cartridge. For two test samples of derivatized carbonyl standards (set 1: oxoglutaric acid, α-ketoisovaleric acid, butanal, 2-pentanone, 4-heptanone, nabumetone, octanal, and nonanal (see Figure 2.8.) and set 2: acetoacetic acid, 3-hydroxybutyric acid, androsterone, methyl propenyl ketone, 3-hexanone, daidzein, 3-methyl-2-oxovaleric acid, and benzaldehyde), HLB gave

on average a 20-25 % greater recovery than ODS. Observed exceptions included oxoglutaric acid and benzaldehyde which showed improved recovery with the ODS cartridge.

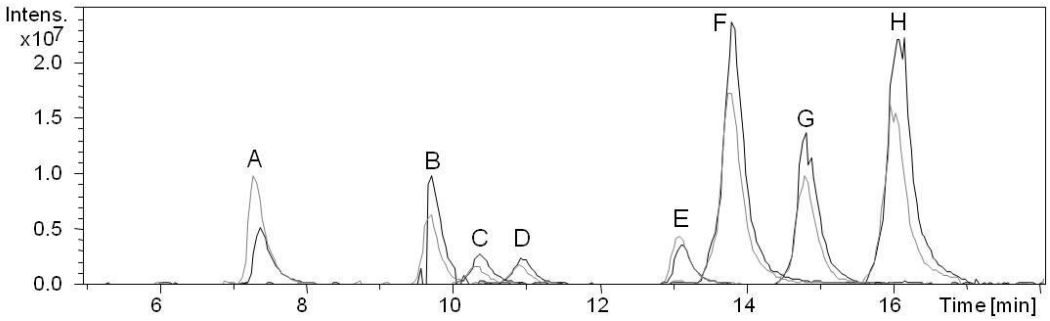

Figure 2.8. Overlaid extracted ion chromatograms (EICs) of eight DH labeled standards acquired via LC-MS (Esquire 3000plus) where the SPE cartridge used is Oasis HLB shown in black and AccuBOND ODS C18 in grey; A = oxoglutaric acid, B = α-ketoisovaleric acid, C = butanal, D = 2-pentanone, E = 4-heptanone, F = nabumetone, G = octanal, and H = nonanal.

Since the use of the HLB cartridge yielded a superior overall performance, it was the SPE cartridge type chosen for use with the method. Other advantages of the HLB Oasis SPE cartridge include that it is stable upon exposure to a wide range of pH 0 – 14. Therefore, if there is residual TFA present in a sample, then the low pH of such a sample would not affect the performance of the sorbent. Another benefit is that the cartridge sorbent bed can run dry without affecting recovery. This allowed for a more reproducible SPE technique and helped to reduce the drying time required using the SpeedVac, by drying the sorbent bed under vacuum prior to elution with methanol. Compared to traditional silica-based C18 sorbents, such as the AccuBOND ODS, there are no unfavorable silanol interactions, the sorbent exhibits a good retention capacity for a broader range of compound polarities, and there is a three times higher retention capacity for hydrophobic compounds, which is desirable as DH derivatized carbonyls are relatively hydrophobic.

2.3.2. Chromatography Improvement and ESI Signal Enhancement

Metabolites display a large diversity of chemical structures and chemophysical properties, and biofluids usually consist largely of very polar components. The detection of ketones and aldehydes containing metabolites in human biofluids has been considered in the past to be a challenging task as these analytes are poorly separated by RPLC as a result of their polarity and suffer from ion suppression effects resulting from the complexity of the sample matrix. Through the use of DH labeling and analysis by LC-MS, such effects have been minimized by altering the chromatographic retention behavior of these often very polar metabolites and improving the ESI responsiveness of these analytes, making quantitative detection of carbonyl metabolites in a variety of human biofluids possible.

Figure 2.9 shows the base peak ion chromatograms (BPCs) for equimolar amounts of the unlabeled versus labeled standards (2 μM) (panel A), unlabeled versus labeled urine (panel B), and unlabeled versus labeled plasma (panel C). It is clearly observed that with equal injection amounts, the overall ion intensity of the DH labeled analytes is much greater than for that of unlabeled standards and plain urine and plasma. There are several important features of the DH labeling for improved carbonyl metabolite identification and quantification.

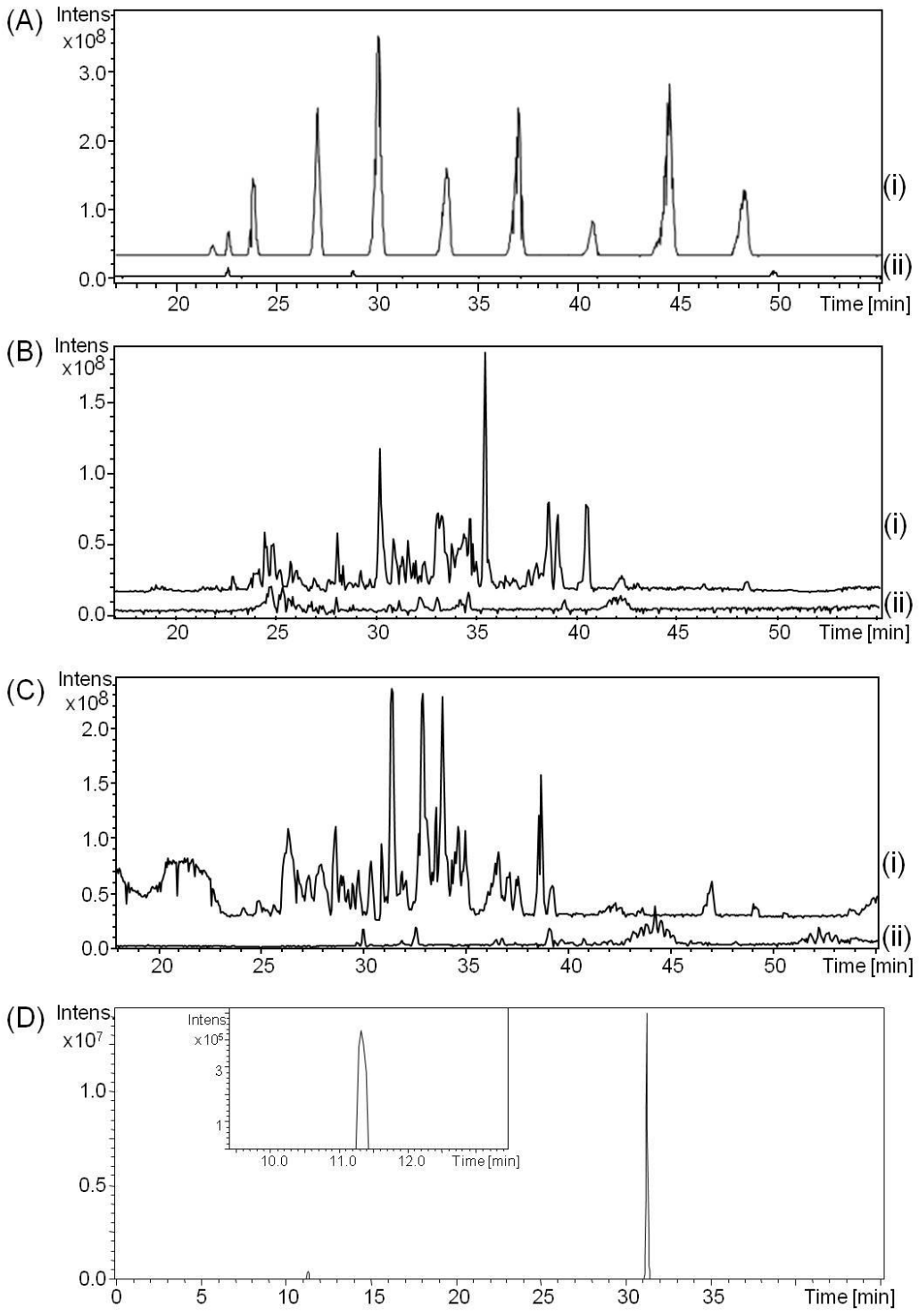

Figure 2.9. (A) BPCs of (i) mixture of nine DH labeled aldehydes and (ii) the same mixture of nine unlabeled aldehydes obtained by nLC FT-ICR-MS. (B) BPCs of (i) DH labeled human urine and (ii) the same amount of unlabeled human urine obtained by nLC FT-ICR-MS. (C) BPCs of (i) DH labeled human

plasma and (ii) the same amount of unlabeled human plasma obtained by nLC FT-ICR-MS. (D) Overlaid EICs of unlabeled phenylacetylglycine (11.3 min) and DH labeled phenylacetylglycine (31.2 min) (the expanded view of the EIC of the unlabeled standard is shown in the inset).

Some carbonyl compounds are very polar and not well retained on RPLC columns. One example is shown in Figure 2.9 of unlabeled and labeled phenylacetylglycine (panel D). Derivatization with DH improves the chromatographic properties by increasing the hydrophobicity of the analyte through the introduction of the relatively hydrophobic naphthalene moiety and hence improving both the retention and separation of the tagged analyte in RPLC. For example, the unlabeled standard was eluted at 11.3 min and after labeling the elution time was increased to 31.2 min, as shown in Figure 2.9 (D). Many of the unlabeled carbonyl standards were not retained on a C18 column and were eluted in the void volume and lost, such as for the unlabeled aldehyde standards which would correspond to the DH labeled standards in Figure 2.9 (Ai). With labeling, these standards of interest could be retained on a C18 column. The chromatographic peaks shown in Figure 2.9 (Bi) for the labeled urine sample are distributed across the entire gradient elution window, suggesting that the labeled carbonyls are well retained and separated in RPLC. Thus, there is no need to use other modes of separations, such as hydrophilic interaction chromatography (HILIC) which usually provides lower efficiencies than RPLC, to handle the very polar carbonyl metabolites in a complex mixture. This is important for high-throughput analysis, as switching columns and running the same sample in multiple modes can increase the overall analysis time.

Carbonyl compounds are also poorly ionized by ESI and the complexity of the biofluid matrix can result in undesirable ion suppression. The conversion of these carbonyls to their dansylhydrazone derivatives was found to improve the sensitivity by four to sixty-five fold (see Table 2.2). Two examples are shown in Figure 2.10 for propanal and nonanal. In comparing the analyte nESI-MS signal intensity before and after labeling, an enhancement factor of four and fifty-seven

was found for DH labeled propanal and nonanal, respectively. Note that unlabeled analytes see much greater ion suppression and may not even be fully converted into gas phase ions by ESI for introduction into the MS system for detection. The signal enhancement observed with labeling is mainly due to the increase in positive ion ESI surface activity of the analyte by the introduction of the easily ionized dimethyl amino moiety which makes it amenable for sensitive detection by mass spectrometry. Also by increasing the hydrophobicity of the carbonyl analyte through the introduction of the naphthalene moiety, the labeled compounds are eluted at a higher percentage of organic mobile phase which results in decreased droplet surface tension and an increased analyte droplet surface affinity. Generally as a result, if an analyte is chargeable, it is observed for the ESI process that hydrophobic analytes display greater electrospray response than analytes which are relatively polar.[40] Therefore labeled analytes are preferentially ionized or more readily ionized as they occupy a greater part of the droplet surface and are able to compete more favorably for space and charge on the droplet surface, with the majority of the analytes being converted to gas phase ions with successful delivery to the MS for detection.

Table 2.2. Enhancement factors observed for eight standards with DH labeling by nESI-MS. Where equimolar amounts (2 μM) of both unlabeled and labeled standards were infused into a nESI source, operating in the positive mode, of an FT-ICR-MS.

Standard	**$[M+H]^+$**	**Observed**		**DH Labeled $[M+H]^+$**	**Observed**		**Enhan-cement Factor**
		m/z	Intensity		m/z	Intensity	
Formaldehyde	31.02	31.36	9.1E+04	278.10	278.10	1.1E+06	**12**
Acetaldehyde	45.03	n.o.	-	292.11	292.11	6.8E+05	**-**
Propanal	59.05	59.07	3.1E+05	306.13	306.13	1.1E+06	**4**
Butanal	73.06	73.08	1.1E+05	320.14	320.14	6.9E+06	**65**
Pentanal	87.08	87.27	2.6E+05	334.16	334.16	8.2E+06	**31**
Hexanal	101.10	101.86	2.3E+05	348.17	348.17	3.0E+06	**13**
Heptanal	115.11	115.41	4.3E+05	362.19	362.19	3.5E+06	**8**
Octanal	129.13	n.o.	-	376.21	376.20	7.5E+06	**-**
Nonanal	143.14	143.10	1.7E+05	390.22	390.22	1.0E+07	**57**
Decanal	157.16	157.71	4.0E+05	404.24	404.24	2.3E+07	**57**

Note: n.o. = not observed

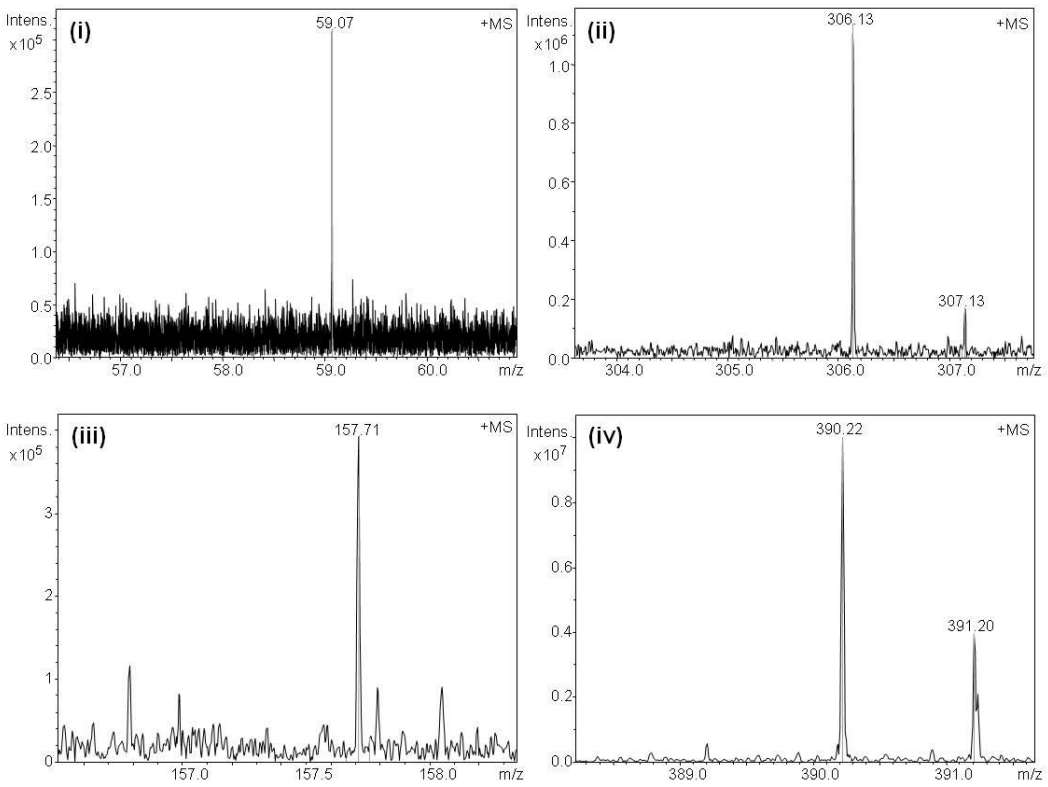

Figure 2.10. Positive nESI FT-ICR-MS of (i) propanal and (ii) DH labeled propanal, and (iii) nonanal and (iv) DH labeled nonanal, showing a four fold and fifty-seven fold ESI signal enhancement with derivatization, respectively.

Another benefit of DH labeling is the shifting of the mass-to-charge ratio of the derivatives out of the low mass region to above m/z 250 allowing for an improved signal-to-noise ratio as well, as interferences from common LC-MS contaminants and solvent clusters often found at the low masses is significantly reduced.

2.3.3. Dansylhydrazine Labeled Standard Library

Usually for "omics" based studies, profiling of a biofluid is carried out by searching analytical data, such as LC-MS results, against a database or a library of standards to identify putative metabolites. Such databases for metabolomics as the Human Metabolome Database (HMDB, http://www.hmdb.ca) have been in construction and seen rapid growth in the past few years. The HMDB contains

over 8000 endogenous human metabolite entries and offers a mass spectra search tool which can be used to identify possible metabolites based on their molecular weight or m/z data. The availability and usefulness of such databases is key for the expansion of metabolome coverage and allowing for the application of metabolomics studies to areas such as biomarker discovery. The data analysis step in untargeted metabolomics studies has long been the bottle-neck to the workflow as these types of studies can provide information on thousands of metabolites and the analysis of such complex data can be quite difficult. The use of metabolome databases and standard libraries greatly facilitates the assignment and identification of the many different compounds composing a metabolome.

By specifically profiling the human carbonyl metabolome we had envisioned developing a metabolite database that could help in our own studies of human biofluids as well as to be made public as part of the HMDB in order to aid others in their data analysis and to enhance the overall coverage of the human metabolome. Our interest was to profile as many carbonyl metabolites as possible, and therefore a variety of standards were chosen to examine the performance of the derivatization method. A DH labeled standard compound library consisting of eighty-one known compounds was constructed; see Table 2.3 for the list of standards and their compound classes. This library was used in the method development as well as profiling of human metabolites in biofluids; urine and plasma.

A wide range of endogenous carbonyl metabolites were chosen for the development of a library of DH derivatives, including ketones, aldehydes, unsaturated aldehydes, keto-acids, aromatic ketones and aldehydes, phenyl amides, steroids and sugars. Ketones, aldehydes, and keto-acids were derivatized using the described optimized DH labeling method. Typically the labeling yield was found to be greater than 90 %. All standards were stored at –20 ^{o}C to prevent degradation, except where storage conditions at 4 ^{o}C or room temperature were indicated by the supplier. There were several instances where labeling of a standard with DH following the optimized protocol was possible with freshly obtained standard but then was not possible on further tests due to believed

dimerization or polymerization of the standard on storage prior to derivatization (as is suspected to be the case for glyceraldehyde (Figure 2.11.), pyruvaldehyde, acrolein, dihydroxyacetone, and succinic acid semialdehyde, as noted in Table 2.3.). Therefore, further quantitative studies, beyond the initial qualitative studies, of these analytes in biological samples were not possible. Optimization of storage conditions for these standards is required in order to prevent polymerization.

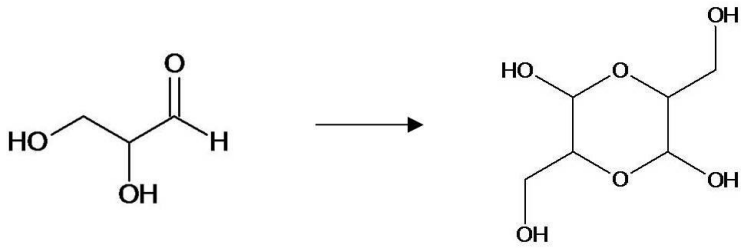

Figure 2.11. Dimerization of glyceraldehyde.

Only mono-derivatized products were observed in the case of compounds containing two or more carbonyl functional groups. The formation of multiply derivatized products has been previously reported for ketosteroids [41] and therefore potential standards, such as steroids and others, were analyzed to see if such products were being produced upon reaction with DH using the developed protocol. Progesterone, 17-hydroxyprogesterone, pyruvaldehyde, diacetyl, and succinylacetone were investigated for mono- and bis-derivatized products. However, for the labeling conditions used, bis-derivatives were not observed. This is likely due to steric hindrance present at the other sites on such compounds, for example for ketosteroids labeling at the 3-position is favorable over the sterically hindered 20-position. For succinylacetone, the labeling at the first position may sterically hinder the labeling reaction at the second position, preventing the formation of a bis-derivative.

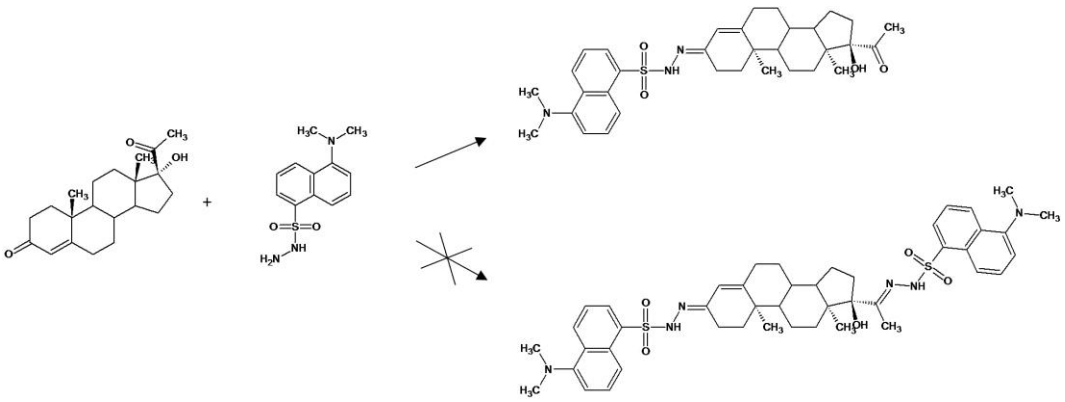

Figure 2.12. Reaction of 17-hydroxyprogesterone with excess DH reagent yields mono-derivatized product (above) and does not yield bis-derivatized product (below).

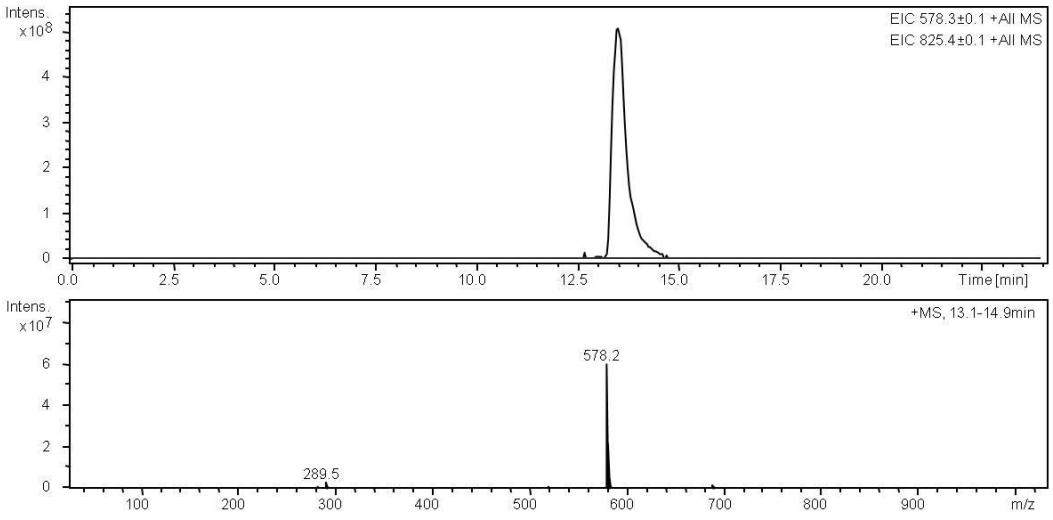

Figure 2.13. Overlay of EICs for mono- and bis-derivatives of DH labeled 17-hydroxyprogesterone. Observation of one mono-derivatized peak (m/z 578) in LC-MS confirms that only one isomer is formed and is believed to be the product that is labeled at the 3-position (shown in Figure 2.11.) rather than at the sterically hindered 20-position (not shown). Bis-derivatized product is not observed (m/z 825).

The labeling studies show that a hydroxy acid, 3-hydroxybutyric acid (3-HBA), was potentially labeled by DH, which is an unexpected result as it is not a carbonyl compound; rather it contains both hydroxyl and carboxylic acid functional groups. This reaction may have proceeded via acid catalyzed esterification of 3-HBA in the heated alcohol medium used. Protonation of 3-HBA at the C=O of the carboxyl group, activates the group for nucleophilic addition of the methanol. Further proton transfer within the intermediate results in a 1,2-elimination dehydration yielding the ester product, methyl 3-hydroxybutyrate. This is an equilibrium reaction and therefore is reversible; removal of water from the reaction as it forms will force the reaction to completion. Then aminolysis of the ester proceeds via the nucleophilic addition of dansylhydrazine to the ester and the 1,2-elimination yielding an amide and the alcohol, methanol. This reaction can be driven to completion by the presence of excess DH reagent and removal of the alcohol. The amide may be the product observed. The possibility of this reaction resulting in an appreciable yield is low since the two main reactions which must occur to obtain the product are performed under conditions in which the reverse reaction would be favored. Also this product is observed to co-elute with the excess DH peak. Hence this standard was used solely for qualitative purposes and requires further investigation as other similar compounds did not yield DH labeled products. It would be interesting if DH could be used to label 3-HBA as it is one of the three diagnostic ketone bodies produced during diabetic ketoacidosis, along with acetone and acetoacetic acid, which is why the standard was initially chosen for testing with DH labeling.

Phenyl amides, such as hippuric acid, and steroids such as androsterone could be labeled using this method, however in a few instances complete labeling of similar compounds was not achieved and therefore further optimization of the labeling method for these two metabolite classes is required. DH labeling of phenyl amide based compounds was investigated using the outlined DH labeling protocol with the following standards: benzamide, methylhippuric acid, 4-aminohippuric acid, salicyluric acid, nicotinuric acid, and hippuric acid. A phenyl amide is loosely defined here as any compound with adjacent amide and phenyl

functional groups. Both benzamide and methylhippuric acid showed no derivatized products following reaction with DH. 4-aminohippuric acid, salicyluric acid, nicotinuric acid, and hippuric acid showed a mixture of unreacted and labeled standard following reaction with DH, with 4-aminohippuric acid and nicotinuric acid reaction equilibrium favoring the reactants (unlabeled standard) and with salicyluric acid and hippuric acid reaction equilibrium favoring the products (labeled standard). It would seem from these observations that the formation of labeled products is favorable where the amide N is a secondary amine and there is an electron donating group in resonance with the carbonyl of the amide group. Further optimization of the labeling protocol may lead to complete derivatization of this class of compounds with DH. As for the complete labeling of steroids, it has been suggested in the literature that basic reaction conditions may be more favorable than the acidic conditions employed here with a longer reaction time.[42]

A variety of saturated and unsaturated aldehydes were chosen for investigation with DH labeling as they are a potentially important class of metabolites for disease biomarker studies. The polyunsaturated fatty acid groups of phospholipids are subject to oxidative attack by reactive oxygen species such as hydroxyl radicals, generated during normal cell processes, which gives rise to lipid aldehydes. An increase in radical production has been noted for a variety of vascular disorders and cancers which results in oxidative stress and can be monitored by the production of an elevated amount of lipid aldehydes and other products.[16] Where research in this area has been mainly focused on the monitoring of elevated concentrations of malondialdehyde, 4-hydroxnonenal, and 4-hydroxyhexenal, we chose to study other compounds including the C_1-C_{12} saturated aliphatic aldehydes, hydroxylated aldehyde, glyceraldehyde, as well as unsaturated aldehydes: acrolein, trans-2-hexen-1-al, trans, trans-2,4-decadienal, and cis-4-decenal. Labeling of these standards with DH was successful and useful for studies of biofluids. It was found that storage conditions were of particular importance for the unsaturated aldehydes pre-derivatization.

A variety of ketone and keto-acid standards were also tested for labeling with DH. There has been a rise in biomarker studies which show a connection between an increased production of ketones such as acetone and keto-acids such as acetoacetic acid in the biofluids of patients with conditions such as diabetes and a growing interest in identifying increased production of other saturated aliphatic ketones as indicators of diseased states such as cancer.[16] The standards successfully labeled with DH in our studies are listed in Table 2.3. Unsuccessfully derivatized standards are listed in Table 2.4.

Table 2.3. List of eighty-one standards composing the DH standard library.

Standard		Class	HMDB Accession #	DH labeled $[M+H]^+$	t_R (min)
1	Formaldehyde	Aldehydes	HMDB01426	278.09577	13.2
2	Acetaldehyde	Aldehydes	HMDB00990	292.11142	15.9
3	Propanal	Aldehydes	HMDB03366	306.12707	17.3
4	Butanal	Aldehydes	HMDB03543	320.14272	22.1
5	Pentanal	Aldehydes	-	334.15837	24.6
6	Hexanal	Aldehydes	HMDB05994	348.17402	27.3
7	Heptanal	Aldehydes	-	362.18967	30.3
8	Octanal	Aldehydes	HMDB01140	376.20532	33.7
9	Nonanal	Aldehydes	-	390.22097	37.4
10	Decanal	Aldehydes	HMDB11623	404.23662	40.8
11	Undecanal	Aldehydes	-	418.25227	44.5
12	Dodecanal	Aldehydes	-	432.26792	48.3
13	Glyceraldehyde	Aldehydes	HMDB01051	338.11690	11.3 */**
14	3-Methylbutanal	Aldehydes	HMDB06478	334.15837	24.2
15	Benzaldehyde	Aldehydes	HMDB06115	354.12707	24.4
16	Phenylacetaldehyde	Aldehydes	HMDB06236	368.14272	24.8
17	Pyruvaldehyde	Ketones/Aldehydes	HMDB01167	320.10634	*
18	Acrolein	Aldehydes	-	304.11142	*

19	trans-2-Hexen-1-al	Aldehydes	-	346.15837	23.0
20	trans, trans-2,4-decadienal	Aldehydes	-	400.20532	35.2; 36.2; 36.8
21	cis-4-Decenal	Aldehydes	-	402.22097	36.2
22	Retinal	Retinoids/ Aldehydes	HMDB01358	532.29922	63.7
23	Acetone	Ketones	HMDB01659	306.12707	17.0
24	2-butanone	Ketones	HMDB00474	320.14272	21.0
25	2-Pentanone	Ketones	-	334.15837	23.4
26	2-Hexanone	Ketones	HMDB05842	348.17402	25.7
27	3-Hexanone	Ketones	HMDB00753	348.17402	27.1
28	2-heptanone	Ketones	HMDB03671	362.18967	28.9
29	4-Heptanone	Ketones	HMDB04814	362.18967	28.4
30	3-Octanone	Ketones	-	376.20532	31.8
31	2-Nonanone	Ketones	-	390.22097	35.6
32	dihydroxyacetone	Ketones	HMDB01882	338.11690	*
33	Diacetyl	Ketones	HMDB03407	334.12199	26.6
34	Cyclohexanone	Ketones	HMDB03315	346.15837	22.8
35	Methyl propenyl ketone	Ketones	HMDB01184	332.14272	22.4
36	Ethyl isopropyl ketone	Ketones	HMDB05846	348.17402	26.3
37	Methyl isobutyl ketone	Ketones	HMDB02939	348.17402	25.2; 26.8
38	Pyruvic acid	Keto-Acids	HMDB00243	336.10125	12.5
39	2-Ketobutyric acid	Keto-Acids	HMDB00005	350.11690	17.1; 18.3
40	Acetoacetic acid	Keto-Acids	HMDB00060	350.11690	19.8
41	Succinic acid semialdehyde	Keto-Acids	HMDB01259	350.11690	*
42	3-Hydroxybutyric acid	Hydroxy-Acids	HMDB00357	352.13255	**
43	α-Ketoisovaleric acid	Keto-Acids	HMDB00019	364.13255	20.6
44	Methylacetoacetic acid	Keto-Acids	HMDB00310	364.13255	18.4
45	2-Oxovaleric acid	Keto-Acids	HMDB01865	364.13255	19.0; 19.7
46	Levulinic acid	Keto-Acids	HMDB00720	364.13255	19.4
47	3-Methyl-2-oxovaleric acid	Keto-Acids	HMDB00491	378.14820	20.2

48	2-Methyl-3-ketovaleric acid	Keto-Acids	HMDB00408	378.14820	22.3
49	Ketoleucine	Keto-Acids	HMDB00695	378.14820	20.4; 21.2
50	2-Ketohexanoic acid	Keto-Acids	HMDB01864	378.14820	20.8; 21.8
51	4-Hydroxyphenyl-pyruvic acid	Keto-Acids	HMDB00707	428.12747	16.5
52	Succinylacetone	Keto-Acids	HMDB00635	406.14312	11.7
53	Oxaloacetic acid	Dicarboxylic Acids	HMDB00223	380.09108	10.5
54	Oxoglutaric acid	Dicarboxylic Acids	HMDB00208	394.10673	9.5
55	3-Oxoadipic acid	Dicarboxylic Acids	HMDB00398	408.12238	15.4
56	2-Methylglutaric acid	Dicarboxylic Acids	HMDB00422	394.14312	9.7
57	(+)-Carvone	Monoterpenes/ Ketones	HMDB04487	398.18967	33.4
58	Nabumetone	Ketone	-	476.20024	30.9
59	Phenylpyruvic acid	Aromatic Acids/Ketones	HMDB00205	412.13255	21.1; 21.7
60	Nutriacholic acid	Bile Acids/Ketones	HMDB00467	638.36222	37.9
61	7α-hydroxy-3-oxo-5β-cholanoic acid	Bile Acids/Ketones	HMDB00503	638.36222	43.5
62	4-(Methylnitros-amino)-1-(3-pyridyl)-1-butanone	Ketones/Nitroso	HMDB11603	455.18599	29.2; 30.0
63	Androsterone	Ketosteroids	HMDB00031	538.30979	32.4
64	Progesterone	Ketosteroids	HMDB01830	562.30979	***
65	17-Hydroxyprogesterone	Ketosteroids	HMDB00374	578.30470	31.0
66	4-Aminohippuric	Acyl Glycines	HMDB01867	442.15435	***
67	Salicyluric acid	Acyl Glycines	HMDB00840	443.13837	17.9 ***
68	Nicotinuric acid	Acyl Glycines	HMDB03269	428.13870	***
69	Hippuric Acid	Acyl Glycines	HMDB00714	427.14345	15.7 ***
70	Phenylacetylglycine	Acyl Glycines	HMDB00821	441.15910	29.1
71	D-glucuronic acid	Carbohydrate	HMDB00127	442.12786	9.2
72	Lactose	Carbohydrate	HMDB00186	590.20142	12.5 ****
73	Galactose	Carbohydrate	HMDB00143	428.14860	14.4 ****
74	Glucose	Carbohydrate	HMDB00122	428.14860	12.9 ****
75	Fructose	Carbohydrate	HMDB00660	428.14860	18.0 ****
76	D-Mannose	Carbohydrate	HMDB00169	428.14860	18.7 ****

77	D-Xylose	Carbohydrate	HMDB00098	398.13803	15.0 ****
78	L-Arabinose	Carbohydrate	HMDB00646	398.13803	17.4 ****
79	D-Ribose	Carbohydrate	HMDB00283	398.13803	29.9 ****
80	L-Fucose	Carbohydrate	HMDB00174	412.15369	24.2 ****
81	L-Rhamnose	Carbohydrate	HMDB00849	412.15369	28.6 ****

* Standard is sensitive to storage conditions and/or polymerizes; derivatized product was observed on initial testing experiments using the LC-MS (Esquire 3000plus) for analysis but not on further derivatization testing when acquired using nLC-nESI FT-ICR-MS with gradient as given in the experimental. Standard stored at -20 ^{o}C degraded and/or polymerized, preventing labeling reaction on following attempts.

** Co-elution of derivatized standard with excess reagent peak prevented use of the standard for quantitation; for qualitative use only.

*** Inconsistent labeling of standard observed using normal protocol and therefore was not used for quantitation; for qualitative use only.

**** Derivatized using slightly modified reaction conditions and LC gradient, will be discussed further in Chapter 3.

Table 2.4. List of sixteen standards that were tested for labeling with DH and were not derivatized.

Standard		**Class**	**HMDB Accession #**
1	Menadione	Naphthoquinones	HMDB01892
2	Benzamide	Amino Ketones	HMDB04461
3	L-Ascorbic Acid	Hydroxy Acids	HMDB00044
4	Allantoin	Amino Ketones	HMDB00462
5	Anserine	Polypeptides	HMDB00194
6	Uric Acid	Purine Derivatives	HMDB00289
7	Sodium Pyruvate	Keto-Acid Salts	-
8	2,5-dimethylfuran	Furans	-
9	Methylhippuric acid	Acyl Glycines	HMDB00859
10	Creatinine	Amino Ketones	HMDB00562

11	Uracil	Pyrimidines	HMDB00300
12	L-Acetylcarnitine	Acyl Carnitines	HMDB00201
13	1-Methylnicotinamide	Amino Ketones	HMDB00699
14	Daidzein	Polyphenols	HMDB03312
15	2-Ethyl-2-Hydroxybutyric acid	Hydroxy Acids	HMDB01975
16	7-Ketocholesterol	Steroids	HMDB00501

2.3.4. Biofluid Labeling and Metabolite Identification with nLC-nESI FT-ICR-MS

In addition to the benefits obtained by DH labeling, nLC-nESI FT-ICR-MS was employed in order to achieve improved separation efficiency and increased sensitivity for the detection of carbonyl metabolites. In comparison to regular LC-ESI MS on the ion trap, much greater information could be obtained using nLC-nESI FT-ICR-MS, allowing for a greater number of metabolites to be detected and identified for both urine and plasma.

Initially regular LC-MS was used for the DH labeling method development and screening of derivatized standards. It was then determined that the use of low flow LC in combination with nanospray and FT-ICR-MS could be highly advantageous in profiling DH labeled biofluids. The miniaturization of column i.d. allows for improved separation efficiency and electrospray ionization efficiency, and reduction in sample size. Improved separation efficiency is primarily achieved by a reduction of the A term (Eddy diffusion) in the Van Deemter equation. Ionization efficiency is improved by the reduction of co-eluting components due to the improved separation. Ionization efficiency was also improved by the use of the nanospray interface in combination with nLC. The smaller emitter tip, 30 μm, used allowed for the tip to be positioned closer to the orifice such that greater ion transmission to the MS could be achieved. On the FT-ICR-MS instrument used, an eyepiece microscope and light in the nanospray interface allowed for the viewing of the spray. The tip position could be finely adjusted in the x, y, and z planes to optimize its position and signal every time the nLC and FT-ICR-MS were interfaced. An optimized position and spray stability

was determined based on signal intensity observed of background and tuning solution with adjustment of tip position and spray voltage over a range of mobile phase compositions. The flow rate was chosen by evaluating the ion intensities of a tuning solution at 0.5 μL/min, 0.8 μL/min, 1.0 μL/min, and 3.0 μL/min by direct infusion to the nESI-FT-ICR-MS, with a constant spray position and voltage. The results are presented in Table 2.5. Ion intensities were observed to be the highest at a flow rate of 1.0 μL/min and therefore this flow rate was chosen for use with nLC-nESI FT-ICR-MS analyses.

Table 2.5. Ion intensities observed for a mixture of tune mix standards at tested flow rates using direct infusion nESI FT-ICR-MS.

Standard	**Conc. (μM)**	**m/z**	**Intensity (x 10^7)**			
			0.5 μL/min	**0.8 μL/min**	**1.0 μL/min**	**3.0 μL/min**
dCMP	2.00	308.06422	0.06	0.02	0.1	0.2
Phe-Tyr	0.250	329.14958	1.5	1.3	1.2	0.8
Trp-Phe	0.125	352.16557	1.9	1.9	1.7	0.8
Trp-Tyr	0.125	368.16048	1.6	2.0	1.8	0.6
Phe-Phe-Phe	0.005	460.22308	9.1	7.8	11.0	4.7
Loperamide	4.000	477.23033	1.8	2.5	2.6	1.9
Citicoline	0.500	489.11461	4.5	5.5	5.9	3.8
D-Panthethine	4.000	555.25168	0.2	--	0.2	0.5
Amikacin	1.000	586.29302	0.1	0.2	0.2	0.2
Reserpine	0.100	609.28066	8.8	10.0	9.0	6.6

Internal and external calibration of the FT-ICR-MS is very important in order to obtain and maintain the high mass accuracy of MS data that can be achieved with this instrument. FT-ICR-MS produces narrow peaks which allows for the precise measurement of the frequency. These frequencies are then converted to m/z values via the use of a calibration equation. The frequency of the image current is the difference between the cyclotron and magnetron frequencies, where the magnetron frequency is independent of m/z and is subject to shifting caused be the trapping electric field. Calibration of the instrument corrects for the

errors that may be introduced to the frequency of the image signal and allows for high mass accuracy data to be obtained. The instrument was calibrated as required by the manager of the MS facility and tuning was performed by the user. Regular tuning of the instrument was performed prior to every batch of analyses in order to check and ensure the high mass accuracy of the data. Typically the accepted m/z error following tuning was less than 2 ppm, often with less than 1 ppm error obtained. For analyses of labeled standards and samples, a mass error of 2 ppm was used as the cut-off when identifying analytes using the MS data, where error in ppm is calculated by:

$$\text{Error (ppm)} = (\text{Measured Mass} - \text{Theoretical Mass} / \text{Theoretical Mass}) \times 10^6 \quad (\textit{Eq. 2.1.})$$

Tuning of the nESI-FT-ICR-MS was performed using the standard mixture as given in Table 2.5. (early qualitative work) and was later replaced with the standard mixture (2.5 μM in 50/50 H_2O/ACN + 0.1 % FA) as given in Table 2.6. (late qualitative work and all quantitative work).

Table 2.6. nESI FT-ICR-MS tuning solution.

Standard	m/z
L-Phenylalanine	166.086255
9-Methylamino-anthracene	222.127725
Dns-L-Glycine	309.090354
Dns-L-Glutamine	380.127469
Dns-L-Phenylalanine	399.137304
Dns-Glycine-Tryptophan	495.169667

Where Dns = dansyl group, $C_{12}H_{12}NO_2S$.

nLC-nESI FT-ICR-MS method development was initially performed using a range of derivatized standards and then applied and adjusted for DH derivatized biofluids, urine and plasma. As derivatized carbonyl metabolites cover a wide range of polarities, with the DH tag rendering the targeted analytes more non-

polar in general, gradient elution was required. A compromise had to be made between throughput and peak resolution in order to afford good labeled metabolite separation combined with moderate throughput. The final optimized LC gradient and MS method chosen for the qualitative profiling studies is as given in experimental section 2.2.4. The example shown in Figure 2.14 is a comparison of the chromatograms of derivatized urine acquired by regular LC-ESI MS using the ion trap (panel A) versus nLC-nESI FT-ICR-MS (panel B). It is evident that with the use of nLC-nESI FT-ICR-MS with an optimized method improved metabolome profiling is achieved.

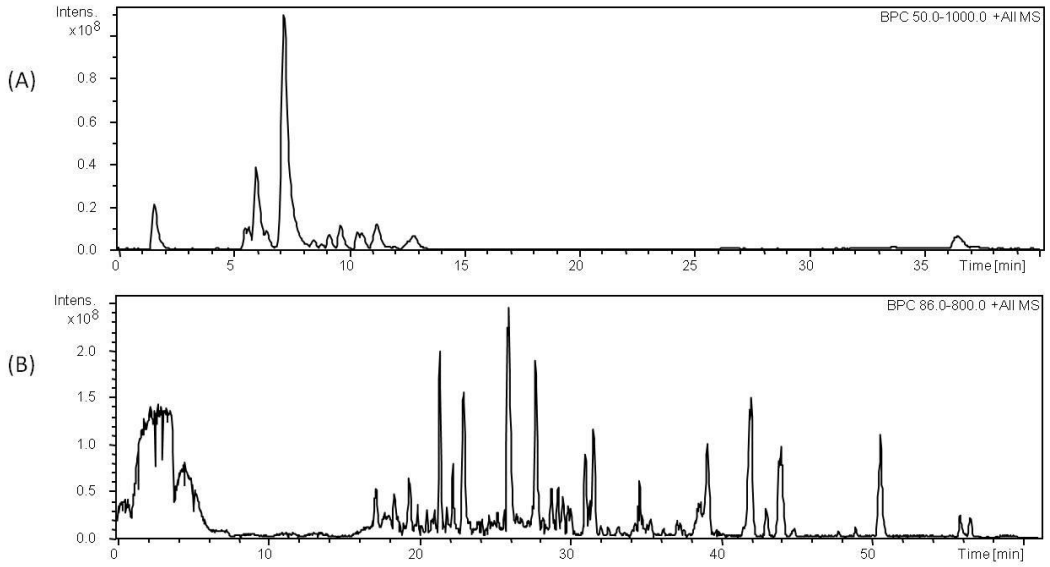

Figure 2.14. (A) BPC of DH derivatized urine (10 x dilution of reconstituted sample with 20 µL injection volume) acquired by regular LC-ESI MS using the Esquire 3000plus ion trap MS instrument with gradient profile as follows: t = 0 min, 15 % B; t = 1 min, 15 % B; t = 7 min, 55 % B; t = 35 min, 100 % B; t = 38 min, 100 % B; t = 38.1 min, 15 % B; t = 40 min, 15 % B; flow rate: 0.2 mL/min. (B) BPC of DH derivatized urine (40 x dilution of reconstituted sample with 2 µL injection volume) acquired by nLC-nESI FT-ICR-MS with gradient profile as follows: 0.00 min – 15 % B, 5.00 min – 15 % B, 12.00 min – 40 % B, 50.00 min – 100 % B, 50.10 min – 15 % B; flow rate: 1 µL/min.

Carbonyl metabolites were tentatively identified in human urine and plasma using t_R and m/z matching to the standard compounds available from our DH standard library with analysis by nLC-nESI FT-ICR-MS. The standard library was initially put together by testing the labeling of a variety of carbonyl standards expected to be present as metabolites in biofluids. Then derivatized urine and plasma was profiled by nLC-nESI FT-ICR-MS and peaks were searched using the HMDB Spectra Search – MS Search tool available on the HMDB website (http://hmdb.ca/search/spectra?type=ms_search). This was done by subtracting the mass, 247.07793, that the DH label would add on to the potential compound. Peaks that gave results in the MS Search were then scrutinized for likelihood of the match, for instance the possible match must be a carbonyl compound. Standards tentatively identified as matches were then obtained either from the HML or from Sigma-Aldrich. These standards were tested for derivatization with DH and added to the library if derivatization was successful. Derivatized standards from the library were analyzed using the same nLC-nESI FT-ICR-MS method as labeled urine and plasma in triplicate and putative carbonyl metabolite matches were confirmed by t_R and m/z matching of peaks from the labeled samples to those of the labeled standards. An example is shown in Figure 2.15 of tentatively identified urinary carbonyl metabolite, nonanal, overlaid with the respective DH labeled nonanal standard. Using the DH labeled standard library for t_R and m/z matching of peaks in profiled urine and plasma, twenty-seven carbonyl metabolites were tentatively identified and are presented in Table 2.7, where six of these metabolites are currently not identified as human metabolites in the HMDB.

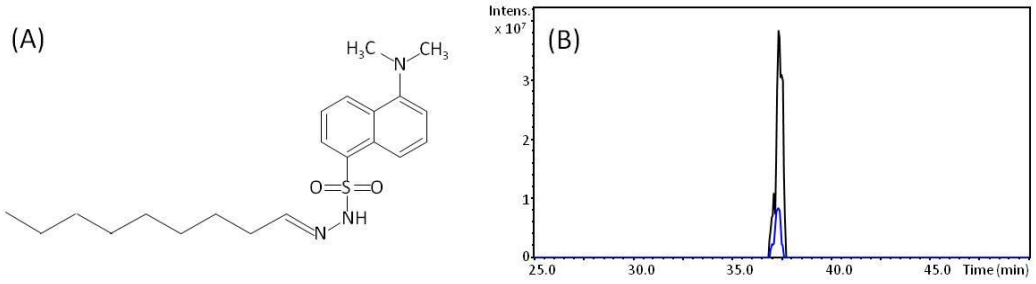

Figure 2.15. (A) DH labeled nonanal. (B) EIC overlay (m/z 390.22097) of DH labeled nonanal standard and tentatively identified nonanal as a metabolite in a DH labeled urine sample acquired by nLC-nESI FT-ICR-MS.

Table 2.7. List of tentatively identified human urinary and plasma metabolites using the DH labeled standard library with nLC-nESI FT-ICR-MS analyses.

Compound Name	**HMDB accession #**	**Urine**	**Plasma**
Formaldehyde	HMDB01426	√	√
Acetaldehyde	HMDB00990	√	√
Propanal	HMDB03366	√	√
Butanal	HMDB03543	√	√
Pentanal	-	√	√
3-Methylbutanal	HMDB06478	√	√
Hexanal	HMDB05994	√	√
Heptanal	-	√	√
Octanal	HMDB01140	√	√
Nonanal	-	√	√
Decanal	HMDB11623	√	√
Undecanal	-	√	√
Dodecanal	-	√	√
Acetone	HMDB01659	√	√
Butanone	HMDB00474	√	√
2-Pentanone	-	√	√
4-Heptanone	HMDB04814	√	√
Pyruvic acid	HMDB00243	√	√
α-Ketoisovaleric acid	HMDB00019	√	√
3-Methyl-2-oxovaleric acid	HMDB00491	√	√
Ketoleucine	HMDB00695	√	√
2-Methyl-3-ketovaleric acid	HMDB00408	√	√

Oxoglutaric acid	HMDB00208	√	√
2-Methylglutaric acid	HMDB00422	√	-
Hippuric Acid	HMDB00714	√	-
D-Glucuronic acid	HMDB00127	√	-
D-Glucose	HMDB00122	√	√

The results demonstrate that column miniaturization and nESI in combination with FT-ICR-MS and DH labeling is capable of yielding improved coverage of the carbonyl metabolome. Tentative identification of further carbonyl metabolites by this strategy is challenging as a result of retention time shifting between runs which is mainly a result of manual sample injection on the LC and the uncontrolled temperature of the column as the LC used did not have a temperature controlled compartment for the column and the room temperature fluctuated between standard and sample runs. A variation on this strategy based on the devised labeling chemistry to achieve improved qualitative and powerful quantitative profiling of the human carbonyl metabolome was desirable and will be presented in Chapter 3.

2.4. Conclusions

In this chapter, the method development and application of the DH labeling technique for the profiling of the human urinary and plasma carbonyl metabolome using LC-MS was presented. The derivatization with DH improves the chromatographic behavior of labeled ketones, aldehydes and keto-acids and significantly enhances the ESI signal of the analyte. Further enhancement of sensitivity and reduction of sample size was achieved using nLC-nESI MS. Nano flow LC methods appropriate for the analysis of DH derivatized biofluids were developed which were suitable for the interface with nESI-MS using a 9.4 Tesla FT-ICR-MS. DH derivatization of carbonyl standards was performed with the goal of building a sizable library for use in identifying carbonyl metabolites in derivatized biofluids. With the mass accuracy offered by FT-ICR-MS and the sensitivity achieved using nLC in combination with the use of the nanospray

interface for the analysis of labeled standards, it was possible to compose a carbonyl metabolite library consisting of eighty-one standards. The use of this DH standard library allowed for the putative identification of twenty-seven human urinary and plasma metabolites from the qualitative profiling studies of these labeled biofluids. Future expansion of the standard library will certainly increase the coverage and understanding of the human carbonyl metabolome. We envisage that this DH labeling method, combined with other high-performance labeling methods such as DnsCl for amines and phenols and DmPA for carboxylic acids developed in our laboratory, will allow us to profile a greater number of metabolites and enable a greater capacity for biological and disease biomarker studies.

2.5. Literature Cited

(1) Fiehn, O. *Plant Mol.Biol.* **2002**, *48*, 155-171.
(2) Fiehn, O. *Compar. Funct. Genom.* **2001**, *2*, 155-168.
(3) Griffiths, W. J.; Koal, T.; Wang, Y. Q.; Kohl, M.; Enot, D. P.; Deigner, H. P. *Angew. Chem.-Int. Edit.* **2010**, *49*, 5426-5445.
(4) Villas-Boas, S. G.; Mas, S.; Akesson, M.; Smedsgaard, J.; Nielsen, J. *Mass Spectrom. Rev.* **2005**, *24*, 613-646.
(5) Want, E. J.; Cravatt, B. F.; Siuzdak, G. *Chembiochem* **2005**, *6*, 1941-1951.
(6) Guo, K.; Ji, C.; Li, L. *Anal. Chem.* **2007**, *79*, 8631-8638.
(7) Guo, K.; Li, L. *Anal. Chem.* **2009**, *81*, 3919-3932.
(8) Guo, K.; Li, L. *Anal. Chem.* **2010**, *82*, 8789-8793.
(9) Lewis-Stanislaus, A. E.; Li, L. *J. Am. Soc. Mass Spectrom.* **2010**, *21*, 2105-2116.
(10) Dettmer, K.; Aronov, P. A.; Hammock, B. D. *Mass Spectrom. Rev.* **2007**, *26*, 51-78.
(11) Want, E. J.; Wilson, I. D.; Gika, H.; Theodoridis, G.; Plumb, R. S.; Shockcor, J.; Holmes, E.; Nicholson, J. K. *Nat. Protoc.* **2010**, *5*, 1005-1018.
(12) Ryan, D.; Robards, K.; Prenzler, P. D.; Kendall, M. *Anal. Chim. Acta.* **2011**, *684*, 17-29.
(13) Psychogios, N.; Hau, D. D.; Peng, J.; Guo, A. C.; Mandal, R.; Bouatra, S.; Sinelnikov, I.; Krishnamurthy, R.; Eisner, R.; Gautam, B.; Young, N.; Xia, J. G.; Knox, C.; Dong, E.; Huang, P.; Hollander, Z.; Pedersen, T. L.; Smith, S. R.; Bamforth, F.; Greiner, R.; McManus, B.; Newman, J. W.; Goodfriend, T.; Wishart, D. S. *PLoS One* **2011**, *6*, 23.
(14) Pysanenko, A.; Wang, T.; Spanel, P.; Smith, D. *Rapid Commun. Mass Spectrom.* **2009**, *23*, 1097-1104.

(15) Pacenti, M.; Dugheri, S.; Traldi, P.; Esposti, F. D.; Perchiazzi, N.; Franchi, E.; Calamante, M.; Kikic, I.; Alessi, P.; Bonacchi, A.; Salvadori, E.; Arcangeli, G.; Cupelli, V. *J. Autom. Methods Manag. Chem.*, 13.
(16) Li, N.; Deng, C. H.; Yao, N.; Shen, X. Z.; Zhang, X. M. *Anal. Chim. Acta* **2005**, *540*, 317-323.
(17) Al-Dirbashi, O. Y.; Rashed, M. S.; Jacob, M.; Al-Ahaideb, L. Y.; Al-Amoudi, M.; Rahbeeni, Z.; Al-Sayed, M. M.; Al-Hassnan, Z.; Al-Owain, M.; Al-Zeidan, H. *Biomed. Chromatogr.* **2008**, *22*, 1181-1185.
(18) Lebovitz, H. E. *Lancet.* **1995**, *345*, 767-772.
(19) Zhang, H. J.; Huang, J. F.; Wang, H.; Feng, Y. Q. *Anal. Chim. Acta.* **2006**, *565*, 129-135.
(20) Zhang, H. J.; Huang, J. F.; Lin, B.; Feng, Y. Q. *J. Chromatogr. A* **2007**, *1160*, 114-119.
(21) Eggink, M.; Wijtmans, M.; Kretschmer, A.; Kool, J.; Lingeman, H.; de Esch, I. J. P.; Niessen, W. M. A.; Irth, H. *Anal. Bioanal. Chem.* **2010**, *397*, 665-675.
(22) Xu, H.; Song, D. D.; Cui, Y. F.; Hu, S.; Yu, Q. W.; Feng, Y. Q. *Chromatographia.* **2009**, *70*, 775-781.
(23) Benson, D. A.; Karsch-Mizrachi, I.; Lipman, D. J.; Ostell, J.; Wheeler, D. L. *Nucleic Acids Res.* **2008**, *36*, D25-D30.
(24) Apweiler, R.; Martin, M. J.; O'Donovan, C.; Magrane, M.; Alam-Faruque, Y.; Antunes, R.; Barrell, D.; Bely, B.; Bingley, M.; Binns, D.; Bower, L.; Browne, P.; Chan, W. M.; Dimmer, E.; Eberhardt, R.; Fazzini, F.; Fedotov, A.; Foulger, R.; Garavelli, J.; Castro, L. G.; Huntley, R.; Jacobsen, J.; Kleen, M.; Laiho, K.; Legge, D.; Lin, Q. A.; Liu, W. D.; Luo, J.; Orchard, S.; Patient, S.; Pichler, K.; Poggioli, D.; Pontikos, N.; Pruess, M.; Rosanoff, S.; Sawford, T.; Sehra, H.; Turner, E.; Corbett, M.; Donnelly, M.; van Rensburg, P.; Xenarios, I.; Bougueleret, L.; Auchincloss, A.; Argoud-Puy, G.; Axelsen, K.; Bairoch, A.; Baratin, D.; Blatter, M. C.; Boeckmann, B.; Bolleman, J.; Bollondi, L.; Boutet, E.; Quintaje, S. B.; Breuza, L.; Bridge, A.; deCastro, E.; Coudert, E.; Cusin, I.; Doche, M.; Dornevil, D.; Duvaud, S.; Estreicher, A.; Famiglietti, L.; Feuermann, M.; Gehant, S.; Ferro, S.; Gasteiger, E.; Gateau, A.; Gerritsen, V.; Gos, A.; Gruaz-Gumowski, N.; Hinz, U.; Hulo, C.; Hulo, N.; James, J.; Jimenez, S.; Jungo, F.; Kappler, T.; Keller, G.; Lara, V.; Lemereier, P.; Lieberherr, D.; Martin, X.; Masson, P.; Moinat, M.; Morgat, A.; Paesano, S.; Pedruzzi, I.; Pilbout, S.; Poux, S.; Pozzato, M.; Redaschi, N.; Rivoire, C.; Roechert, B.; Schneider, M.; Sigrist, C.; Sonesson, K.; Staehli, S.; Stanley, E.; Stutz, A.; Sundaram, S.; Tognolli, M.; Verbregue, L.; Veuthey, A. L.; Wu, C. H.; Arighi, C. N.; Arminski, L.; Barker, W. C.; Chen, C. M.; Chen, Y. X.; Dubey, P.; Huang, H. Z.; Mazumder, R.; McGarvey, P.; Natale, D. A.; Natarajan, T. G.; Nchoutmboube, J.; Roberts, N. V.; Suzek, B. E.; Ugochukwu, U.; Vinayaka, C. R.; Wang, Q. H.; Wang, Y. Q.; Yeh, L. S.; Zhang, J. A.; UniProt, C. *Nucleic Acids Res.* **2011**, *39*, D214-D219.

(25) Wishart, D. S.; Tzur, D.; Knox, C.; Eisner, R.; Guo, A. C.; Young, N.; Cheng, D.; Jewell, K.; Arndt, D.; Sawhney, S.; Fung, C.; Nikolai, L.; Lewis, M.; Coutouly, M. A.; Forsythe, I.; Tang, P.; Shrivastava, S.; Jeroncic, K.; Stothard, P.; Amegbey, G.; Block, D.; Hau, D. D.; Wagner, J.; Miniaci, J.; Clements, M.; Gebremedhin, M.; Guo, N.; Zhang, Y.; Duggan, G. E.; MacInnis, G. D.; Weljie, A. M.; Dowlatabadi, R.; Bamforth, F.; Clive, D.; Greiner, R.; Li, L.; Marrie, T.; Sykes, B. D.; Vogel, H. J.; Querengesser, L. *Nucleic Acids Res.* **2007**, *35*, D521-D526.

(26) Wishart, D. S.; Knox, C.; Guo, A. C.; Eisner, R.; Young, N.; Gautam, B.; Hau, D. D.; Psychogios, N.; Dong, E.; Bouatra, S.; Mandal, R.; Sinelnikov, I.; Xia, J. G.; Jia, L.; Cruz, J. A.; Lim, E.; Sobsey, C. A.; Shrivastava, S.; Huang, P.; Liu, P.; Fang, L.; Peng, J.; Fradette, R.; Cheng, D.; Tzur, D.; Clements, M.; Lewis, A.; De Souza, A.; Zuniga, A.; Dawe, M.; Xiong, Y. P.; Clive, D.; Greiner, R.; Nazyrova, A.; Shaykhutdinov, R.; Li, L.; Vogel, H. J.; Forsythe, I. *Nucleic Acids Res.* **2009**, *37*, D603-D610.

(27) Kanehisa, M.; Goto, S.; Hattori, M.; Aoki-Kinoshita, K. F.; Itoh, M.; Kawashima, S.; Katayama, T.; Araki, M.; Hirakawa, M. *Nucleic Acids Res.* **2006**, *34*, D354-D357.

(28) Fahy, E.; Sud, M.; Cotter, D.; Subramaniam, S. *Nucleic Acids Res.* **2007**, *35*, W606-W612.

(29) Wheeler, D. L.; Barrett, T.; Benson, D. A.; Bryant, S. H.; Canese, K.; Chetvernin, V.; Church, D. M.; DiCuccio, M.; Edgar, R.; Federhen, S.; Geer, L. Y.; Kapustin, Y.; Khovayko, O.; Landsman, D.; Lipman, D. J.; Madden, T. L.; Maglott, D. R.; Ostell, J.; Miller, V.; Pruitt, K. D.; Schuler, G. D.; Sequeira, E.; Sherry, S. T.; Sirotkin, K.; Souvorov, A.; Starchenko, G.; Tatusov, R. L.; Tatusova, T. A.; Wagner, L.; Yaschenko, E. *Nucleic Acids Res.* **2007**, *35*, D5-D12.

(30) Degtyarenko, K.; De Matos, P.; Ennis, M.; Hastings, J.; Zbinden, M.; McNaught, A.; Alcantara, R.; Darsow, M.; Guedj, M.; Ashburner, M. *Nucleic Acids Res.* **2008**, *36*, D344-D350.

(31) Cui, Q.; Lewis, I. A.; Hegeman, A. D.; Anderson, M. E.; Li, J.; Schulte, C. F.; Westler, W. M.; Eghbalnia, H. R.; Sussman, M. R.; Markley, J. L. *Nat. Biotechnol.* **2008**, *26*, 162-164.

(32) Smith, C. A.; O'Maille, G.; Want, E. J.; Qin, C.; Trauger, S. A.; Brandon, T. R.; Custodio, D. E.; Abagyan, R.; Siuzdak, G. *Ther. Drug Monit.* **2005**, *27*, 747-751.

(33) Taguchi, R.; Nishijima, M.; Shimizu, T. In *Lipidomics and Bioactive Lipids: Mass-Spectrometry-Based Lipid Analysis*; Elsevier Academic Press Inc: San Diego, 2007; Vol. 432, pp 185-211.

(34) Appelblad, P.; Ponten, E.; Jaegfeldt, L. H.; Backstrom, T.; Irgum, K. *Anal. Chem.* **1997**, *69*, 4905-4911.

(35) Rodler, D. R.; Nondek, L.; Birks, J. W. *Environ. Sci. Technol.* **1993**, *27*, 2814-2820.

(36) Binding, N.; Kläning, H.; Karst, U.; Pötter, W.; Czeschinski, P.; Witting, U. *Fresenius J. Anal. Chem.* **1998**, *362*, 270-273.

(37) Banos, C. E.; Silva, M. *Anal. Lett.* **2009**, *42*, 1352-1367.

(38) Uchiyama, S.; Ando, M.; Aoyagi, S. *J. Chromatogr. A.* **2003**, *996*, 95-102.
(39) Herrington, J.; Zhang, L.; Whitaker, D.; Sheldon, L.; Zhang, J. *J. Environ. Monit.* **2005**, *7*, 969-976.
(40) Cech, N. B.; Enke, C. G. *Mass Spectrom. Rev.* **2001**, *20*, 362-387.
(41) Weinberger, R.; Koziol, T.; Millington, G. *Chromatographia.* **1984**, *19*, 452-456.
(42) Visser, S. A. G.; Smulders, C. G. M. A.; Gladdines, W. W. F. T.; Irth, H.; van der Graaf, P. H.; Danhof, M. *J. Chromatogr. B.* **2000**, *745*, 357-363.

Chapter 3: Differential $^{15}N_2$-/$^{14}N_2$-isotope Dansylhydrazine Labeling and LC-MS for Absolute and Relative Quantification of the Human Carbonyl Metabolome.

3.1. Introduction

Metabolomics aims at the study of the full complement of endogenous small molecules composing biological systems. Metabolomics has rapidly evolved to facilitate biological studies and potential disease biomarker discovery.[1-4] The detection, identification, and quantification of metabolites are key for a thorough understanding of living systems. The development of sensitive techniques for the quantitative profiling of the metabolome is essential in order to achieve a complete overview and a better understanding of a biosystem. LC-MS has become an increasingly important analytical tool for metabolome profiling and quantitation. LC-MS is widely used for quantitative analysis because of its high sensitivity, specificity, and speed. An ideal LC-MS platform would enable the comprehensive identification and quantification of all the metabolites present in a biological sample, such as biofluids urine and plasma.[5]

However, as a result of the great diversity in chemophysical properties of metabolites, the presence of metabolites over extended dynamic ranges, and the sheer number of metabolites which are present in a biosystem, the universal detection and quantitation of all metabolites is extremely challenging.[6-8] As presented in Chapter 2, the strategy we have devised to achieve a more comprehensive view of the human metabolome is to break down the metabolome into sub-metabolomes, each consisting of the metabolites that share a common functional group (for example all carbonyl-containing metabolites or carbonyl metabolome) and use tailored methods of analysis in order to study the smaller class of metabolites (for example DH labeling of carbonyl-containing metabolites). By breaking down the task into several targeted studies of the sub-metabolomes and then compiling the results to provide a comprehensive view of the metabolome as a whole, it is our goal to achieve a more complete and accurate profile of the human metabolome.

This strategy also helps to overcome the difficulty encountered with quantitative metabolome profiling. Due to the sheer complexity of the metabolome there is a trade-off between quantitative and profiling capability. As with high metabolome coverage there is low throughput for quantitative metabolome analysis. Therefore by reducing the size of the metabolome to be profiled, a sub-metabolome, the quantitative throughput increases as well. Additionally, the use of RPLC as a separation technique can help to improve the coverage for quantitative studies as it helps to reduce background interference and ion suppression from other compounds in combination with ESI-MS. With the use of nLC-nESI MS further benefits can be achieved for the quantitative analysis of the metabolome, particularly for low abundance small molecules such as carbonyls, including improved separation efficiency, greater sensitivity, enhanced dynamic range, minimized ion suppression, and smaller sample size requirements. When combined with high resolution mass analysis, such as the use of the FT-ICR-MS, the contribution from interfering ions can be reduced as well. The high mass accuracy data provided by FT-ICR-MS analysis allows for improved accuracy in quantitation as analyte identification can be assigned with high confidence.

There are three types of calibration which can be used for quantitative analysis; the external standard method, the standard addition method, and the internal standard method. The external standard method involves the analysis of standard solutions of known concentrations and plotting of peak area (or signal intensity) of the chromatographic peak (the MS response) against the known standard concentration in order to build a calibration curve which can be used to determine the concentration of an unknown analyte based on the measured peak area. However, this method offers limited accuracy and precision as the standards and samples are run at different points in time and within that time the MS response may drift and also it is often difficult to match the matrix of the standard solutions to the sample. The standard addition method is able to overcome the effects of the matrix and fluctuations in the instrument response by measuring the peak area following the addition of known concentrations of standard solution to

the unknown sample where the concentration of the unknown is given by the intercept of the calibration curve with the x-axis. This method is very laborious and therefore inappropriate for high throughput analysis of complex samples. The internal standard method is widely used for quantitative analysis as it allows for high accuracy and precision. In this method, a known, constant amount of an internal standard (IS) compound is added to solutions of known analyte concentrations and the ratio of their MS response is plotted against concentration. The IS is added to the sample solution and the ratio of the internal standard and analyte as determined by MS is used to determine the concentration of the unknown analyte based on the ratio and the curve. The IS is added to the unknown sample early on during the sample preparation and therefore corrects for any losses that may occur during the sample handling and chromatography, as well as correcting for fluctuations in MS response. This method also overcomes any matrix effects by the direct addition of the IS to the sample and avoids fluctuations in instrument response by the analysis of the IS and sample together in the same run. Careful selection of an IS is critical to the quality of the results. In order to accurately account for sample losses and detection variations, the chemophysical properties of the analyte must be an exact match to the IS and the chromatographic properties of the IS and analyte must match so that they co-elute closely in time or preferably are co-eluting. The MS properties of the IS and analyte must also match in terms of ionization efficiency, fragmentation behavior, and detector response. And it is also important that the chosen IS in not present as a sample component. Given this selection criteria, there are two main types of IS, a structural homologue of the analyte and a stable isotope-labeled (SIL) analogue of the analyte. A SIL standard is the ideal IS as it has the same structure as the analyte but with one or more of the atoms replaced by a different isotope than the analyte.

The use of SIL analogues is complementary to LC-MS based quantification as it aids to overcome matrix and ion suppression effects. However, for metabolome quantification a large number of SIL standards would be required and the availability of SIL standards is quite limited. The synthesis of a SIL for

every metabolite would be very time consuming and expensive and is therefore impractical. To overcome these limitations, we have devised a differential isotope labeling technique for the quantitative profiling of sub-metabolomes which uses a chemical reaction to introduce an isotope tag to the analyte(s) of interest in one sample and another mass-difference isotope tag to the same analyte(s) in another standard mixture or comparative sample to achieve absolute or relative quantification, respectively. With this methodology, a SIL IS is generated for every metabolite targeted. The labeled samples are combined for analysis and metabolite isoforms are co-eluted by RPLC and detected using MS. The peak area ratio of the isotope labeled analyte pair provides the basis for the absolute quantification of the analyte if the other sample is a standard of known concentration or relative quantification of the analyte in two comparative samples. Our work includes the quantitative profiling of amine-containing metabolites with ^{13}C-/^{12}C-formaldehyde[9], amine- and phenol-containing metabolites with $^{13}C_2$-/$^{12}C_2$-dansyl chloride (DnsCl)[10], and carboxylic acid-containing metabolites with $^{13}C_2$-/$^{12}C_2$-p-dimethylaminophenacyl (DmPA) bromide[11]. Studies are on-going for the isotopic labeling of the acylcarnitine and acylglycine sub-metabolomes. The development and application of the quantitative profiling technique for the human carbonyl sub-metabolome with $^{15}N_2$-/$^{14}N_2$-dansylhydrazine using LC-MS are presented in this Chapter.

By introducing isotopes into the developed DH labeling reagent for carbonyls, the tag not only improves the performance of LC separation and MS detection for the targeted analytes but also provides the ability to perform robust, high throughput comprehensive quantitation of the carbonyl metabolome. The synthesis of $^{15}N_2$-DH will be given and the use of the labeling strategy for the quantitative profiling of human urine and plasma will be discussed.

DH has previously been used for the labeling of sugars in addition to ketones and aldehydes.[12-14] The identification of sugars in complex biofluid samples is also important for biological studies and disease biomarker discovery. Studies performed on the biofluids of humans with conditions such as diabetes and specific inherited metabolomic diseases have shown elevated concentrations

of sugars such as glucose. For example, a high concentration of glucose in the urine and blood can be indicative of diabetes. As such the development of sensitive techniques for the global profiling and quantitation of sugars in the metabolome is significant. Sugars are relatively polar compounds and suffer from the same effects as carbonyls for RPLC-MS analysis. They are poorly separated by RPLC and often elute in the void volume and are poorly ionized by ESI. With modification of the DH labeling method and LC-MS methods for carbonyl metabolites presented in Chapter 2, labeling of sugar-based metabolites was possible. Identification and quantification of sugars in the human urine and plasma was achieved using the differential isotope labeling method in combination with the DH standard library and will be discussed.

3.2. Experimental

3.2.1. Materials and Reagents

All chemicals, standards, and reagents were purchased from Sigma-Aldrich Canada (Markham, ON) except those otherwise noted. The following standards, given by HMDB accession number, were obtained from the Human Metabolite Library (HML): 00005, 00019, 00031, 00044, 00060, 00098, 00127, 00169, 00174, 00194, 00201, 00205, 00208, 00223, 00243, 00283, 00289, 00300, 00310, 00357, 00374, 00398, 00408, 00422, 00462, 00467, 00474, 00491, 00501, 00503, 00562, 00635, 00646, 00695, 00699, 00707, 00714, 00720, 00753, 00821, 00840, 00849, 00859, 00990, 01015, 01051, 01140, 01167, 01184, 01259, 01358, 01864, 01867, 01882, 01892, 01975, 02939, 03269, 03312, 03315, 03366, 03407, 03543, 03543, 04461, 05842, 05846, 05994, 06115, 06236, 11603, and 11623. The isotope reagent, $^{15}N_2$-hydrazine sulfate, used in the synthesis of $^{15}N_2$-dansylhydrazine, was purchased from Cambridge Isotope Laboratories (Andover, MA). LC-MS grade water, methanol (MeOH), and acetonitrile (ACN), LC grade chloroform, and ACS grade ethyl acetate and dichloromethane (DCM) were purchased from Fisher Scientific (Edmonton, AB). LC grade tetrahydrofuran (THF) and reagent grade hexanes were purchased from EMD Chemicals

(Gibbstown, NJ). LC-MS grade formic acid (FA) and trifluroroacetic acid (TFA) was purchased from Sigma-Aldrich Canada (Markham, ON). TFA and H_2O were stored at 4 ^oC upon opening. LC grade ethanol (EtOH) was provided as a gift from Dr. Randy Whittle. Oasis hydrophilic-lipophilic balance (HLB) solid phase extraction (SPE) cartridges (30 mg, 1 mL) were purchased from Waters Corporation (Milford, MA). Urine and blood samples used in absolute quantitation studies were provided by a healthy individual. Urine samples used in the three-day study were provided by ten female and ten male volunteers.

3.2.2. Synthesis of $^{15}N_2$-Dansylhydrazine

$^{15}N_2$-dansylhydrazine (5-(dimethylamino)naphthalene-1-sulfonohydrazide-$^{15}N_2$) was synthesized by a one-step reaction. Figure 3.1 depicts the synthetic scheme. In a 100 mL round-bottom flask, 0.38 g sodium hydroxide was dissolved in 8 mL H_2O with stirring at room temperature. To this NaOH solution, 0.32 g $^{15}N_2$-hydrazine sulfate salt was added and dissolved. In a glass vial, 0.53 g dansylchloride (DnsCl) was dissolved in 10 mL THF. This DnsCl mixture was then added dropwise with stirring at room temperature to the mixture in the round bottom flask using a glass pipette over a period of 10 min. 2 mL THF was used to rinse the glass vial and was combined into the reaction mixture. The reaction mixture was stirred at room temperature for 40 min and then the THF was removed using a rotary evaporator. LC-MS was used to confirm reaction completion. Liquid-liquid extraction was performed on the crude product. The aqueous crude reaction mixture was combined with 5 mL DCM in a 50 mL glass separatory funnel, shaken and the organic (DCM) layer was collected. The aqueous layer was then extracted with 10 x 2 mL DCM and the organic layer was collected and combined after each extraction. LC-MS was used to check the aqueous layer to ensure complete extraction of the product into the organic layer. The combined organic layer (DCM) containing the crude product was reduced to dryness using a rotary evaporator. Flash chromatography using solvents ethyl acetate (EtAc) and hexanes was performed to obtain the purified product. 100 mL hexanes was used to pack the column with silica gel. The crude product was

loaded onto the column in ~ 3 mL DCM. Elution was then performed with the following gradient: 120 mL 5:1 hexanes:EtAc, 80 mL 3:1 hexanes:EtAc, 210 mL 2.5:1 hexanes:EtAc, and 270 mL 2:1 hexanes:EtAc. Fractions containing the product were collected with the addition of the 270 mL 2:1 hexanes:EtAc. Fractions containing the product as verified by TLC were combined and reduced using a rotary evaporator and then fully dried under a stream of N_2 (g). Purified $^{15}N_2$-dansylhydrazine was obtained in a reaction yield of 98.8 %. The purity of the product was confirmed by LC-MS and ^{1}H NMR analysis with comparison to commercially available $^{14}N_2$-dansylhydrazine standard and synthesized $^{14}N_2$-dansylhydrazine standard. $^{15}N_2$-dansylhydrazine is not commercially available.

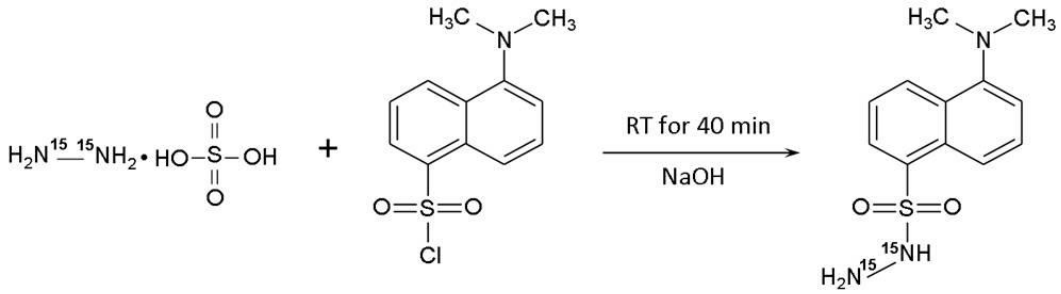

Figure 3.1. Reaction scheme for the synthesis of the isotope labeling reagent, $^{15}N_2$-dansylhydrazine.

3.2.3. Sample Collection and Pre-treatment

3.2.3.1. Standards

Standards obtained from Sigma-Aldrich were stored in the fridge at 4 ^{o}C unless otherwise indicated by the MSDS for storage at room temperature or at -20 ^{o}C. Standards obtained from the HML were stored at -20 ^{o}C. 5 mM stock solutions of standards were prepared in MeOH and stored at -20 ^{o}C prior to derivatization with DH. Stock standard solutions were prepared fresh prior to each batch of analyses or as required.

3.2.3.2. Urine

Urine that was used for the absolute quantitation profiling with the differential $^{15}N_2$-/$^{14}N_2$-DH labeling scheme was provided by a healthy individual. Urine was obtained following a 12 hour fast, during which only water was consumed. Second void volume, midstream urine was supplied in a 500 mL borosilicate glass bottle. Urine was cooled on ice for 20 min in the containment level II laboratory and was then mixed 1:1 with LC-MS grade MeOH and centrifuged for 10 min at 4,000 rpm. Using a SpeedVac the volume of supernatant obtained was reduced back to the original volume of urine collected. Then 100 µL aliquots were taken to dryness using a SpeedVac and then stored at -80 ^{o}C in the dried concentrate form until reconstitution in MeOH and derivatization with DH. (Note this is the same protocol as outlined in Section 2.2.2).

3.2.3.3. Plasma

Blood that was used for the absolute quantitation profiling with the differential $^{15}N_2$-/$^{14}N_2$-DH labeling scheme was provided by a healthy individual following a 12 hour fast (no food or water). The blood was collected in polypropylene tubes containing EDTA as the anti-coagulant and was transported on ice in a cooler to the containment level II biosafety laboratory. The blood was transferred from the EDTA tubes into 50 mL polypropylene BD Falcon tubes that had been pre-cleaned with LC-MS grade MeOH and H_2O. In total ~ 200 mL blood was collected. It was then centrifuged for one hour at 4,000 rpm resulting in ~ 100 mL of supernatant, plasma. 1 mL aliquots of plasma were then transferred to pre-cleaned 15 mL BD Falcon tubes. To each 1 mL aliquot, 0.5 mL of cold 0.1 % FA in ACN (-20 ^{o}C) was added and then kept at 4 ^{o}C for 30 min. This was repeated until a final volume of 4 mL of cold 0.1 % FA in ACN had been added. At this stage, samples could be further processed at the regular level I laboratory. The tubes were then centrifuged for 10 min at 4,000 rpm. ~ 4.5 mL of supernantant was obtained from each tube and was diluted with LC-MS grade water to obtain a mixture that was ~ 20 % ACN. This mixture was then passed through Microcon MWCO filters of 3,000 Da using a centrifuge at 10,500 rpm, 4

^{o}C until complete. The filters had been pre-cleaned with LC-MS grade H_2O and the collection vials had been pre-cleaned with LC-MS grade MeOH and H_2O. The filtrate was combined and then 1 mL aliquots of the filtrate were reduced to dryness using the SpeedVac and then stored at -80 ^{o}C in the dried concentrate form prior to reconstitution in MeOH and derivatization with DH. (Note this is the same protocol as outlined in Section 2.2.2).

3.2.3.4. Research study urine samples

A research study was conducted to determine baseline concentrations of urinary metabolites and to study the variation of inter- and intra-sample concentrations of the observed metabolites. Ten male and ten female volunteers, who claimed to be healthy, provided a first void volume (morning), midstream urine sample following an 8 hour fast (no food or water), once a day for three consecutive days. Those of us conducting the study and performing the sample preparation were only aware of the gender and age of the volunteer, as well as the urine sample collection time and date as recorded on the sample tube. Identity of the volunteers remained anonymous and volunteers were recruited by members of the Li group who were not involved with the study. The study was conducted in accordance with the codes of the University of Alberta's Arts, Science, and Law Research Ethics Board. Once the urine sample was collected in the provided 50 mL BD Falcon polypropylene conical tube, volunteers were asked to report to a designate (not involved with the study) within two hours of sample collection and were directed to store the sample in the 4 ^{o}C refrigerator in the containment level II laboratory. Samples were processed within four hours of receipt. Samples were centrifuged for 10 min at 4000 rpm. The urine supernatant was then filtered twice through a 0.2 μm polyvinylidene fluoride (PVDF) filter and collected into a BD Falcon tube. 1 mL aliquots of the double filtered urine were stored at -80 ^{o}C. Within a week of storage at -80 ^{o}C, a 1 mL aliquot of each sample (20 samples provided over a 3 day period) was thawed on ice and then divided up into 100 μL aliquots in triplicate and reduced to dryness using the SpeedVac. An additional 1 mL aliquot of each sample was thawed on ice and then a pooled urine sample was

prepared consisting of 1 mL aliquots of each of the sixty samples from the study. The pooled urine was vortexed and then 100 μL aliquots of the pooled urine were reduced to dryness using the SpeedVac. All dried urine concentrates were stored at -80 ^{o}C until reconstitution in MeOH and derivatization with DH.

3.2.4. Dansylhydrazine Labeling Reaction Conditions

3.2.4.1. DH labeling protocol for carbonyl metabolome profiling

This labeling protocol was applied to both standards and biofluids (i.e., urine and plasma). (Note this is the same protocol as outlined in Section 2.2.2). For derivatization, carbonyl standards solutions were prepared in MeOH and urine and plasma were reconstituted in 1 mL MeOH using sonication at room temperature and combined with 125 μL 3 % (v/v) TFA in MeOH and 125 μL 20 mM DH. The reaction mixtures were vortexed for 1 min and then centrifuged for 1 min at 14,000 rpm. The reaction was then allowed to proceed for one hour at 60 ^{o}C at 300 rpm in an Innova-4000 benchtop incubator shaker. After which, the mixture was again vortexed and centrifuged and then the reaction was quenched by cooling it at -20 ^{o}C, followed by evaporation of acid and solvent using a SpeedVac concentrator system. SPE using HLB Oasis cartridges was then performed separately on the DH labeled standards, urine, and plasma. The cartridges were conditioned with 5 mL MeOH, 1 mL H_2O and equilibrated with 1 mL of 10 % MeOH/H_2O. Labeled urine was reconstituted in 1.2 mL 10 % MeOH and loaded onto the SPE cartridge, the reaction vial was rinsed with 50 μL 10 % MeOH and loaded with the sample. The cartridge was then washed with 1 mL 40 % MeOH/H_2O and the dansylhydrazones were eluted with 1.2 mL MeOH. The labeled standards, urine or plasma collected eluate was reduced to dryness using the SpeedVac concentrator system and stored at -80 ^{o}C overnight (or up to a week) if the analysis could not be performed immediately. At time of analysis, the sample was reconstituted in 200 μL MeOH and further diluted in the initial LC gradient mobile phase for injection and analysis by LC-MS. Labeling of the standard set or sample with $^{14}N_2$-DH or $^{15}N_2$-DH depended on the type of

quantitation to be achieved. Reaction conditions for both isotope forms were the same using the outlined protocol. Figure 3.2 shows the labeling scheme.

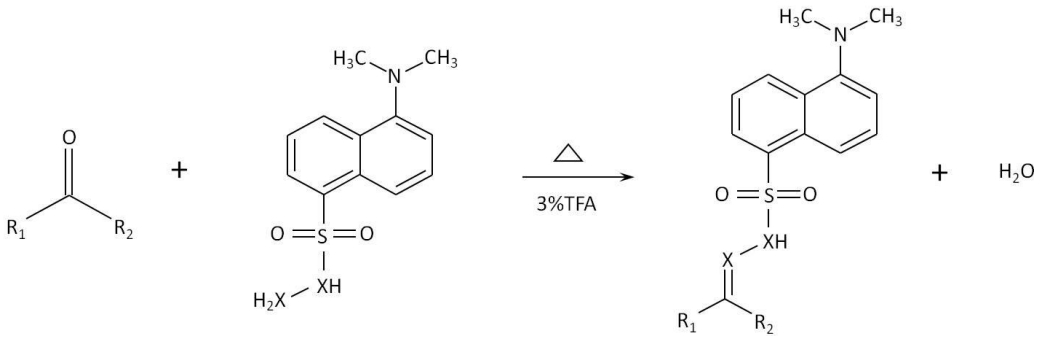

Figure 3.2. Dansylhydrazine labeling scheme, where X = ^{14}N, or X = ^{15}N.

3.2.4.2. DH labeling protocol for sugar metabolome profiling and group study urine profiling for carbonyls and sugars

This labeling protocol was applied to both standards and biofluids (i.e., urine and plasma). For derivatization, sugar and carbonyl standard solutions were prepared in EtOH and urine and plasma were reconstituted in 1 mL EtOH using sonication at room temperature and combined with 125 µL 3 % (v/v) TFA in EtOH and 125 µL 20 mM DH. The reaction mixtures were vortexed for 1 min and then centrifuged for 1 min at 14,000 rpm. The reaction was then allowed to proceed for 100 min at 60 ^{o}C at 300 rpm in an Innova-4000 benchtop incubator shaker. After which, the mixture was again vortexed and centrifuged and then the reaction was quenched by cooling it at -20 ^{o}C, followed by evaporation of acid and solvent using a SpeedVac concentrator system. The labeled standards, urine or plasma concentrates were stored at -80 ^{o}C overnight (or up to a week) if the analysis could not be performed immediately. At time of analysis, the sample was reconstituted in 200 µL EtOH and further diluted in the initial LC gradient mobile phase for injection and analysis by LC-MS. Labeling of the standard set or sample with $^{14}N_2$-DH or $^{15}N_2$-DH depended on the type of quantitation to be achieved. Reaction conditions for both isotope forms were the same using the outlined protocol.

3.2.5. LC Ion Trap MS Conditions

The HPLC system used was an Agilent 1100 series equipped with an auto sampler, binary pump, and degasser. The column used was an ACE C18 3 μm, 50 mm x 2.1 mm, 100 Å, column (Aberdeen, Scotland). The LC system was interfaced to the ESI source of a Bruker Esquire 3000plus quadrupole ion trap MS (Bruker, Bremen, Germany). The LC auto sampler was set at 4 ^{o}C and the column was at room temperature. LC mobile phase A was 0.1 % (v/v) LC-MS grade FA in LC-MS grade H_2O, and mobile phase B was 0.1 % (v/v) LC-MS grade FA in LC-MS grade ACN. The main binary gradient elution profile used for confirming DH derivatized carbonyls was as follows: t = 0.0 min, 15 % B; t = 1.0 min, 15 % B; t = 5.0 min, 55 % B; t = 18.0 min, 100 % B; t = 22.0 min, 100 % B; t = 22.1 min, 15 % B; t = 26.0 min, 15 % B. The flow rate was 0.2 mL/min and the injection volume was 20 μL. The main binary gradient elution profile used for confirming DH derivatized sugars was as follows: t = 0.0 min, 14 % B; t = 20.0 min, 14 % B; t = 24.0 min, 50 % B; t = 26.0 min, 100 % B; t = 26.1 min, 14 % B; t = 30.0 min, 14 % B. The flow rate was 0.2 mL/min and the injection volume was 10 μL.

Using the Esquire 3000plus MS, all spectra were acquired in positive ion mode. MS source parameters include: capillary voltage 3500 V, end plate offset -500 V, nebulizer gas 20.0 psi, dry gas flow 6.0 L/min, and dry temperature 300 ^{o}C. Further MS settings include: skimmer voltage 40.0 V, capillary exit 118.0 V, octopole (1) DC 12.00 V, octopole (2) DC 1.70 V, octopole RF 125.0 Vpp, lens (1) -5.0 V, lens (2) -60.0 V, and trap drive 53.9. The scan range was set at 50 to 1000 m/z. Calibration and tuning was performed using direct infusion of the commercially available Bruker ESI tune mix.

3.2.6. nLC-nESI FT-ICR-MS Conditions

The HPLC system used was an Agilent 1100 series capillary LC system with modified flow rate of 1.0 μL/min and equipped with manual injector, binary pump, and degasser. The column used was a Waters Xterra MS C18 3.5 μm, 150 μm x 150 mm, 125 Å, NanoEase column (Milford, MA). The LC system was

interfaced to the nESI source of a Bruker 9.4 T Apex-Qe FT-ICR-MS (Bruker, Billerica, MA). The nESI tip used in the interface of the NanoEase column to the nESI source of the FT-ICR-MS was a New Objective PicoTip Emitter Silica Tip 30 ± 2 μm (Woburn, MA). nLC separation on column was performed at room temperature (which was monitored). LC mobile phase A was 0.1 % (v/v) LC-MS grade FA in LC-MS grade H_2O, and mobile phase B was 0.1 % (v/v) LC-MS grade FA in LC-MS grade ACN. The flow rate was 1.0 μL/min and the sample loop injection volume was 2.0 μL. The binary gradient elution profile used for DH labeled carbonyl profiling was as follows: t = 0.0 min, 15 % B; t = 5.0 min, 15 % B; t = 12.0 min, 55 % B; t = 50.0 min, 100 % B; t = 65.0 min, 100 % B. The binary gradient elution profile used for DH labeled sugar profiling was as follows: t = 0.0 min, 18 % B; t = 18.0 min, 10 % B; t = 22.0 min, 50 % B; t = 25.0 min, 100 % B; t = 30.0 min, 100 % B; t = 30.10 min, 10 % B. The binary gradient elution profile used for combined DH labeled carbonyl and sugar profiling was as follows: t = 0.0 min, 10 % B; t = 18.0 min, 10 % B; t = 20.0 min, 25 % B; t = 25.0 min, 55 % B; t = 63.0 min, 100 % B; t = 65.0 min, 100 % B; t = 65.10 min, 10 % B.

Using the FT-ICR-MS, all spectra were acquired in positive ion mode; the negative ion mode was found to be much less sensitive for the detection of DH labeled metabolites. FT-ICR-MS spray chamber (nESI) parameters used include: capillary voltage 1800 V (typically), dry temperature 120 ^{o}C, and dry gas flow 2.0 L/min. Accumulation settings include: TD (Fid Size) 256 k, average spectra 2, source accumulation time 0.0010 s, ion accumulation time 0.1 s, TOF (AQS) 0.0007 s, and DC extract bias voltage 0.7 V. Source optics settings include: capillary exit 240 V, deflector plate 250.0 V, funnel (1) 180 V, skimmer (1) 18.0 V, funnel (2) 6.1 V, skimmer (2) 5.0 V, hexapole DC 4.0 V, trap 20 V, and extract -10 V. Qh settings include: focus lens -100 V, entrance lens 1.8 V, entrance lens trap 4.7 V, entrance lens extract 20 V, DC extract bias 0.7 V, exit lens trap 22.0 V, and exit lens extract -12.0 V. Transfer optics settings include: accelerator (1) 45 V, high voltage -3000 V, vertical beam steer (1) 0.5 V, horizontal beam steer (1) 17.5 V, focusing lens (1) -160 V, focusing lens (2) -20 V, and focusing lens

(3) -100 V. Analyzer settings include: side kick -12.7 V, side kick offset -1.8 V, excitation amplitude 4.00 dB, front trap plate 1.0 V, back trap plate 1.2 V, and analyzer entrance -4.0 V. The scan range was set at 86.62 to 800.00 m/z using broadband detection and spectra were acquired in chromatography mode with a run time of 65.0 min. The instrument was calibrated and tuned using the prepared nESI-FT-ICR-MS tuning mixture as discussed in Chapter 2 and given in Table 2.6. The maximum resolution and transient length varied per instrument calibration but were typically 28000 (at m/z 400) and 0.0786 s, respectively.

3.2.7. capLC-ESI FT-ICR-MS Conditions for Group Study DH Labeled Urine

The HPLC system used was an Agilent 1100 series capillary LC system with automatic injector, binary pump, and degasser. The column used was an Agilent Zorbax Eclipse XDB-C18 3.5 μm, 1.0 x 150 mm, 80 Å, MicroBore Rapid Resolution column. The capLC system was interfaced to the ESI source of a Bruker 9.4 T Apex-Qe FT-ICR-MS (Bruker, Billerica, MA). Bruker BioSpin software HyStar^{TM} was used to control the capLC and coordinate the communication between the capLC system and the FT-ICR-MS so that sample sequences could be set-up and run automatically without the need for constant monitoring. LC separation on column was performed at room temperature. LC mobile phase A was 0.1 % (v/v) LC-MS grade FA in LC-MS grade H_2O, and mobile phase B was 0.1 % (v/v) LC-MS grade FA in LC-MS grade ACN. The flow rate was 50.0 μL/min and the injection volume was 8.0 μL. The binary gradient elution profile used for DH labeled carbonyl and sugar profiling was as follows: t = 0.0 min, 15 % B; t = 15.0 min, 15 % B; t = 25.0 min, 50 % B; t = 30.0 min, 100 % B; t = 40.0 min, 100 % B; t = 40.1 min, 15 % B; 60.0 min, 15 % B.

Using FT-ICR-MS, all spectra were acquired in positive ion mode. FT-ICR-MS spray chamber (ESI) parameters used include: capillary voltage 4200 V, spray shield 3700 V, nebulizer gas flow 2.3 L/min, dry gas flow 7.0 L/min, and dry temperature 190 ^{o}C. Accumulation settings include: average spectra = 5, source accumulation time 0.01 s, ion accumulation time 0.1 s, and TOF (AQS)

0.0007 s. Source optics settings include: capillary exit 300 V, deflector plate 260.0 V, funnel (1) 160 V, skimmer (1) 20.0 V, funnel (2) 5.0 V, skimmer (2) 5.2 V, hexapole DC 3.5 V, trap 20 V, and extract -10 V. RF control settings include: funnel RF 200 V, hexapole RF amplitude 400 Vpp, and hexapole frequency 5.0 MHz. Qh optics settings include: focus lens -100 V, entrance lens 2.0 V, pre-filter DC bias 0.0 V, DC bias 0.0 V, post-filter DC bias 0.0 V, entrance lens trap 4.2 V, entrance lens extract 20 V, collision voltage -2.0 V, DC extract bias 0.7 V, exit lens trap 20.0 V, and exit lens extract -10.0 V. Gas control settings include: collision gas flow 0.30 L/s. ICR transfer settings include: accelerator (1) 25 V, accelerator (2) 0.0 V, accelerator (3) 0.0 V, vertical beam steer (1) 3.5 V, vertical beam steer (2) 0.0 V, horizontal beam steer (1) 25.0 V, horizontal beam steer (2) 0.0 V, focusing lens (1) -180 V, focusing lens (2) -20 V, and focusing lens (3) -150 V. Analyzer settings include: side kick -10.0 V, side kick offset -1.800 V, excitation amplitude 5.25 dB, front trap plate 1.000 V, back trap plate 1.200 V, and analyzer entrance -4.000 V. The scan range was set at 202.11 to 1000.00 m/z. The instrument was calibrated and tuned using the prepared nESI-FT-ICR-MS tuning mixture as discussed in Chapter 2 and given in Table 2.6. The maximum resolution and transient length varied per instrument calibration but were typically 33000 (at m/z 400) and 0.1835 s, respectively.

3.3. Results and Discussion

3.3.1. The Differential $^{15}N_2$-/$^{14}N_2$-Dansylhydrazine Strategy for Absolute and Relative Metabolome Quantification

MS-based identification and quantification of a large number of metabolites can be extremely challenging. The use of paired labeling reagents that are chemically identical but isotopically different provides a simple and robust means of quantitative metabolome profiling. Our research has the goal of developing paired isotope labeling reagents to selectively react with the metabolites containing specific functional groups, followed by high mass accuracy LC-MS analysis for unambiguous identification and precise and accurate quantification. In Chapter 2, an optimized method for the determination of

carbonyl-containing metabolites in human biofluids using DH labeling was presented. The conversion of carbonyl metabolites into their dansylhydrazone derivatives has shown significant improvement of RPLC chromatographic properties and enhancement of ESI-MS signals. Further enhancement of sensitivity and reduction of sample size was achieved using nLC-nESI FT-ICR-MS. DH labeling proved to be a powerful technique for carbonyl metabolite profiling and identification. To advance this technique to allow for confident metabolite identification and quantification, a strategy based on the use of isotope-labeled DH was developed.

In order to perform absolute quantification of the human carbonyl metabolome the differential $^{15}N_2$-/$^{14}N_2$-DH isotope labeling method was devised. This method of derivatization is used to generate a $^{15}N_2$-stable isotope labeled internal standard for each corresponding $^{14}N_2$-labeled analyte. This is done by labeling known amounts of carbonyl standards from our metabolite library with $^{15}N_2$-DH and labeling human biofluid samples with $^{14}N_2$-DH and then combining the two samples and analyzing by high mass accuracy LC-MS. The DH isoforms are co-eluted and simultaneously detected and hence no isotopic effect is observed, as is common when using deuterium labeled standards for RPLC, where the MS intensity ratio of co-eluted isoforms is used for reliable, absolute quantitation of the metabolites.

In order to perform relative quantification, a pooled biofluid sample in which absolute quantification has been performed is used as the standard and a known amount is labeled with $^{15}N_2$-DH and the other sample of interest is labeled with $^{14}N_2$-DH. Again the two samples are combined and isoforms are co-eluted and detected simultaneously. The ratio of the MS signal of the isoforms is used for relative quantitation of the metabolites in the sample of interest. An overview of the absolute/relative quantitative strategy for human metabolome profiling using differential $^{15}N_2$-/$^{14}N_2$-DH labeling is presented in Figure 3.3.

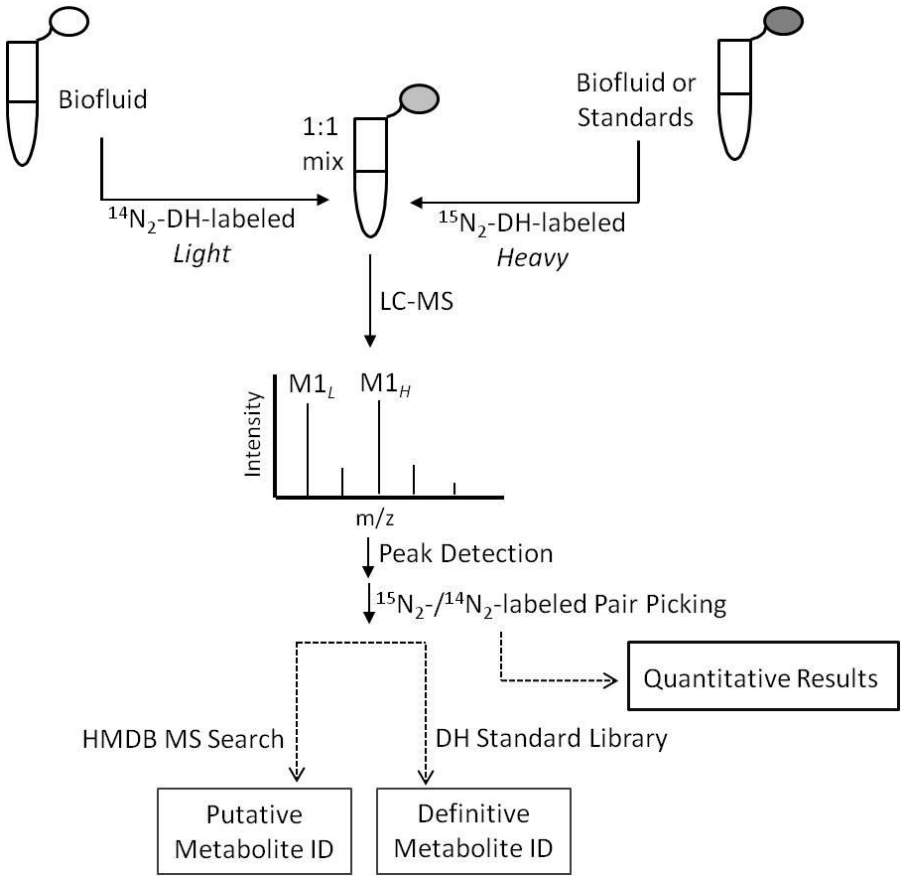

Figure 3.3. Overview of $^{15}N_2$-/$^{14}N_2$-DH isotope labeling LC-MS method for quantitative metabolome profiling.

The developed strategy required an isotope labeled dansylhydrazine reagent. An isotopic form of this compound is not presently available commercially and therefore a scheme for the synthesis of the compound was developed. First, the type of isotope form had to be decided upon. The use of paired labeling reagents with deuterium as the isotope is not ideal for LC-MS applications as it results in an isotope effect where the pairs are not co-eluted or simultaneously detected.[15] This can result in interference from other peaks overlapping with the light or heavy form and also a seemingly reduced labeling efficiency, ultimately rendering quantitation unreliable. Commonly, ^{13}C-isotope labeled compounds are used with LC-MS as internal standards as there is no observed isotope effect and ^{13}C isotope reagents can occasionally be purchased

commercially. The simplest synthesis of DH attempted, a variation on a synthesis described in the literature[16], was the reaction of dansylchoride (DnsCl) with 35 % hydrazine hydrate in toluene, represented in Figure 3.4. The reaction went to completion within minutes at room temperature and produced a pure product as verified by TLC plate and LC-MS analyses.

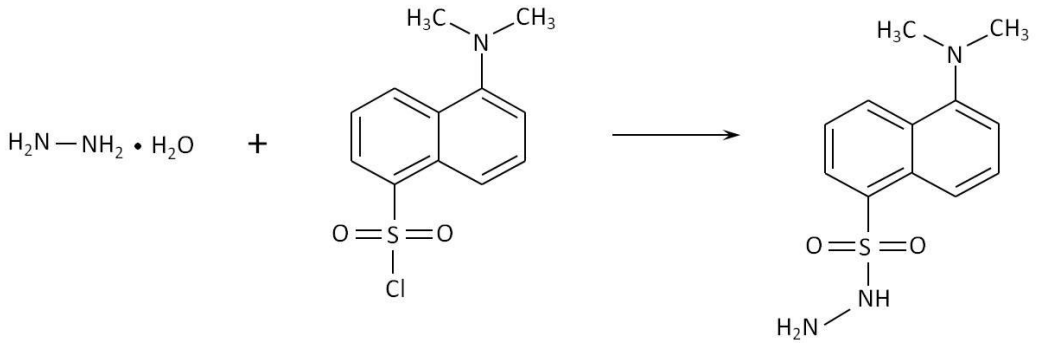

Figure 3.4. Synthetic scheme for the preparation of dansylhydrazine from the reaction of hydrazine hydrate with dansylchloride.

A synthesis for $^{13}C_2$-DnsCl has been developed in our research group and is based on the two-step reaction of $^{13}C_2$-dimethylsulfate with 5-aminonaphthalene-1-sulfonic acid to produce $^{13}C_2$-5-dimethylamino-naphthalene-1-sulfonic acid and then further reaction with phosphorous pentachloride to yield $^{13}C_2$-DnsCl.[10] Based on this synthetic scheme, one preparation devised for the production of an isotope form of DH was the reaction of purified $^{13}C_2$-DnsCl with hydrazine hydrate to produce $^{13}C_2$-DH, as outlined in Figure 3.5. While this synthesis would have been very likely to have produced the desired product, a three-step reaction, including a rigorous purification procedure to obtain $^{13}C_2$-DnsCl prior to the synthesis of $^{13}C_2$-DH, was undesirable.

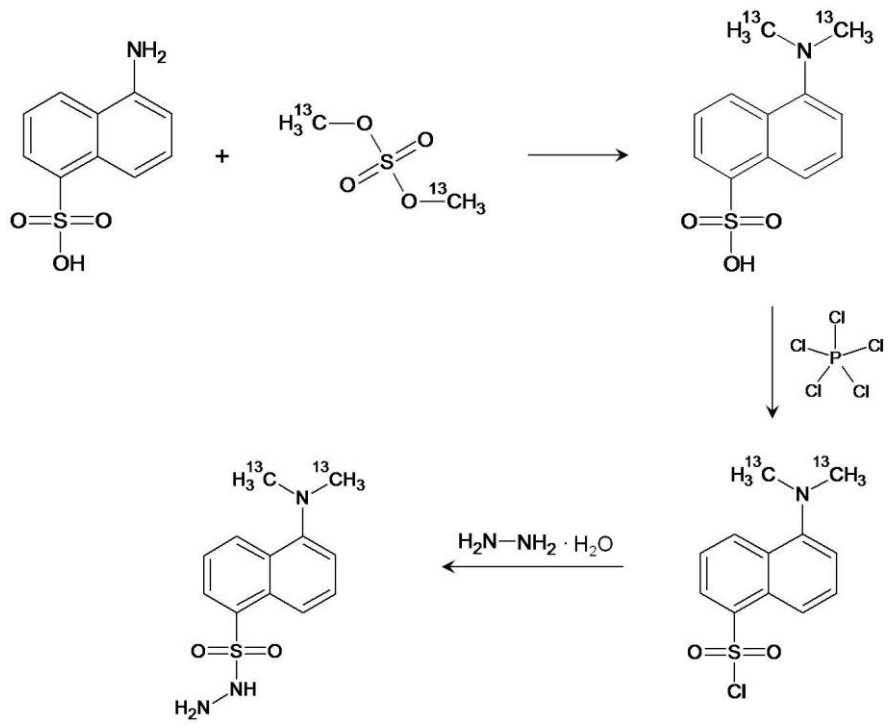

Figure 3.5. Synthetic scheme for the production of $^{13}C_2$-dansylhydrazine.

Another isotope form of DH considered was the ^{15}N isotope form. ^{15}N isotope standards are not as common for LC-MS based studies, most likely due to their poor availability and high cost. Based on a review of literature material, an isotope effect was not expected for the paired labeling reagents $^{15}N_2$-/$^{14}N_2$-DH. Using our synthetic scheme to obtain DH as the product of the reaction of DnsCl with hydrazine, a one-step reaction of DnsCl with $^{15}N_2$-hydrazine was devised for the production of $^{15}N_2$-DH. This reaction scheme was chosen due to its simplicity. $^{15}N_2$-hydrazine was available commercially in the forms of $^{15}N_2$-hydrazine monohydrate ($H_2{}^{15}N{}^{15}NH_2 \cdot H_2O$) and $^{15}N_2$-hydrazine sulfate salt ($H_2{}^{15}N{}^{15}NH_2 \cdot H_2SO_4$). Both forms were very expensive. $^{15}N_2$-hydrazine sulfate salt was half the cost of the monohydrate and was therefore chosen as the reagent for the synthesis, where the reaction scheme used to obtain $^{15}N_2$-DH is shown in Figure 3.1. Use of the sulfate salt required modification of our previously developed synthesis of DH to accommodate the change in forms of hydrazine from the hydrate solution to the sulfate salt. Mainly a base needed to be used in

order to consume the acid produced during the reaction by the release of the sulfate salt to form sulfuric acid. Bases evaluated for use with the reaction included sodium hydroxide, triethylamine, pyridine, 1,8-Diazabicyclo[5.4.0]undec-7-ene, sodium hydride, and sodium methoxide, as well as a carbonate buffer (pH 9.4). An aqueous solution of sodium hydroxide was found to be the most appropriate base for use with the reaction. Other bases lead to incomplete reactions or formation of reaction by-products. Also since this is an S_N2 reaction, a polar aprotic solvent was desirable. Toluene, a non-polar solvent, was inappropriate. The hydrazine sulfate salt was also found to be insoluble in toluene which was problematic. Tetrahydrofuran (THF) was found to be an appropriate reaction solvent, due to the fact that it is both a polar aprotic solvent and it was able to solvate the salt. THF was to be removed from the crude product immediately as it was found to react with the product if left overnight at room temperature. Dichloromethane (DCM), also a polar aprotic solvent, was determined to be appropriate for reconstitution of the product for crude purification as the product was found to be both soluble and stable for extended periods of time in this solvent. The product was purified first by liquid-liquid extraction and then by flash chromatography. LC-MS chromatograms showing the purity of the starting material, DnsCl, the commercially available DH standard, the crude DH synthesis product, and the final DH synthesis product following liquid-liquid extraction and flash chromatography purification are shown in Figure 3.6, panels (A), (B), (C), and (D), respectively. The chromatograms presented in Figure 3.7 display the step-wise extraction of the crude product from the aqueous layer to the organic layer during liquid-liquid extraction. Figure 3.8 shows the LC-MS chromatograms of the crude and final purified $^{15}N_2$-DH product.

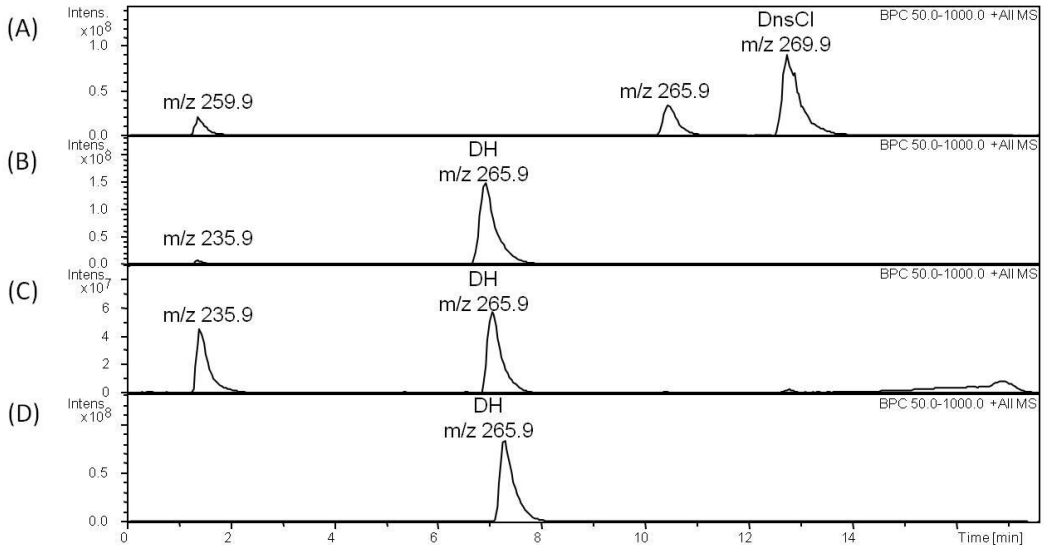

Figure 3.6. BPCs acquired by LC-MS (Esquire 3000plus) of (A) commercially available DnsCl standard used for synthesis, (B) commercially available DH standard, (C) crude DH product after 45 min reaction time, and (D) final purified DH reaction product.

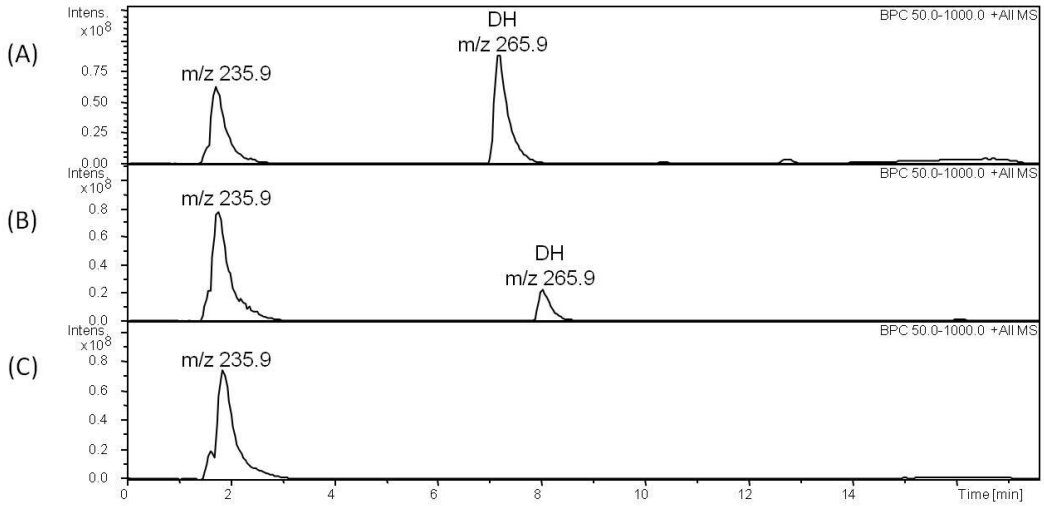

Figure 3.7. BPCs acquired by LC-MS (Esquire 3000plus) of (A) crude DH product following reconstitution in DCM prior to liquid-liquid extraction, (B) the liquid-liquid extraction aqueous layer showing diminished DH content, and (C) the final liquid-liquid extraction aqueous layer showing that DH was completely

recovered to the organic layer, while removing the major impurity 5-dimethylaminonaphthalene-1-sulfonyl, m/z 235.9, from the product.

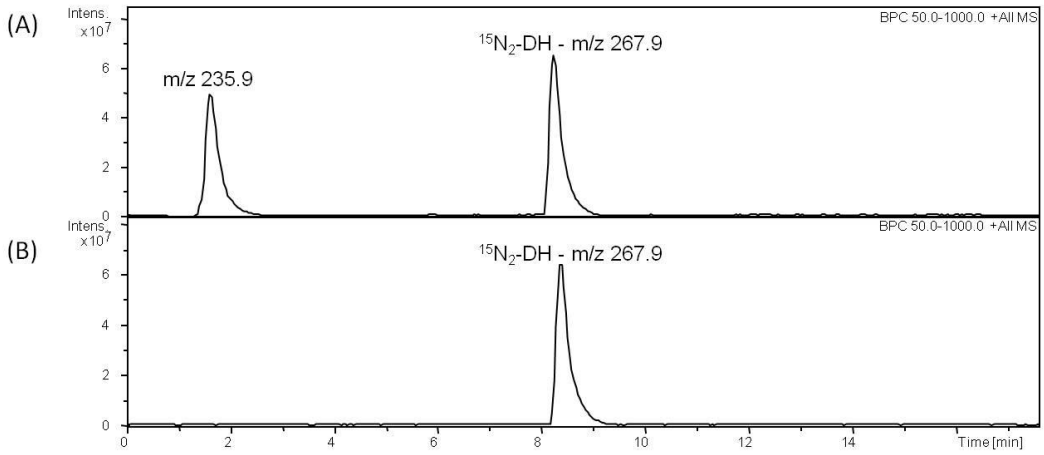

Figure 3.8. BPCs acquired by LC-MS (Esquire 3000plus) of (A) crude $^{15}N_2$-DH reaction product, and (B) final purified $^{15}N_2$-DH reaction product.

As desired, the synthesized $^{15}N_2$-DH was found to co-elute exactly with $^{14}N_2$-DH in LC-MS with no observed isotope effect or ionization suppression. In Figure 3.9, the LC-MS chromatogram is presented showing the co-elution of equimolar amounts of the commercially purchased $^{14}N_2$-DH and the synthesized $^{15}N_2$-DH in panel (A). Panels (B) and (C) show the MS of the isotopic signature obtained by LC ion trap MS and panel (D) shows the MS of the isotopic signature and mass accuracy obtained by nLC-nESI FT-ICR-MS. The utility of the differential $^{15}N_2$-/$^{14}N_2$-DH isotope labeling technique was initially tested by labeling a human urine sample with $^{14}N_2$-DH and a set of ten aldehyde standards with $^{15}N_2$-DH, as would be done for absolute quantitation experiments. The LC-MS chromatogram is presented in Figure 3.10. The metabolite isoforms co-eluted and confirmed the potential of this strategy for carbonyl metabolite identification and quantitation.

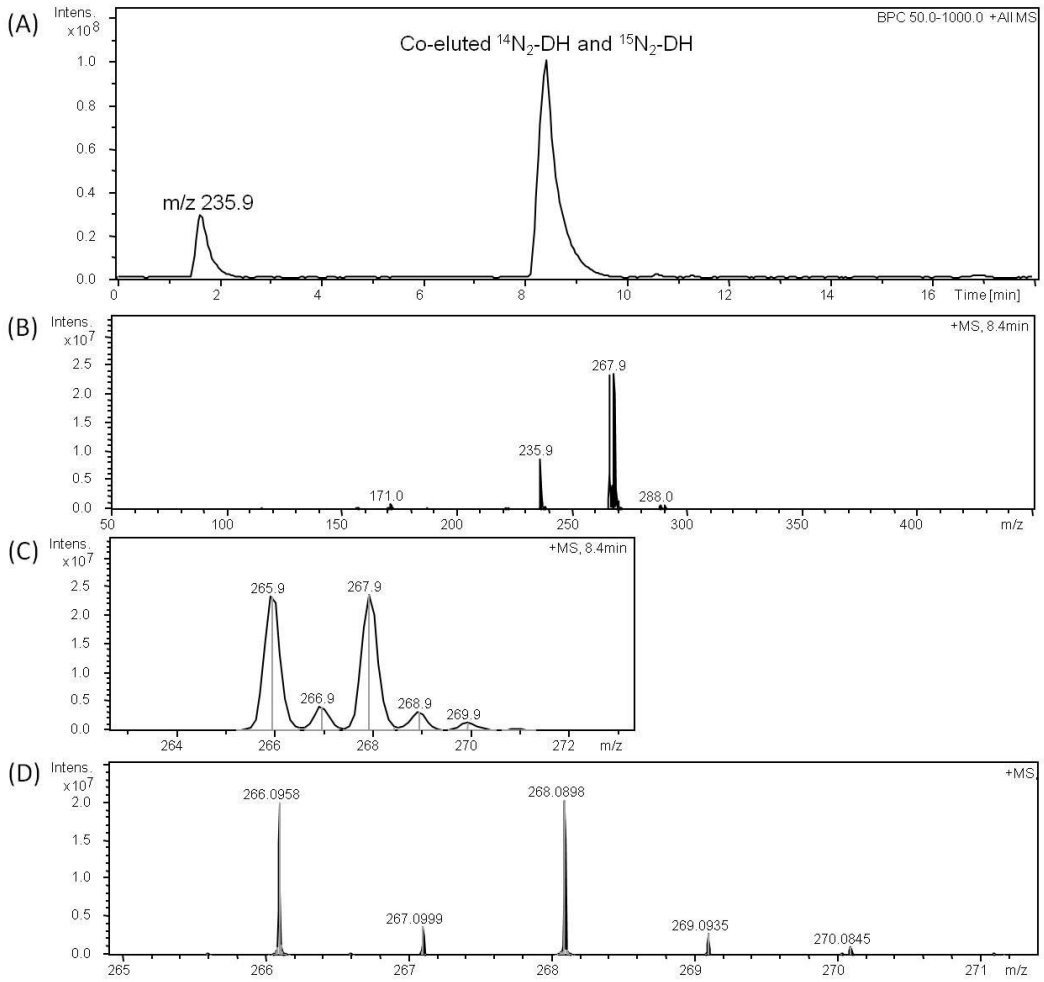

Figure 3.9. (A) BPC of a 1:1 mixture of the commercially available $^{14}N_2$-DH standard and the synthesized purified $^{15}N_2$-DH product acquired by LC-MS (Esquire 3000plus), where m/z 235.9 is a contaminant of the commercially available $^{14}N_2$-DH. (B) MS of the co-eluted peak of $^{14}N_2$-DH and $^{15}N_2$-DH. (C) Zoomed in view of (B) showing the isotopic pattern in the MS. (D) Zoomed in view of the MS of co-eluted $^{14}N_2$-DH and $^{15}N_2$-DH showing the observed isotopic pattern and mass accuracy obtained by nLC-nESI FT-ICR-MS.

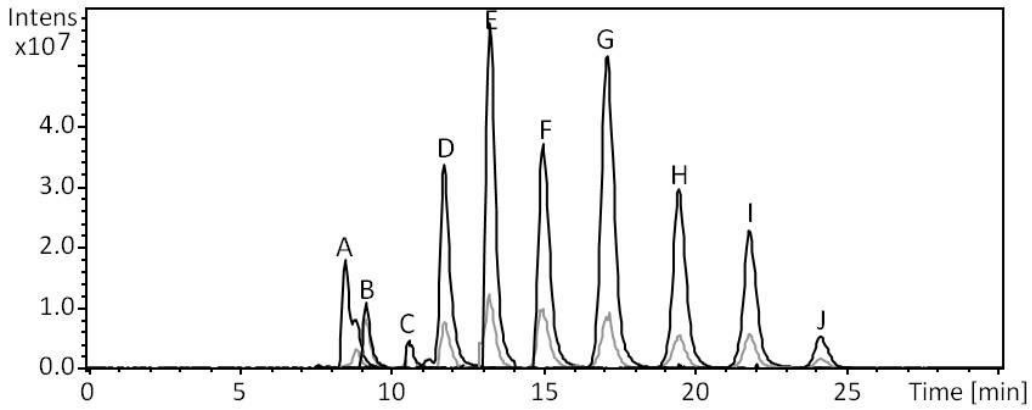

Figure 3.10. EICs of $^{14}N_2$-DH labeled human urinary aldehydes (shown in grey) and $^{15}N_2$-DH labeled aldehyde standards (shown in black) obtained by LC-MS (Esquire 3000plus) displaying co-elution of the isoforms. Where A = formaldehyde, B = acetaldehyde, C = propanal, D = butanal, E = pentanal, F = hexanal, G = heptanal, H = octanal, I = nonanal, and J = decanal.

The use of differential isotope labeling, along with accurate mass measurement, can be used to facilitate the identification of metabolites in complex samples. For differential $^{15}N_2$-/$^{14}N_2$-DH labeling, the mass difference of the ion pair from the $^{14}N_2$- and $^{15}N_2$-labeled metabolite is 1.994070 Da. In the FT-ICR-MS experiments, it was found that the error in the actual mass difference of an ion pair, compared to the theoretical difference, was less than 2 ppm. Thus, the ion pair belonging to the same metabolite can be readily picked up based on the criterion that the error in mass difference must be within 2 ppm. Other non-carbonyl signals such as chemical noise, background signals and unlabeled compounds will not show such characteristic ion pairing. They would show as singlet peaks and the coincidence of two adjacent singlet peaks with their mass difference corresponding to 1.994070 within 2 ppm is rare.

Labeling efficiency was tested by derivatizing equimolar amounts of standards from our DH standard library with $^{14}N_2$-DH and $^{15}N_2$-DH and then combining prior to nLC-nESI FT-ICR-MS. The peak area ratios of co-eluted labeled standard isoforms were measured and were observed to be acceptable,

with an average ratio of 0.97 based on the thirty standards tested, as presented in Table 3.1.

Table 3.1. Peak area ratios of co-eluted $^{15}N_2$-/$^{14}N_2$-DH labeled standards.

Differentially Labeled Standard	**HMDB #**	**Peak Area Ratio**
Formaldehyde	-	0.80
Acetaldehyde	HMDB00990	0.97
Propanal	HMDB03366	1.01
Butanal	HMDB03543	0.96
Pentanal	-	0.95
Hexanal	HMDB05994	1.02
Heptanal	-	0.94
Octanal	HMDB01140	0.98
Nonanal	-	0.92
Decanal	HMDB11623	1.00
Acetone	HMDB01659	1.15
Diacetyl	HMDB03407	0.86
2-Heptanone	HMDB03671	0.93
4-Heptanone	HMDB04814	0.92
3-Octanone	-	1.15
Cyclohexanone	HMDB03315	1.02
Succinic acid semialdehyde	HMDB01259	0.94
Glyceraldehyde	HMDB01051	1.06
Phenylacetaldehyde	HMDB06236	0.94
3-Methylbutanal	HMDB06478	0.85
2-Methyl-3-ketovaleric acid	HMDB00408	1.16
Levulinic acid	HMDB00720	0.81
Ketoleucine	HMDB00695	0.95
Oxaloacetic acid	HMDB00223	0.87
Methylacetoacetic acid	HMDB00310	0.87
Phenylacetylglycine	HMDB00821	0.99
Salicyluric acid	HMDB00840	0.90
Hippuric acid	HMDB00714	1.15
Androsterone	HMDB00031	0.97
17-Hydroxyprogesterone	HMDB00374	1.09
	Average =	**0.97**

The devised differential isotope $^{15}N_2$-/$^{14}N_2$-labeling strategy was developed to provide quantitative information on the metabolites labeled in biofluids. Recovery was evaluated by (A) spiking 100 μL aliquots of urine with standards (in triplicate) and then reducing to dryness as per the normal protocol, followed by reconstitution in methanol and labeling with $^{14}N_2$-DH. Known amounts of the standards were labeled with $^{15}N_2$-DH and the light and heavy labeled samples combined prior to nLC-nESI FT-ICR-MS analysis. The ion pair ratios were then used to calculate recoveries. Alternatively, in experiment (B), 100 μL aliquots of urine were reduced to dryness and reconstituted in methanol as per the normal protocol; the samples were then spiked with standards (in triplicate) and then labeled with $^{14}N_2$-DH. Then similarly, known amounts of the standards were labeled with $^{15}N_2$-DH and the light and heavy labeled samples combined prior to nLC-nESI FT-ICR-MS analysis with the ion pair ratios used to determine recoveries of the spiked analytes. Recovery was evaluated in both manners (A and B) in order to determine if reducing the urine sample to dryness using a SpeedVac was affecting metabolite concentrations in the sample. Recoveries were found to fall within 80-100 % and reducing the urine aliquots to dryness had no effect on the yield of spiked carbonyl standards (see Table 3.2.). Labeling experiments were carried out in triplicate and reproducibility was high, with relative standard deviation on average of less than 5 %.

Table 3.2. Recoveries for (A) carbonyl standards spiked into urine and then reduced to dryness and labeled and (B) urine reduced to dryness and then spiked with standards and labeled.

Compound	A (% Recovery)	B (% Recovery)
2-Pentanone	88.3 ± 0.9	88.2 ± 5.2
Octanal	90.1 ± 5.1	93.2 ± 5.4

The linear range was investigated and was found to be limited by the instrument. Typically, the linear range was determined to be ~ 10-fold (see an example given for DH labeled nonanal in Figure 3.11). And therefore it was

important when performing quantitative experiments with the differential labeling technique that the amount of heavy labeled standard be close in concentration to the amount of light labeled analyte in the biofluid. For example, where sample analyte concentrations were found to be ~ 1 μM, the heavy labeled standards used for quantitation were of known concentrations in the range of 1 – 10 μM. Where analyte concentrations were not found at the expected concentration range, the experiment was repeated such that the heavy labeled standards were in the appropriate concentration range for accurate quantitation. Limits of detection and quantification were determined to be compound dependent.

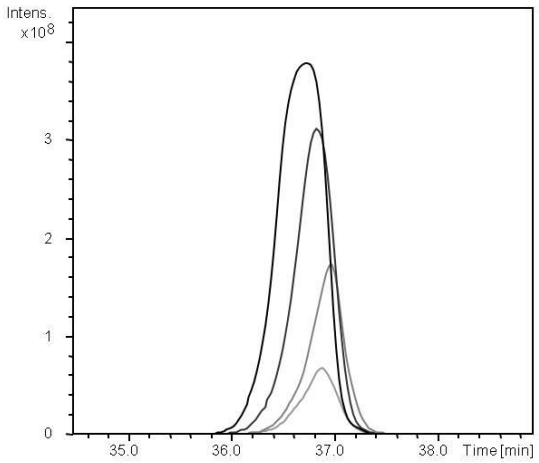

Figure 3.11. Overlaid EICs of injections of DH labeled nonanal at 0.52 μM, 1.0 μM, 2.1 μM, and 4.2 μM acquired by nLC-nESI FT-ICR-MS. Linear relationship based on MS intensity gives $R^2 = 0.997$ over this concentration range.

The differential isotope labeling method can be used to generate both a qualitative and quantitative carbonyl metabolome profile for biofluids. In order to produce a qualitative metabolome profile using the $^{15}N_2$-/$^{14}N_2$-DH labeling method, a biofluid sample must first be split into two equal amounts. One aliquot is labeled with $^{14}N_2$-DH and the other with $^{15}N_2$-DH. The two labeled portions are then re-combined and analyzed by nLC-nESI FT-ICR-MS. With the high resolution and mass accuracy provided by this analysis, metabolite ion pairs can then be picked based on their exact co-elution as well as the criterion that the error

in the characteristic mass difference be no greater than 2 ppm. Qualitative profiles were acquired for both human urine and plasma samples.

For the 1:1 $^{15}N_2$-/$^{14}N_2$-DH labeled urine sample, seventy-three ion pairs were detected from one nLC-nESI FT-ICR-MS run and eighty-three ion pairs were detected from a replicate analysis of a replicate sample (see Table 3.3). Fifty-six common ion pairs were found in the two runs. Tentative identification of these metabolites was carried out by searching the accurate mass of the metabolite peaks against the Human Metabolome Database (HMDB). The results are also shown in Table 3.3. Among ninety-nine ion pairs detected from the two runs, seventeen peaks matched with one metabolite entry and sixty-four matched with more than one entry.

For the 1:1 $^{15}N_2$-/$^{14}N_2$-DH labeled plasma sample, forty-nine ion pairs were detected from one nLC-nESI FT-ICR-MS run and forty-one ion pairs were detected from a replicate analysis of a replicate sample (see Table 3.4). Twenty-nine common ion pairs were found in the two runs. Tentative identification of these metabolites was carried out by searching the accurate mass of the metabolite peaks against the HMDB. Among sixty-one total ion pairs detected from the two runs, twelve peaks matched with one metabolite entry and thirty-eight matched with more than one entry.

Table 3.3. Ion pairs detected and identified by nLC-nESI FT-ICR-MS from a duplicate 1:1 $^{15}N_2$-/$^{14}N_2$-DH labeled urine sample.

Sample # 1					
Putative ID	**m/z(light)**	**m/z(heavy)**	**diff.**	**ratio**	**+MS Spectra**
Unknown	442.1284	444.1214	1.994	1.06	8.1-11.9min #(139-206)
Unknown	590.2032	592.1982	1.995	1.02	8.1-11.9min #(139-206)
Unknown	428.1480	430.1418	1.994	0.99	8.1-11.9min #(139-206)
Unknown	469.1729	471.1670	1.994	1.05	8.1-11.9min #(139-206)
Unknown	398.1381	400.1320	1.994	0.91	8.1-11.9min #(139-206)
Unknown	560.1918	562.1864	1.995	0.97	8.1-11.9min #(139-206)
Unknown	442.1264	444.1197	1.993	1.08	12.0-15.0min #(207-259)
Unknown	469.1737	471.1676	1.994	0.99	12.0-15.0min #(207-259)
Unknown	398.1383	400.1323	1.994	0.88	12.0-15.0min #(207-259)
Unknown	428.1486	430.1425	1.994	0.92	12.0-15.0min #(207-259)
Unknown	557.1929	559.1867	1.994	1.03	12.0-15.0min #(207-259)
Unknown	412.1536	414.1473	1.994	0.97	15.1-18.0min #(260-294)
Unknown	428.1484	430.1422	1.994	0.93	15.1-18.0min #(260-294)
Unknown	469.1760	471.1696	1.994	1.03	15.1-18.0min #(260-294)
Unknown	557.1929	559.1869	1.994	1.03	15.1-18.0min #(260-294)
Unknown	398.1386	400.1329	1.994	0.93	15.1-18.0min #(260-294)
Cyclohexanone	346.1588	348.1531	1.994	1.4	15.1-18.0min #(260-294)
Unknown	456.1445	458.1385	1.994	0.83	18.0-20.0min #(312-346)
Unknown	412.1544	414.1482	1.994	0.93	18.0-20.0min #(312-346)
Unknown	412.1541	414.1480	1.994	1.02	20.0-21.0min #(347-364)
Unknown	294.0907	296.0848	1.994	1.01	23.0-24.0min #(400-417)
Unknown	361.1443	363.1378	1.994	0.9	23.0-24.0min #(400-417)
Unknown	363.1851	365.1792	1.994	1.04	23.0-24.0min #(400-417)
Unknown	426.1332	428.1272	1.994	1.13	23.0-24.0min #(400-417)

Unknown	435.1820	437.1760	1.994	1.1	25.0-26.0min #(437-454)
Unknown	394.1070	396.1008	1.994	0.85	26.0-26.9min #(455-472)
Unknown	449.1971	451.1910	1.994	0.81	26.0-26.9min #(455-472)
Unknown	336.1018	338.0960	1.994	1.09	27.0-28.0min #(473-491)
Unknown	571.2074	573.2014	1.994	0.94	27.0-28.0min #(473-491)
Unknown	278.0963	280.0905	1.994	1.27	28.0-29.0min #(492-509)
Unknown	292.1119	294.1060	1.994	0.83	28.0-29.0min #(492-509)
Unknown	364.1703	366.1639	1.994	1.25	28.0-29.0min #(492-509)
Unknown	292.1120	294.1061	1.994	0.94	29.0-30.0min #(510-528)
Unknown	306.1276	308.1217	1.994	0.98	29.0-30.0min #(510-528)
Unknown	403.1809	405.1752	1.994	1.03	29.0-30.0min #(510-528)
Unknown	408.1235	410.1173	1.994	1.24	29.0-30.0min #(510-528)
Unknown	427.1445	429.1382	1.994	0.91	29.0-30.0min #(510-528)
Unknown	364.1361	366.1273	1.991	1.66	30.0-31.0min #(529-546)
11-beta-hydroxyl-androsterone-3-glucuronide	730.3413	732.3364	1.995	1.26	30.0-31.0min #(529-546)
Unknown	306.1276	308.1217	1.994	0.94	31.0-32.0min #(547-563)
Unknown	362.0756	364.0694	1.994	0.61	31.0-32.0min #(547-563)
Unknown	320.1430	322.1368	1.994	0.93	32.0-33.0min #(564-582)
Indole-5,6-quinone	395.1180	397.1121	1.994	0.91	32.0-33.0min #(564-582)
Unknown	420.1957	422.1897	1.994	0.84	32.0-33.0min #(564-582)
Unknown	320.1432	322.1371	1.994	0.92	33.1-34.0min #(583-599)
Unknown	461.2569	463.2505	1.994	1.07	33.1-34.0min #(583-599)
6-Succino-aminopurine	483.1537	485.1475	1.994	0.86	33.1-34.0min #(583-599)
Unknown	714.3467	716.3429	1.996	0.9	33.1-34.0min #(583-599)
3-Methylbutanal	334.1578	336.1516	1.994	0.86	34.0-35.0min #(600-617)
Cyclohexanone	346.1569	348.1505	1.994	0.89	34.0-35.0min #(600-617)
Unknown	599.2019	601.1961	1.994	0.68	34.0-35.0min #(600-617)

3-Methylbutanal	334.1575	336.1513	1.994	0.94	35.0-36.0min #(618-635)
Cyclohexanone	346.1579	348.1516	1.994	1.16	35.0-36.0min #(618-635)
Unknown	354.1265	356.1206	1.994	0.91	35.0-36.0min #(618-635)
Unknown	475.2690	477.2630	1.994	0.98	35.0-36.0min #(618-635)
Unknown	348.1739	350.1675	1.994	0.98	36.0-37.0min #(636-654)
Unknown	382.1349	384.1293	1.994	0.71	36.0-37.0min #(636-654)
Unknown	348.1729	350.1667	1.994	0.97	37.0-38.0min #(655-671)
Unknown	462.2439	464.2374	1.993	1.07	37.0-38.0min #(655-671)
Unknown	348.1745	350.1682	1.994	0.97	38.0-39.0min #(672-689)
Unknown	362.1903	364.1842	1.994	1.14	39.0-40.0min #(690-707)
Unknown	382.1588	384.1527	1.994	1.19	39.0-40.0min #(690-707)
Unknown	567.2110	569.2055	1.995	0.97	39.0-40.0min #(690-707)
Unknown	581.2057	583.2036	1.998	1.43	39.0-40.0min #(690-707)
Unknown	362.1902	364.1841	1.994	1.18	40.0-41.0min #(708-724)
Unknown	400.2060	402.1997	1.994	1.02	41.0-42.0min #(725-741)
Octanal	376.2058	378.1997	1.994	0.99	43.0-43.9min #(760-776)
Octanal	376.2054	378.1993	1.994	0.91	44.0-45.0min #(777-793)
Unknown	390.2215	392.2154	1.994	1.06	45.0-46.0min #(794-810)
Unknown	390.2214	392.2154	1.994	1.01	46.0-47.0min #(811-828)
Unknown	390.2213	392.2151	1.994	0.93	47.0-48.0min #(829-845)
Unknown	404.2373	406.2310	1.994	1.02	50.0-51.0min #(881-897)
Unknown	418.2529	420.2470	1.994	1.05	54.0-55.0min #(950-967)
Sample # 2					
Putative ID	**m/z(light)**	**m/z(heavy)**	**diff.**	**ratio**	**+MS Spectra**
Unknown	444.1451	446.1386	1.993	1.43	7.0-12.0min #(113-194)
Unknown	560.1909	562.1855	1.995	1.1	7.0-12.0min #(113-194)
Unknown	442.1242	444.1171	1.993	1.04	7.0-12.0min #(113-194)
Unknown	469.1719	471.1660	1.994	1.05	7.0-12.0min

					#(113-194)
Unknown	590.2016	592.1963	1.995	1.01	7.0-12.0min #(113-194)
Unknown	398.1369	400.1305	1.994	0.96	7.0-12.0min #(113-194)
Unknown	428.1450	430.1387	1.994	1.03	7.0-12.0min #(113-194)
Unknown	398.1379	400.1318	1.994	0.97	12.0-14.9min #(195-244)
Unknown	428.1480	430.1418	1.994	1.01	12.0-14.9min #(195-244)
Unknown	469.1722	471.1663	1.994	1.03	12.0-14.9min #(195-244)
Unknown	557.1914	559.1854	1.994	1.14	12.0-14.9min #(195-244)
Unknown	560.1907	562.1855	1.995	1.2	12.0-14.9min #(195-244)
Unknown	412.1537	414.1475	1.994	1.06	12.0-14.9min #(195-244)
Methyl bisnor-biotinyl ketone	462.1470	464.1452	1.998	4.07	12.0-14.9min #(195-244)
Unknown	398.1384	400.1327	1.994	1.09	15.0-18.0min #(245-295)
Unknown	428.1489	430.1424	1.993	1.07	15.0-18.0min #(245-295)
Unknown	469.1755	471.1693	1.994	1.16	15.0-18.0min #(245-295)
Unknown	557.1929	559.1868	1.994	1.12	15.0-18.0min #(245-295)
Cyclohexanone	346.1587	348.1529	1.994	1.29	15.0-18.0min #(245-295)
Unknown	456.1436	458.1371	1.993	0.89	15.0-18.0min #(245-295)
Unknown	571.2077	573.2026	1.995	1.23	15.0-18.0min #(245-295)
Unknown	304.0522	306.0462	1.994	1.02	15.0-18.0min #(245-295)
Unknown	412.1545	414.1483	1.994	1.03	15.0-18.0min #(245-295)
Unknown	412.1545	414.1484	1.994	1.04	18.0-21.0min #(296-345)
Unknown	304.0520	306.0461	1.994	1.05	18.0-21.0min #(296-345)
Unknown	361.1445	363.1383	1.994	1.01	18.0-21.0min #(296-345)
Unknown	294.0910	296.0851	1.994	1.35	22.0-23.0min #(362-378)
Unknown	361.1447	363.1385	1.994	0.99	22.0-23.0min #(362-378)
Unknown	416.1391	418.1330	1.994	0.97	23.0-23.9min #(379-394)
Unknown	433.1651	435.1584	1.993	0.98	23.0-23.9min #(379-394)
Unknown	294.0911	296.0853	1.994	1.42	24.0-25.0min #(395-411)

Unknown	539.1801	541.1741	1.994	0.98	24.0-25.0min #(395-411)
Unknown	380.1648	382.1590	1.994	0.96	25.0-26.0min #(412-428)
Unknown	394.1068	396.1005	1.994	0.9	25.0-26.0min #(412-428)
Unknown	449.1969	451.1902	1.993	0.98	25.0-26.0min #(412-428)
Unknown	394.1072	396.1010	1.994	0.95	26.0-27.0min #(429-445)
Unknown	571.2070	573.2010	1.994	0.96	26.0-27.0min #(429-445)
Unknown	336.1019	338.0960	1.994	1.15	27.0-28.0min #(446-461)
Unknown	571.2058	573.2002	1.994	0.93	27.0-28.0min #(446-461)
Unknown	292.1120	294.1061	1.994	0.96	28.0-29.0min #(462-478)
Unknown	364.1698	366.1637	1.994	1.35	28.0-29.0min #(462-478)
Unknown	427.1435	429.1376	1.994	1.1	28.0-29.0min #(462-478)
Unknown	306.1275	308.1217	1.994	1.21	29.1-30.0min #(479-495)
Unknown	403.1809	405.1748	1.994	1.19	29.1-30.0min #(479-495)
Unknown	408.1235	410.1174	1.994	1.06	29.1-30.0min #(479-495)
Unknown	362.0764	364.0702	1.994	0.78	30.0-31.0min #(496-512)
Unknown	362.0766	364.0707	1.994	0.75	31.0-32.0min #(513-529)
Unknown	320.1429	322.1368	1.994	1.04	32.0-33.0min #(530-546)
Indole-5,6-quinone	395.1182	397.1123	1.994	0.99	32.0-33.0min #(530-546)
Unknown	420.1960	422.1899	1.994	0.92	32.0-33.0min #(530-546)
N-Acetyl-9-O-lactoylneur-aminic acid	629.2125	631.2059	1.993	0.83	32.0-33.0min #(530-546)
Unknown	320.1429	322.1370	1.994	1.11	33.0-34.0min #(547-563)
Cyclohexanone	346.1576	348.1515	1.994	0.93	33.0-34.0min #(547-563)
6-Succino-aminopurine	483.1502	485.1443	1.994	1.01	33.0-34.0min #(547-563)
N-Acetyl-9-O-lactoylneur-aminic acid	629.2119	631.2057	1.994	0.79	33.0-34.0min #(547-563)
Unknown	714.3453	716.3413	1.996	0.75	33.0-34.0min #(547-563)
3-Methylbutanal	334.1576	336.1514	1.994	0.98	34.0-35.0min #(564-580)
Cyclohexanone	346.1576	348.1512	1.994	1.11	34.0-35.0min

					#(564-580)
Unknown	380.1426	382.1404	1.998	1.15	34.0-35.0min #(564-580)
Unknown	599.2010	601.1950	1.994	0.75	34.0-35.0min #(564-580)
3-Methylbutanal	334.1589	336.1529	1.994	1.14	35.0-36.0min #(581-595)
Cyclohexanone	346.1587	348.1527	1.994	1.17	35.0-36.0min #(581-595)
Unknown	475.2693	477.2632	1.994	1.06	35.0-36.0min #(581-595)
Unknown	657.2028	659.2007	1.998	2.59	35.0-36.0min #(581-595)
Unknown	348.1736	350.1673	1.994	1.09	36.0-37.0min #(596-612)
Unknown	382.1353	384.1297	1.994	0.73	36.0-37.0min #(596-612)
Indole-5,6-quinone	395.1164	397.1105	1.994	0.72	36.0-37.0min #(596-612)
Unknown	421.1589	423.1488	1.99	1.25	36.0-37.0min #(596-612)
Unknown	348.1735	350.1671	1.994	1.03	37.0-38.0min #(613-629)
Unknown	462.2436	464.2370	1.993	1.03	37.0-38.0min #(613-629)
Unknown	539.1793	541.1736	1.994	1.08	37.0-38.0min #(613-629)
Unknown	348.1746	350.1680	1.993	1.05	38.0-39.0min #(630-647)
Unknown	382.1591	384.1530	1.994	1.52	38.0-39.0min #(630-647)
Unknown	539.1794	541.1738	1.994	0.99	38.0-39.0min #(630-647)
Entacapone	553.1956	555.1895	1.994	1.01	38.0-39.0min #(630-647)
Unknown	362.1905	364.1844	1.994	1.29	39.1-40.0min #(648-664)
Unknown	567.2112	569.2058	1.995	1.06	39.1-40.0min #(648-664)
Unknown	581.2091	583.2081	1.999	1.36	39.1-40.0min #(648-664)
Unknown	362.1905	364.1844	1.994	1.24	40.0-41.0min #(665-682)
Unknown	400.2061	402.1999	1.994	0.9	41.0-42.0min #(683-699)
Octanal	376.2059	378.1999	1.994	1.11	43.0-44.0min #(717-734)
Unknown	390.2213	392.2152	1.994	1.11	47.0-48.0min #(783-798)
Unknown	404.2370	406.2307	1.994	1.13	50.1-51.0min #(831-847)

Table 3.4. Ion pairs detected and identified by nLC-nESI FT-ICR-MS from a duplicate 1:1 $^{15}N_2$-/$^{14}N_2$-DH labeled plasma sample.

Sample # 1					
Putative ID	**m/z(light)**	**m/z(heavy)**	**diff.**	**ratio**	**+MS Spectra**
Unknown	428.1446	430.1386	1.994	0.94	7.0-13.0min #(130-243)
Cyclohexanone	346.1590	348.1531	1.994	1.39	13.0-14.0min #(244-262)
Cyclohexanone	346.1591	348.1532	1.994	1.38	14.0-15.0min #(263-281)
Unknown	288.0780	290.0721	1.994	0.96	17.0-18.0min #(319-337)
Unknown	294.0908	296.0844	1.994	0.79	19.0-20.0min #(357-375)
Unknown	587.1777	589.1717	1.994	0.58	19.0-20.0min #(357-375)
Unknown	589.1721	591.1658	1.994	2.09	20.1-21.0min #(376-393)
Unknown	363.1859	365.1799	1.994	1.02	24.0-25.0min #(450-468)
Unknown	394.1077	396.1017	1.994	1.49	24.0-25.0min #(450-468)
Unknown	456.1452	458.1392	1.994	0.90	24.0-25.0min #(450-468)
Unknown	426.1338	428.1277	1.994	1.02	25.0-26.0min #(469-487)
Unknown	278.0966	280.0907	1.994	1.07	26.0-27.0min #(488-505)
Unknown	336.0996	338.0934	1.994	0.89	26.0-27.0min #(488-505)
Unknown	292.1110	294.1046	1.994	0.68	27.0-28.0min #(506-524)
Unknown	336.1020	338.0956	1.994	1.05	27.0-28.0min #(506-524)
Unknown	364.1682	366.1621	1.994	0.91	27.0-28.0min #(506-524)
Unknown	585.2119	587.2058	1.994	1.36	27.0-28.0min #(506-524)
Unknown	292.1113	294.1050	1.994	0.62	28.1-29.0min #(525-542)
Unknown	585.2128	587.2068	1.994	1.48	28.1-29.0min #(525-542)
Unknown	306.1272	308.1208	1.994	0.75	29.0-30.0min #(543-560)
Unknown	362.1523	364.1463	1.994	0.78	29.0-30.0min #(543-560)
Unknown	380.1643	382.1582	1.994	1.02	29.0-30.0min #(543-560)
Unknown	512.2359	514.2300	1.994	1.05	29.0-30.0min #(543-560)
Unknown	306.1259	308.1196	1.994	0.77	30.0-31.0min #(561-578)

Unknown	362.0772	364.0708	1.994	0.64	30.0-31.0min #(561-578)
Unknown	380.1639	382.1577	1.994	1.16	30.0-31.0min #(561-578)
Unknown	306.1272	308.1212	1.994	1.04	31.0-32.0min #(579-597)
Unknown	320.1426	322.1364	1.994	0.81	31.0-32.0min #(579-597)
Unknown	364.1687	366.1629	1.994	0.95	31.0-32.0min #(579-597)
Unknown	378.1461	380.1399	1.994	0.98	31.0-32.0min #(579-597)
Unknown	320.1422	322.1360	1.994	0.82	32.0-33.0min #(598-615)
Unknown	378.1458	380.1397	1.994	1.31	32.0-33.0min #(598-615)
Unknown	380.1643	382.1584	1.994	0.33	32.0-33.0min #(598-615)
3-Methylbutanal	334.1584	336.1523	1.994	0.87	33.0-34.0min #(616-633)
Unknown	378.1458	380.1397	1.994	1.61	33.0-34.0min #(616-633)
Unknown	334.1572	336.1511	1.994	0.81	34.0-35.0min #(634-652)
Unknown	475.2695	477.2636	1.994	0.90	34.0-35.0min #(634-652)
3-Methylbutanal	334.1570	336.1511	1.994	0.92	35.0-36.0min #(653-670)
Unknown	348.1736	350.1673	1.994	0.84	36.0-37.0min #(671-689)
3-Oxodecanoic acid	434.2107	436.2044	1.994	0.88	36.0-37.0min #(671-689)
Unknown	348.1741	350.1677	1.994	0.80	37.1-38.0min #(690-707)
3-Oxodecanoic acid	434.2096	436.2032	1.994	0.92	37.1-38.0min #(690-707)
Unknown	382.1567	384.1507	1.994	0.63	38.0-39.0min #(708-725)
Unknown	581.2283	583.2227	1.994	0.90	39.0-40.0min #(726-744)
Unknown	362.1910	364.1847	1.994	1.18	40.0-41.0min #(745-762)
Octanal	376.2063	378.2003	1.994	0.97	43.0-44.0min #(800-817)
Unknown	390.2211	392.2147	1.994	0.87	46.0-47.0min #(855-872)
Unknown	390.2216	392.2152	1.994	0.95	47.0-48.0min #(873-891)
Unknown	404.2380	406.2319	1.994	0.86	50.0-51.0min #(928-946)
Sample # 2					
Putative ID	**m/z(light)**	**m/z(heavy)**	**diff.**	**ratio**	**+MS Spectra**
Unknown	428.1450	430.1390	1.994	0.96	8.0-13.0min

					#(148-165)
Unknown	338.1177	340.1118	1.994	0.92	16.0-17.0min #(295-313)
Cyclohexanone	346.1591	348.1533	1.994	1.32	16.0-17.0min #(295-313)
Unknown	288.0781	290.0721	1.994	0.93	17.0-18.0min #(314-331)
Unknown	294.0904	296.0840	1.994	0.98	20.0-21.0min #(369-387)
Unknown	585.1615	587.1558	1.994	0.51	22.1-23.0min #(407-424)
Unknown	278.0965	280.0906	1.994	1.05	28.0-29.0min #(519-536)
Unknown	292.1110	294.1048	1.994	0.81	28.0-29.0min #(519-536)
Unknown	585.2120	587.2055	1.994	1.53	28.0-29.0min #(519-536)
Unknown	292.1121	294.1062	1.994	0.76	29.0-30.0min #(537-554)
Unknown	306.1279	308.1220	1.994	0.87	29.0-30.0min #(537-554)
Unknown	362.0789	364.0729	1.994	0.89	30.0-31.0min #(555-572)
Estrone sulfate	598.1907	600.1847	1.994	0.68	30.0-31.0min #(555-572)
Unknown	306.1267	308.1205	1.994	0.81	31.0-32.0min #(573-590)
Unknown	362.0769	364.0706	1.994	0.66	31.0-32.0min #(573-590)
Unknown	378.1460	380.1398	1.994	1.05	31.0-32.0min #(573-590)
Unknown	542.2412	544.2353	1.994	0.94	31.0-32.0min #(573-590)
Estrone sulfate	598.1937	600.1875	1.994	0.72	31.0-32.0min #(573-590)
Unknown	320.1436	322.1376	1.994	0.85	32.0-33.0min #(591-609)
Unknown	364.1699	366.1639	1.994	1.13	32.0-33.0min #(591-609)
Unknown	420.1959	422.1897	1.994	0.97	32.0-33.0min #(591-609)
Unknown	320.1430	322.1370	1.994	0.90	33.1-33.9min #(610-626)
Cyclohexanone	346.1582	348.1520	1.994	0.75	33.1-33.9min #(610-626)
Unknown	378.1459	380.1397	1.994	1.19	33.1-33.9min #(610-626)
Unknown	610.2978	612.2920	1.994	1.25	33.1-33.9min #(610-626)
3-Methylbutanal	334.1591	336.1528	1.994	0.84	34.0-35.0min #(627-645)
Unknown	378.1464	380.1404	1.994	1.80	34.0-35.0min #(627-645)
Unknown	475.2700	477.2638	1.994	0.88	34.0-35.0min #(627-645)

Unknown	334.1571	336.1511	1.994	0.87	35.1-36.0min #(646-663)
Unknown	346.1574	348.1510	1.994	0.86	35.1-36.0min #(646-663)
Unknown	475.2692	477.2633	1.994	0.93	35.1-36.0min #(646-663)
Unknown	348.1750	350.1690	1.994	0.87	36.0-37.0min #(664-681)
Unknown	497.1326	499.1270	1.994	1.01	36.0-37.0min #(664-681)
Unknown	348.1748	350.1684	1.994	0.83	37.0-38.0min #(682-699)
3-Oxodecanoic acid	434.2104	436.2040	1.994	0.91	37.0-38.0min #(682-699)
Unknown	382.1558	384.1497	1.994	0.81	38.0-39.0min #(700-717)
Unknown	382.1554	384.1492	1.994	0.87	39.0-40.0min #(718-735)
Octanal	376.2066	378.2005	1.994	0.91	43.0-44.0min #(791-808)
Unknown	390.2220	392.2160	1.994	0.99	45.1-46.0min #(828-845)
Unknown	390.2216	392.2152	1.994	0.92	47.0-48.0min #(864-881)
Unknown	404.2379	406.2318	1.994	0.90	50.0-51.0min #(919-937)

For positive identification of the carbonyl metabolites, the DH standard library was used to compare the mass and retention time of the ion pairs in combination with quantitative labeling studies. Absolute quantification of urinary and plasma metabolites was performed by first labeling the biofluid sample of interest with $^{14}N_2$-DH (light label) and separately labeling a set of standards with $^{15}N_2$-DH (heavy label) (see Figure 3.12). The light labeled sample was combined with the heavy labeled standards and introduced into the LC-MS generating a $^{15}N_2$-labeled internal standard for each of the $^{14}N_2$-labeled analytes. Figure 3.13 panel (A) shows the ion chromatogram of a $^{14}N_2$-DH labeled urine sample spiked with twelve $^{15}N_2$-DH labeled aldehydes. Figure 3.13 panel (B) shows the expanded mass spectrum of the peak pair of co-eluted decanal. No isotopic effect was observed in RPLC, allowing accurate quantification. The peak abundance ratio of the $^{15}N_2$-/$^{14}N_2$-labeled pair can be obtained from the mass spectra such as the one shown in Figure 3.13, panel (B). From the known concentration of $^{15}N_2$-

DH labeled standard used, the absolute concentration of the metabolite in the biofluid sample can be determined.

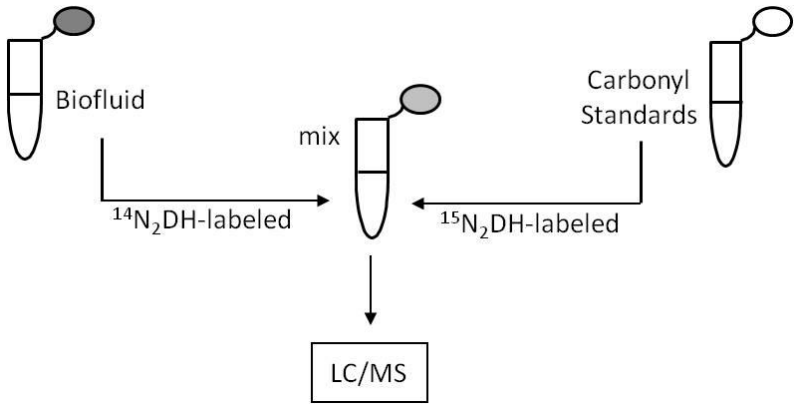

Figure 3.12. $^{15}N_2$-/$^{14}N_2$-DH labeling strategy for the absolute quantitation of the human carbonyl metabolome using nLC-nESI FT-ICR-MS.

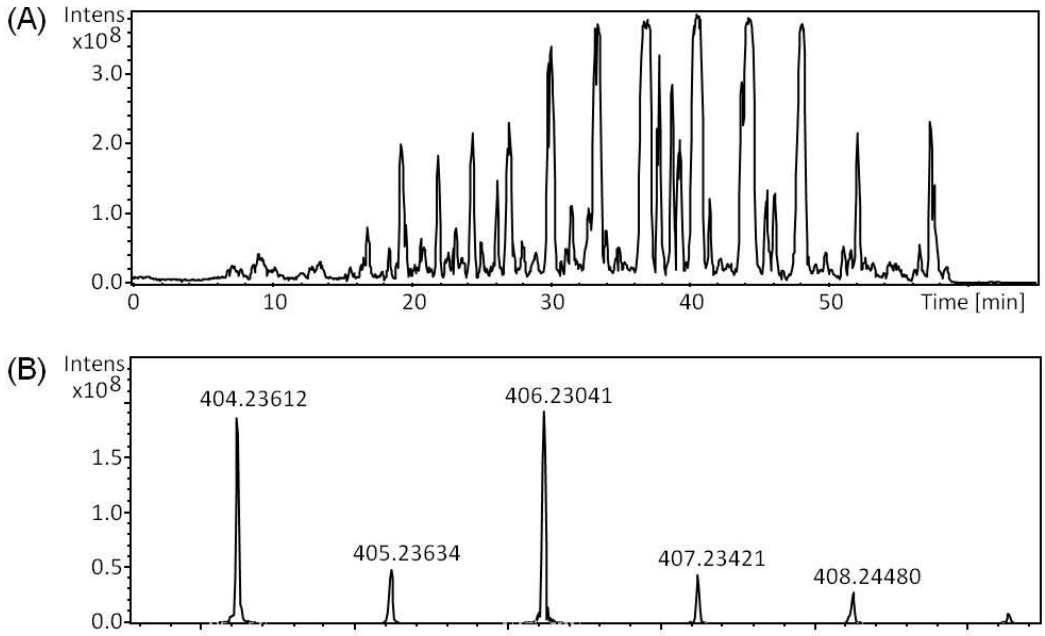

Figure 3.13. (A) BPC of $^{14}N_2$-DH labeled human urine with known quantities of twelve $^{15}N_2$-DH labeled aldehydes obtained using nLC-nESI FT-ICR-MS. (B) Expanded mass spectrum of the $^{15}N_2$-/$^{14}N_2$-DH-decanal ion pair from (A).

Of fifty-four carbonyls tested from our developed DH standard library, thirty-six carbonyl metabolites, including a variety of ketones, aldehydes, and keto-acids were identified in human urine and thirty-six carbonyl metabolites were identified in human plasma. Table 3.5 shows the list of concentrations of the carbonyl metabolites positively identified and quantified in the human urine sample. They range from 0.4 nM – 5.5 μM with an average RSD of 8.7 % between triplicate experiments. Table 3.6 shows the list of concentrations of the carbonyl metabolites positively identified and quantified in the human plasma sample. They range from 0.3 nM – 3.09 μM with an average RSD of 9.6 % between triplicate experiments. Thirty-one common metabolites were positively identified and quantified in both the urine and plasma samples. Five unique metabolites were positively identified and quantified in each of the biofluids.

Table 3.5. List of thirty-six carbonyl metabolites quantified in human urine using the differential $^{15}N_2$-/$^{14}N_2$-DH labeling method with analysis by nLC-nESI FT-ICR-MS.

Standard	**HMDB Accession #**	**t_R (min)**	**$^{14}N_2$-DH $[M+H]^+$**	**$^{15}N_2$-DH $[M+H]^+$**	**Conc. in Urine (μM)**
Formaldehyde	HMDB01426	13.2	278.09577	280.08984	0.071 ± 0.005
Acetaldehyde	HMDB00990	15.9	292.11142	294.10549	5.54 ± 0.42
Propanal	HMDB03366	17.3	306.12707	308.12114	5.15 ± 0.44
Butanal	HMDB03543	22.1	320.14272	322.13679	3.88 ± 0.07
Pentanal	-	24.6	334.15837	336.15244	2.47 ± 0.21
Hexanal	HMDB05994	27.3	348.17402	350.16809	1.27 ± 0.19
Heptanal	-	30.3	362.18967	364.18374	2.13 ± 0.02
Octanal	HMDB01140	33.7	376.20532	378.19939	2.538 ± 0.073
Nonanal	-	37.4	390.22097	392.21504	2.51 ± 0.24
Decanal	HMDB11623	40.8	404.23662	406.23069	3.50 ± 0.29
Undecanal	-	44.5	418.25227	420.24634	2.379 ± 0.081
Dodecanal	-	48.3	432.26792	434.26199	3.46 ± 0.26
3-Methylbutanal	HMDB06478	24.2	334.15837	336.15244	3.58 ± 0.21

Benzaldehyde	HMDB06115	24.4	354.12707	356.12114	0.00136 ± 0.00026
Phenyl-acetaldehyde	HMDB06236	24.8	368.14272	370.13679	2.17 ± 0.24
Trans-2-hexen-1-al	-	23.0	346.15837	348.15244	1.14 ± 0.23
Cis-4-decenal	-	36.2	402.22097	404.21504	2.43 ± 0.19
Acetone	HMDB01659	17.0	306.12707	308.12114	1.45 ± 0.27
2-butanone	HMDB00474	21.0	320.14272	322.13679	4.12 ± 0.17
2-Pentanone	-	23.4	334.15837	336.15244	0.726 ± 0.019
2-Hexanone	HMDB05842	25.7	348.17402	350.16809	0.0532 ± 0.0095
2-heptanone	HMDB03671	28.9	362.18967	364.18374	0.0179 ± 0.0006
4-Heptanone	HMDB04814	28.4	362.18967	364.18374	2.74 ± 0.34
3-Octanone	-	31.8	376.20532	378.19939	1.78 ± 0.15
2-Nonanone	-	35.6	390.22097	392.21504	1.71 ± 0.19
Ethyl isopropyl ketone	HMDB05846	26.3	348.17402	350.16809	0.232 ± 0.027
Methyl isobutyl ketone	HMDB02939	25.2; 26.8	348.17402	350.16809	2.50 ± 0.63 *
Pyruvic acid	HMDB00243	12.5	336.10125	338.09532	0.611 ± 0.025
Acetoacetic acid	HMDB00060	19.8	350.11690	352.11097	0.0377 ± 0.0011
α-Ketoisovaleric acid	HMDB00019	20.6	364.13255	366.12662	0.0252 ± 0.0023
3-Methyl-2-oxovaleric acid	HMDB00491	20.2	378.14820	380.14227	0.0543 ± 0.0030
2-Methyl-3-ketovaleric acid	HMDB00408	22.3	378.14820	380.14227	0.000367 ± 0.000041
Ketoleucine	HMDB00695	20.4; 21.2	378.14820	380.14227	0.000414 ± 0.000011 *
Oxoglutaric acid	HMDB00208	9.5	394.10673	396.10080	0.162 ± 0.004
3-Oxoadipic acid	HMDB00398	15.4	408.12238	410.11645	0.0797 ± 0.0022
2-Methylglutaric acid	HMDB00422	9.7	394.14312	396.13719	0.0525 ± 0.0056

* Concentration is the total of both E- and Z-isomers.

Table 3.6. List of thirty-six carbonyl metabolites quantified in human plasma using the differential $^{15}N_2$-/$^{14}N_2$-DH labeling method with analysis by nLC-nESI FT-ICR-MS.

Standard	**HMDB Accession #**	**t_R (min)**	**$^{14}N_2$-DH $[M+H]^+$**	**$^{15}N_2$-DH $[M+H]^+$**	**Conc. in Plasma (μM)**
Formaldehyde	HMDB01426	13.2	278.09577	280.08984	0.450 ± 0.043
Acetaldehyde	HMDB00990	15.9	292.11142	294.10549	1.71 ± 0.13
Propanal	HMDB03366	17.3	306.12707	308.12114	1.68 ± 0.03
Butanal	HMDB03543	22.1	320.14272	322.13679	1.83 ± 0.03
Pentanal	-	24.6	334.15837	336.15244	1.96 ± 0.02
Hexanal	HMDB05994	27.3	348.17402	350.16809	2.20 ± 0.04
Heptanal	-	30.3	362.18967	364.18374	1.93 ± 0.11
Octanal	HMDB01140	33.7	376.20532	378.19939	2.25 ± 0.12
Nonanal	-	37.4	390.22097	392.21504	2.30 ± 0.07
Decanal	HMDB11623	40.8	404.23662	406.23069	2.94 ± 0.19
Undecanal	-	44.5	418.25227	420.24634	2.38 ± 0.33
Dodecanal	-	48.3	432.26792	434.26199	2.42 ± 0.34
3-Methylbutanal	HMDB06478	24.2	334.15837	336.15244	0.0581 ± 0.0019
Benzaldehyde	HMDB06115	24.4	354.12707	356.12114	0.000334 ± 0.000029
Phenyl-acetaldehyde	HMDB06236	24.8	368.14272	370.13679	1.45 ± 0.10
Cis-4-decenal	-	36.2	402.22097	404.21504	0.0582 ± 0.0045
Acetone	HMDB01659	17.0	306.12707	308.12114	1.66 ± 0.14
2-Butanone	HMDB00474	21.0	320.14272	322.13679	0.0473 ± 0.0097
2-Pentanone	-	23.4	334.15837	336.15244	1.54 ± 0.07
2-Hexanone	HMDB05842	25.7	348.17402	350.16809	1.70 ± 0.13
3-Hexanone	HMDB00753	27.1	348.17402	350.16809	3.09 ± 0.29
2-Heptanone	HMDB03671	28.9	362.18967	364.18374	1.55 ± 0.13
4-Heptanone	HMDB04814	28.4	362.18967	364.18374	2.82 ± 0.65
3-Octanone	-	31.8	376.20532	378.19939	1.82 ± 0.23
2-Nonanone	-	35.6	390.22097	392.21504	1.81 ± 0.16
Ethyl isopropyl ketone	HMDB05846	26.3	348.17402	350.16809	0.00195 ± 0.00027

Methyl isobutyl ketone	HMDB02939	25.2; 26.8	348.17402	350.16809	2.50 ± 0.34 *
Pyruvic acid	HMDB00243	12.5	336.10125	338.09532	0.680 ± 0.053
α-Ketoisovaleric acid	HMDB00019	20.6	364.13255	366.12662	0.00109 ± 0.00005
Methylacetoacetic acid	HMDB00310	18.4	364.13255	366.12662	0.00404 ± 0.00041
Levulinic acid	HMDB00720	19.4	364.13255	366.12662	2.59 ± 0.34
3-Methyl-2-oxovaleric acid	HMDB00491	20.2	378.14820	380.14227	0.00161 ± 0.000006
2-Methyl-3-ketovaleric acid	HMDB00408	22.3	378.14820	380.14227	2.22 ± 0.53
Ketoleucine	HMDB00695	20.4; 21.2	378.14820	380.14227	0.00593 ± 0.00059 *
2-Ketohexanoic acid	HMDB01864	20.8; 21.8	378.14820	380.14227	0.000579 ± 0.000148 *
Succinylacetone	HMDB00635	11.7	406.14312	408.13719	0.129 ± 0.027

* Concentration is the total of both E- and Z-isomers.

3.3.2. Development and Application of the $^{15}N_2$-/$^{14}N_2$-Dansylhydrazine Method for the Identification and Quantification of the Human Sugar Metabolome.

The potential of DH as a quantitative labeling reagent for sugars in biofluids was examined as sugars were found to have been readily labeled in urine and plasma using the carbonyl labeling protocol. The fluorescent labeling of carbohydrates with DH has previously been reported.[12,13,17] Therefore optimization of the developed $^{15}N_2$-/$^{14}N_2$-DH labeling strategy for carbonyls was performed such that it could be applied to the identification and quantification of sugars in human biofluids as well using LC-MS for analysis. Both the derivatization protocol and RPLC conditions were optimized for carbohydrate labeling and quantitation of the human sugar metabolome.

Using carbohydrate standards glucose, fructose, lactose and galactose, a variety of reaction solvents were tested for use with the DH derivatization reaction, including methanol (MeOH), ethanol (EtOH), isopropanol (iPA), and acetonitrile (ACN) (see Figure 3.14). EtOH was found to give the greatest overall product yield and was chosen as the optimal solvent. Reaction time was optimized

using a test sample of three sugar standards (glucose, fructose, and galactose) with the reaction carried out at 60 ^{o}C using EtOH as the solvent. DH labeled product formation progress was monitored by LC-MS at 0, 20, 40, 60, 80, 100, 120, 140, 160 and 180 min following the addition of the acid catalyst, 3 % TFA, and the reagent, DH, in triplicate. As shown in Figure 3.15, optimal product formation was observed at a reaction time of 100 min. Note that the reduced yield observed at 120 - 180 min is most likely due to the degradation of the reagent and derivatized products as a result of side reactions such as hydrolysis.

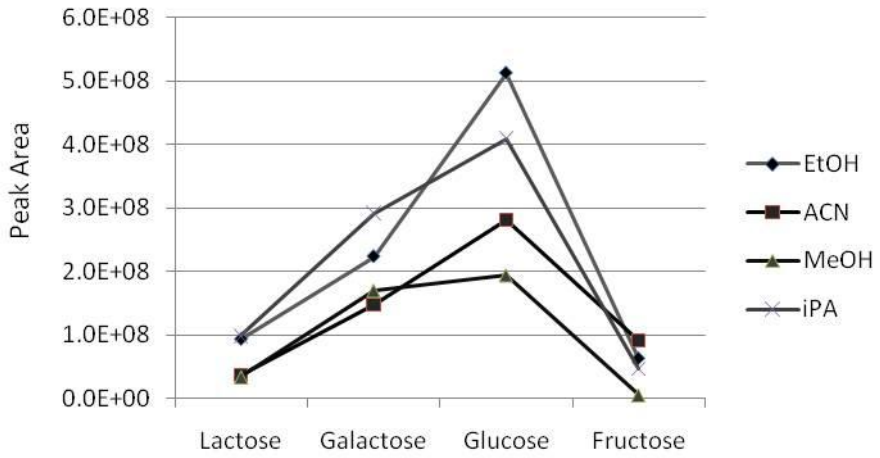

Figure 3.14. LC-MS peak areas of four sugars labeled with DH in four different solvents to test reaction solvent suitability.

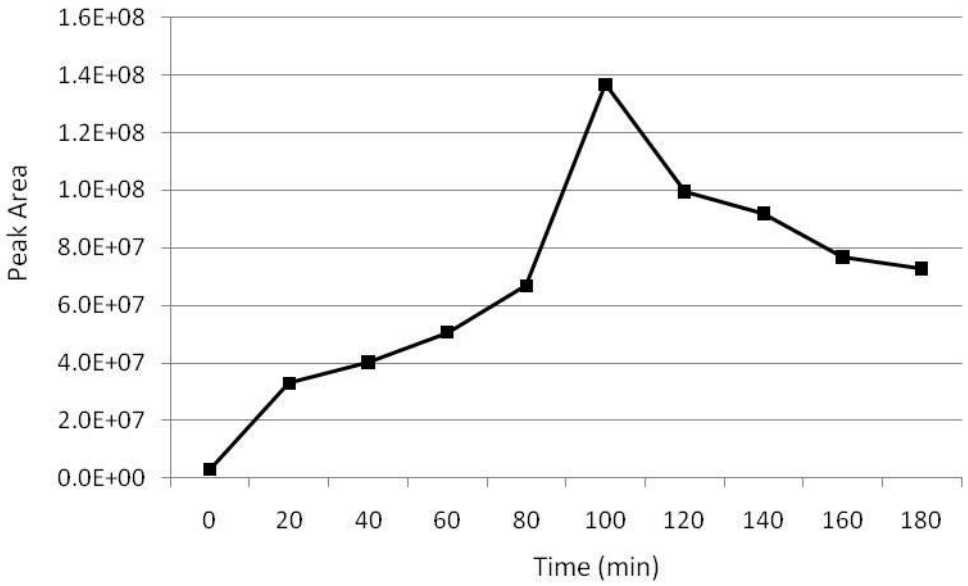

Figure 3.15. Average LC-MS peak areas of three DH derivatized sugar standards monitored during the course of the reaction to show the effect of reaction time on yield.

In order to confirm the completeness of the reaction, thin-layer chromatography (TLC) was employed. The TLC plates used were sheets of glass coated in silica. A 45 mM solution of glucose was derivatized with 67.5 mM DH in EtOH for 100 min at 60 ^{o}C. The glucose starting material, the DH reagent, and the product all dissolved in chloroform were spotted on a TLC plate and developed in a 1:1 hexane:EtAc mixture. One spot was observed for the starting material (glucose), reagent (DH), and product (DH labeled glucose) with retention factors (R_f) of 0.45, 0.58, and 0.73, respectively, viewed with a long wave UV lamp (λ = 365 nm). A second TLC plate, spotted with glucose, DH, and the product, was dipped in cerium molybdate stain (Hanessian's stain) and developed with vigorous heating on a hot plate. Again, only one spot was observed for each of the starting material, reagent, and product with R_fs of 0.10, 0.52, and 0.62, respectively, confirming reaction completion and product purity.

Recovery was evaluated by spiking plasma samples with carbohydrate standards. 100 μL aliquots of plasma were reduced to dryness and reconstituted in EtOH; the samples were then spiked with standards (in triplicate) to give a

concentration of 0.83 μM of each and labeled with $^{14}N_2$-DH. Then known amounts of the standards were labeled with $^{15}N_2$-DH to give a concentration of 2.08 μM of each. The light and heavy labeled samples were combined prior to nLC-nESI FT-ICR-MS analysis and the ion pair peak area ratios from the MS were used to determine recoveries of the spiked analytes (see Table 3.7). The average recovery was 95.3 %.

Table 3.7. Recoveries for plasma reduced to dryness and then spiked with carbohydrate standards and labeled, with analysis by nLC-nESI FT-ICR-MS.

Compound	% Recovery
L-Arabinose	98.4 ± 11.0
L-Fucose	92.2 ± 10.2

Carbohydrate standard and biofluid sample labeling experiments were carried out in triplicate and reproducibility was high, with relative standard deviation on average less than 10 %. As a result of the polar nature of carbohydrates, SPE was not used for this protocol as the sugars would mostly be removed in the wash step.

Sugar standards were obtained from the HML and stored at -20 ^{o}C. They were tested for derivatization using the optimized protocol (outlined in Section 3.2.4.2.) and analyzed using the LC Ion trap MS (Esquire 3000plus). All standards tested were successfully derivatized by DH and added to the DH standard library, as given in Table 2.3, with the sugars listed again below in Table 3.8.

Table 3.8. List of ten carbohydrate standards used for metabolome analysis with the optimized protocol.

Standard	HMDB Accession #	$^{14}N_2$-DH $[M+H]^+$	$^{15}N_2$-DH $[M+H]^+$	t_R (min)
Lactose	HMDB00186	590.20142	592.19549	12.5
Galactose	HMDB00143	428.14860	430.14267	14.4
Glucose	HMDB00122	428.14860	430.14267	12.9
Fructose	HMDB00660	428.14860	430.14267	18.0
D-Mannose	HMDB00169	428.14860	430.14267	18.7
D-Xylose	HMDB00098	398.13803	400.13210	15.0
L-Arabinose	HMDB00646	398.13803	400.13210	17.4
D-Ribose	HMDB00283	398.13803	400.13210	29.9
L-Fucose	HMDB00174	412.15368	414.14775	24.2
L-Rhamnose	HMDB00849	412.15368	414.14775	28.6

Unlabeled sugars are not retained on RPLC columns and therefore LC separation using different separation mechanisms from RPLC such as HILIC or different analysis techniques such as NMR are employed. However NMR lacks the sensitivity that can be achieved from an LC-MS method and HILIC suffers from poor separation efficiency for complex samples such as biofluids in comparison to RPLC. The use of different instruments or columns for analyzing one sample increases the overall analysis time and increases cost per sample. It is highly desirable for all metabolites to be analyzed using the same method and therefore the use of the DH labeling strategy to alter the chemical properties of the analytes of interest such that all targeted metabolites can be analyzed using RPLC-MS was the goal. The addition of the DH group containing a hydrophobic aromatic ring to a polar, hydrophilic sugar increases its hydrophobicity and therefore enhances its retention on a RPLC column. The LC gradient was optimized in order to improve the separation and resolution of the derivatized sugars in human biofluids. Figure 3.16 shows the nLC-nESI FT-ICR-MS chromatograms of labeled human urine and plasma (panel A and B, respectively) acquired using the optimized method as given in Section 3.2.6. DH labeled sugars are still relatively polar and elute in high % aqueous mobile phase. The sugar

metabolites are observed in the first half of the acquisition where the LC conditions are more aqueous than previously and the derivatized ketones, aldehydes, and keto-acids elute later where the LC conditions are higher in organic composition, as previously.

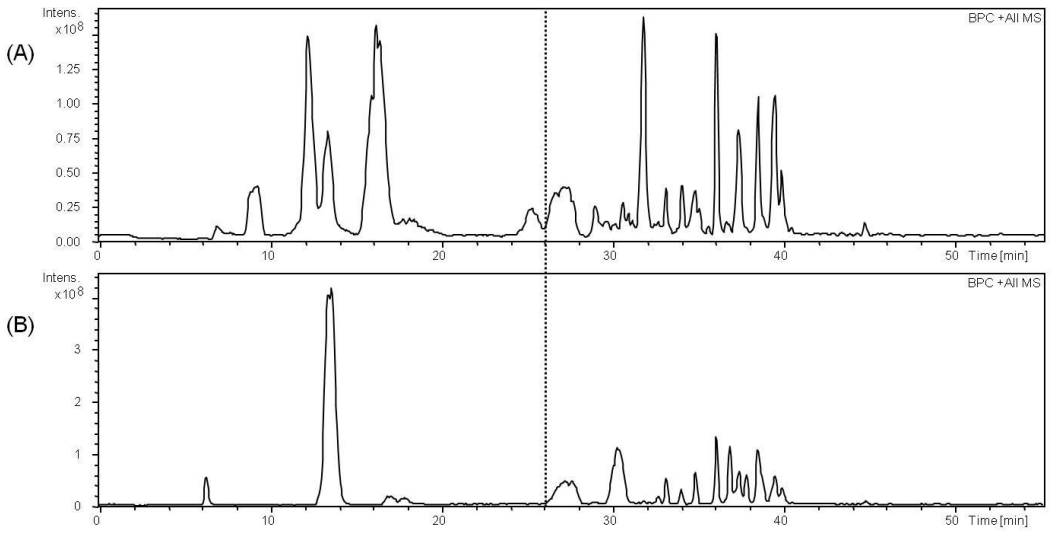

Figure 3.16. BPCs acquired by nLC-nESI FT-ICR-MS of (A) DH labeled human urine and (B) DH labeled human plasma using the optimized analysis protocol for carbohydrate and carbonyl metabolites.

The differential $^{15}N_2$-/$^{14}N_2$-DH labeling strategy for absolute quantitation of the sugar metabolome was applied to human urine and plasma. This strategy follows the same outline as for the absolute quantitation of the carbonyl metabolome as shown previously in Figure 3.12. Aliquots of biofluids were labeled light with $^{14}N_2$-DH and the ten sugar standards of known concentrations were labeled heavy with $^{15}N_2$-DH. They were combined for analysis by nLC-nESI FT-ICR-MS. Co-eluted isoforms confirmed metabolite id and ion pair peak area ratios were used for accurate quantitation. Figure 3.17 shows the MS of glucose (0.03 ppm error) and xylose (0.14 ppm error) ion pairs in a urine analysis. The results of these absolute quantitation experiments, performed in triplicate, are presented for urine in Table 3.9 and for plasma in Table 3.10. Five sugar

metabolites were positively identified and quantified in human urine, ranging from 14 – 289 nM with an average RSD of 9.4 %. Two sugar metabolites were positively identified and quantified in human plasma, ranging from 0.2 – 1.9 μM with an average RSD of 9.4 %.

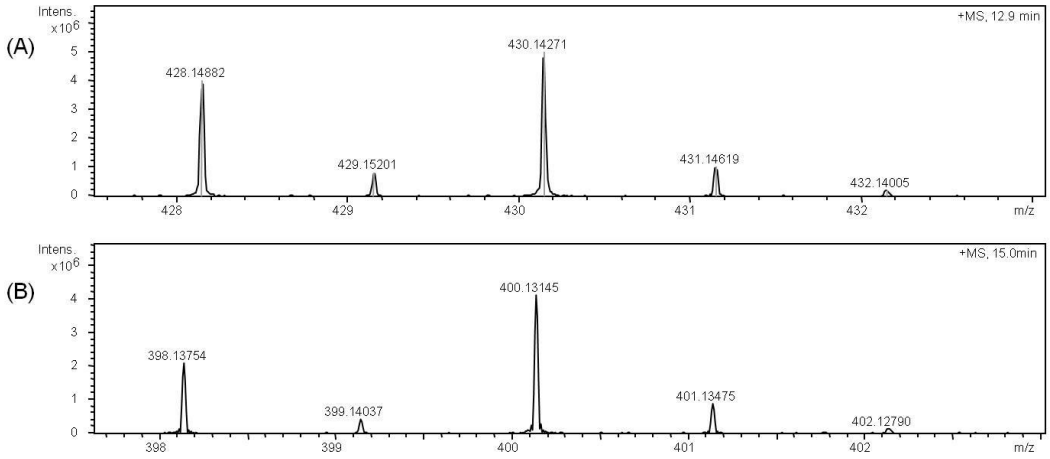

Figure 3.17. MS of co-eluted ion pairs of (A) glucose and (B) xylose obtained by differential $^{15}N_2$-/$^{14}N_2$-DH labeling of human urine and sugar standards for absolute quantitation with analysis by nLC-nESI FT-ICR-MS.

Table 3.9. List of five sugar metabolites quantified in human urine using the differential $^{15}N_2$-/$^{14}N_2$-DH labeling method with analysis by nLC-nESI FT-ICR-MS.

Standard	**HMDB Accession #**	**t_R (min)**	**$^{14}N_2$-DH [M+H]+**	**$^{15}N_2$-DH [M+H]+**	**Conc. in Urine (μM)**
Glucose	HMDB00122	12.9	428.14860	430.14267	0.289 ± 0.002
D-Xylose	HMDB00098	15.0	398.13803	400.13210	0.171 ± 0.018
L-Arabinose	HMDB00646	17.4	398.13803	400.13210	0.0662 ± 0.0097
L-Fucose	HMDB00174	24.2	412.15368	414.14775	0.0575 ± 0.0061
L-Rhamnose	HMDB00849	28.6	412.15368	414.14775	0.0140 ± 0.0028

Table 3.10. List of two sugar metabolites quantified in human plasma using the differential $^{15}N_2$-/$^{14}N_2$-DH labeling method with analysis by nLC-nESI FT-ICR-MS.

Standard	HMDB Accession #	t_R (min)	$^{14}N_2$-DH [M+H]+	$^{15}N_2$-DH [M+H]+	Conc. in Plasma (μM)
Glucose	HMDB00122	12.9	428.14860	430.14267	1.87 ± 0.06
Fructose	HMDB00660	18.0	428.14860	430.14267	0.173 ± 0.027

3.3.3. Application of the $^{15}N_2$-/$^{14}N_2$-Dansylhydrazine labeling strategy for the Absolute and Relative Quantification of Research Study Human Urine Samples.

A research study was conducted to determine baseline concentrations of urinary metabolites and to study the variation of inter- and intra-sample concentrations of the observed metabolites. Profiling of the human urinary metabolome was performed using the $^{15}N_2$-/$^{14}N_2$-DH labeling strategy to determine the range in which carbonyls and carbohydrates are typically present in the urine provided by individuals who self-identified as healthy. This was performed as part of a pilot study that was being carried out within our laboratory for the targeted profiling of a variety of classes of metabolites in human urine in order to provide a comprehensive overview of a typical healthy human urine sample. With average baseline concentrations characterized for human urinary metabolites, this study is the initial step towards performing further biological and disease biomarker studies.

Relative quantitation of metabolites present in the urine of samples collected from ten female and ten male volunteers over a three day period was performed in duplicate using the differential isotope DH labeling technique. First, a pooled urine sample was prepared by combining 1 mL of each of the sixty urine samples collected. This sample was then labeled light and combined with heavy labeled standards for identification and absolute quantification of the carbonyl metabolites. This pooled urine sample was then used as the standard to perform relative quantification of the metabolites in the sixty urine samples (in duplicate)

provided by the volunteers. For the relative quantification experiments, the volunteer urine samples were labeled with $^{14}N_2$-DH and the pooled urine was labeled with $^{15}N_2$-DH.

Four of the quantified carbonyls in the pooled urine sample were used for relative quantification of the four metabolites in the sixty urine samples. The four metabolites quantified were sugars, namely glucose, xylose, arabinose, and fucose. The absolute concentration of these four sugars in the pooled urine sample is given in Table 3.11. A nLC-nESI FT-ICR-MS chromatogram is shown in Figure 3.18 for the relative quantification of one of the volunteer urine samples (identified as female # 2) labeled light combined with heavy labeled pooled urine. Panel A of Figure 3.19 shows an EIC overlay of light labeled metabolite, glucose, from a volunteer urine sample (identified as male # 1) which co-eluted with heavy labeled metabolite, glucose, from the pooled urine. Panel B shows the isotopic pattern of the ion pair of co-eluted glucose (0.17 ppm error).

Difficulty in quantifying other carbonyl standards was encountered and believed to be a result from the change in sample preparation from the protocol outlined in 3.2.3.2. to the protocol outlined in 3.2.3.4. used for the samples collected for this generic study. The original protocol treated the urine with MeOH whereas the protocol used for this group study treated the urine by double filtering through 0.2 μm PVDF membrane filters. This change in sample pre-treatment may have negatively affected the concentrations of the more volatile carbonyls present in the urine. Since the urine samples were collected such that they could be studied comprehensively, a generic sample pre-treatment was applied rather than the pre-treatment method tailored for the analysis of carbonyl metabolites. The protocol for this study also required the collection of morning urine samples rather than a second void volume urine sample required by the protocol outlined specifically for carbonyl metabolome profiling by the differential DH labeling method. Metabolite concentrations in the urine can vary throughout the day and this change in collection time may also have affected the range of carbonyls observed and their concentrations. The change in analytical techniques from nLC-nESI MS to capLC-ESI MS also results in a less sensitive

analysis of the biofluids rendering the quantification of the very low abundance carbonyl metabolites challenging.

Table 3.11. List of four metabolites quantified in $^{14}N_2$-DH labeled pooled urine using the differential labeling method for absolute quantitation using $^{15}N_2$-DH labeled standards with analysis by capLC-ESI FT-ICR-MS.

Standard	HMDB Accession #	t_R (min)	$^{14}N_2$-DH [M+H]+	$^{15}N_2$-DH [M+H]+	Conc. in Pooled Urine (µM)
Glucose	HMDB00122	15.1	428.14860	430.14267	52.0 ± 8.4
D-Xylose	HMDB00098	19.2	398.13803	400.13210	7.59 ± 0.69
L-Arabinose	HMDB00646	22.8	398.13803	400.13210	5.97 ± 0.63
L-Fucose	HMDB00174	30.4	412.15368	414.14775	7.45 ± 1.44

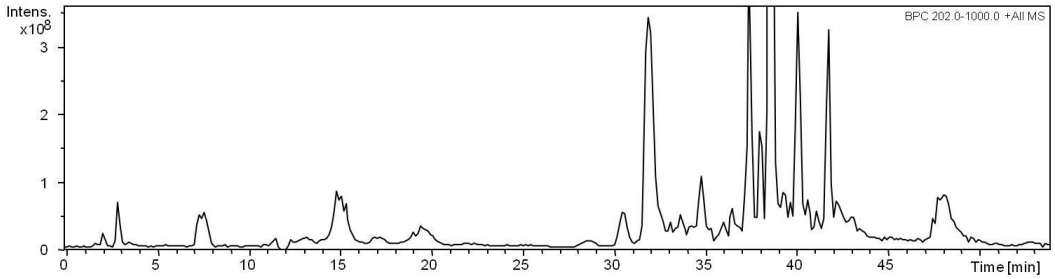

Figure 3.18. BPC of 1:1 $^{15}N_2$-/$^{14}N_2$-DH labeled pooled urine and urine sample F2 obtained by capLC-ESI FT-ICR-MS.

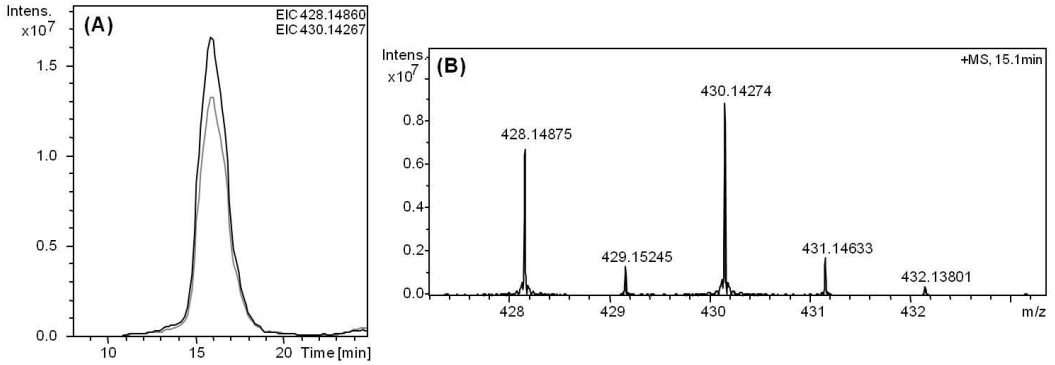

Figure 3.19. (A) Overlaid EICs and (B) MS of 1:1 $^{15}N_2$-/$^{14}N_2$-DH labeled glucose isoforms in pooled urine and urine sample M1 obtained by capLC-ESI FT-ICR-MS.

Presented in Tables 3.12, 3.13, 3.14, and 3.15 are the results of the relative quantitation experiments giving the determined concentrations of glucose, xylose, arabinose, and fucose, respectively, for each of the ten female and ten male urine samples collected once a day for three days at the morning (first) void volume. In the tables where no standard deviation is given, there was a problem with the analysis of the duplicate sample (e.g., inconsistent spray). Where no concentration is given, the metabolite was not present, there was a problem with the acquisition (F7, 8, 9, 10 - Day 3 and M5, 6, 7, 8, 9, 10 - Day 3), or the data were rejected using the t-test (F6 - Day 3). Following each table are plots of the female, male, and combined average female and male concentrations of each of the metabolites over the three days of collection (Figures 3.20, 3.21, 3.22, and 3.23) such that variations in the inter- and intra-day concentrations of each metabolite could be compared for each sample and between samples and for female versus male samples. No significant difference was observed between male and female concentrations of each of the sugars. Slight variations may be a result of the statistically small sample size (N). Using relative quantitation, the average concentrations of each metabolite in healthy human urine for glucose was 55.5 μM, xylose was 7.32 μM, arabinose was 6.99 μM, and fucose 7.51 μM. For glucose, the observed range was 17 – 141 μM, for xylose, the observed range was 2.4 – 16.5 μM, for arabinose, the observed range was 2.4 – 11.9 μM, and for fucose, the observed range was 2.2 – 23 μM.

Table 3.12. List of glucose concentrations determined for the ten female and ten male human urine samples obtained over a three day period by relative quantitation with a three day pooled urine sample using the differential $^{15}N_2$-/$^{14}N_2$-DH labeling strategy with analysis by capLC-ESI FT-ICR-MS.

Gender Sample #	Day 1 Conc (μM)	Day 2 Conc (μM)	Day 3 Conc (μM)	Average of 3 Days
F1	82.4 ± 3.2	59.8 ± 6.5	59.9 ± 5.0	67.4
F2	21.9 ± 1.0	48.5 ± 1.7	37.1 ± 5.0	35.8
F3	70.8 ± 5.8	29.8 ± 3.3	26.65 ± 0.01	42.4
F4	22.2 ± 1.3	16.7 ± 0.5	31.6 ± 4.5	23.5
F5	61.7	48.8 ± 4.2	41.7 ± 6.4	50.7
F6	25.1 ± 0.3	58.3 ± 4.1	-	41.7
F7	33.4 ± 0.8	89.3 ± 12.8	-	61.4
F8	29.0 ± 2.2	55.9 ± 1.3	-	42.5
F9	57.0	36.3 ± 2.4	-	46.7
F10	61.2 ± 0.1	93.5	-	77.4
M1	24.2 ± 0.7	40.1	17.4 ± 0.7	27.2
M2	41.9 ± 0.4	55.7	45.8 ± 5.6	47.8
M3	75.7 ± 4.6	52.0 ± 7.5	49.5 ± 8.8	59.1
M4	57.3 ± 0.2	54.2 ± 9.2	61.0	57.5
M5	74.1 ± 0.4	133 ± 17	-	103.6
M6	35.7 ± 1.7	76.3 ± 12.4	-	56.0
M7	32.5 ± 1.2	65.5 ± 2.0	-	49.0
M9	48.1 ± 3.3	51.2 ± 3.7	-	49.7
M9	70.8 ± 5.5	141 ± 41	-	105.9
M10	50.5 ± 3.3	81.1 ± 3.8	-	65.8
			Average of Female	**48.9**
			Average of Male	**62.2**
			Average of Female and Male	**55.5**

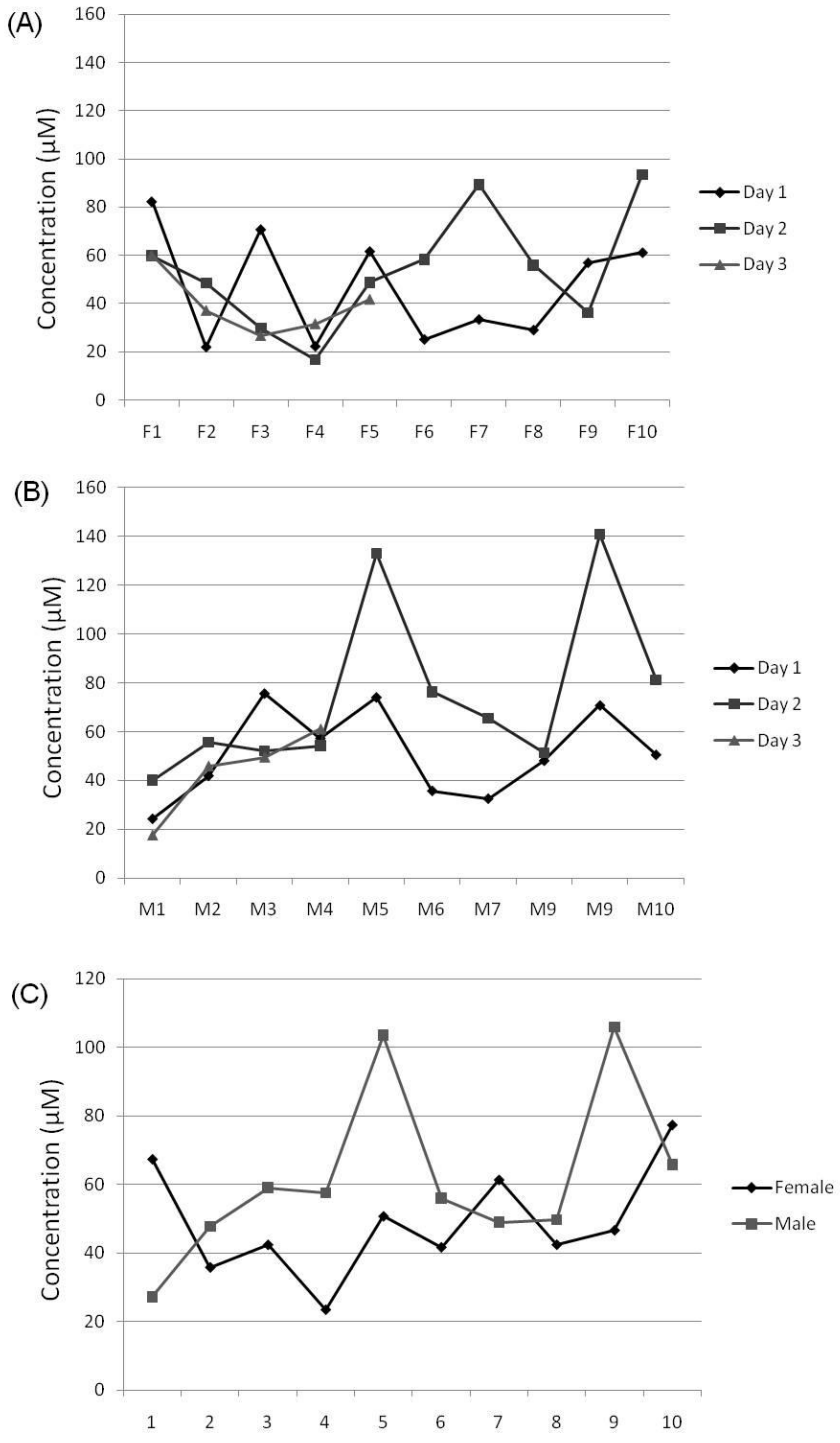

Figure 3.20. (A) Day 1, 2, and 3 glucose concentrations found for the ten female volunteers. (B) Day 1, 2, and 3 glucose concentrations found for the ten male volunteers. (C) The average glucose concentration over the three days for each of the ten female and ten male volunteers.

Table 3.13. List of xylose concentrations determined for the ten female and ten male human urine samples obtained over a three day period by relative quantitation with a three day pooled urine sample using the differential $^{15}N_2$-/$^{14}N_2$-DH labeling strategy with analysis by capLC-ESI FT-ICR-MS.

Gender Sample #	Day 1 Conc (μM)	Day 2 Conc (μM)	Day 3 Conc (μM)	Average of 3 Days
F1	13.6 ± 0.3	16.3 ± 2.2	11.4 ± 0.8	13.8
F2	3.09 ± 0.30	6.68 ± 0.04	5.17 ± 0.13	5.0
F3	12.4 ± 1.4	2.64 ± 0.10	2.69 ± 0.19	5.9
F4	4.20 ± 0.13	6.39 ± 0.05	1.97 ± 0.25	4.2
F5	16.45 ± 0.06	23.2 ± 0.4	16.6 ± 1.0	18.8
F6	3.12 ± 0.47	2.61	7.16	4.3
F7	2.87 ± 0.12	5.22 ± 0.17	-	4.0
F8	3.88 ± 0.18	3.34 ± 0.38	-	3.6
F9	-	3.34 ± 0.05	-	3.3
F10	7.32 ± 0.11	9.86	-	8.6
M1	5.82 ± 0.19	3.98	2.40 ± 0.15	4.1
M2	4.50 ± 0.80	7.61	6.79 ± 0.65	6.3
M3	13.3 ± 0.7	11.2	13.6 ± 0.2	12.7
M4	9.11 ± 0.01	4.63 ± 0.53	9.0	7.6
M5	10.5 ± 0.1	3.56 ± 0.55	-	7.0
M6	6.77 ± 0.68	11.8 ± 0.3	-	9.3
M7	3.61	3.06 ± 0.17	-	3.3
M9	5.23 ± 0.03	3.10 ± 0.08	-	4.2
M9	11.7 ± 0.5	14.1 ± 4.0	-	12.9
M10	7.86 ± 0.16	7.44 ± 0.01	-	7.7
			Average of Female	**7.15**
			Average of Male	**7.50**
			Average of Female and Male	**7.32**

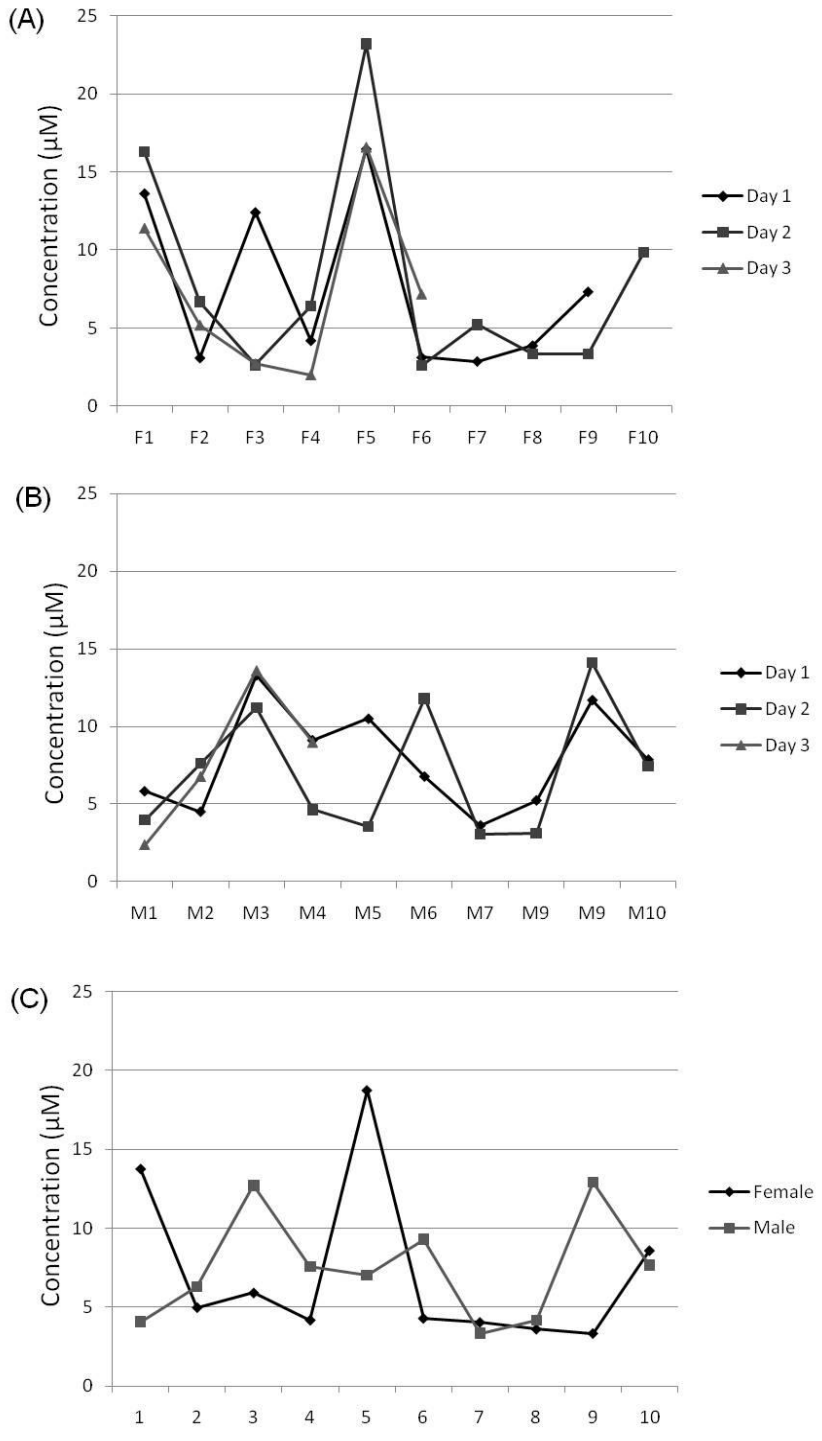

Figure 3.21. (A) Day 1, 2, and 3 xylose concentrations found for the ten female volunteers. (B) Day 1, 2, and 3 xylose concentrations found for the ten male volunteers. (C) The average xylose concentration over the three days for each of the ten female and ten male volunteers.

Table 3.14. List of arabinose concentrations determined for the ten female and ten male human urine samples obtained over a three day period by relative quantitation with a three day pooled urine sample using the differential $^{15}N_2$-/$^{14}N_2$-DH labeling strategy with analysis by capLC-ESI FT-ICR-MS.

Gender Sample #	Day 1 Conc (μM)	Day 2 Conc (μM)	Day 3 Conc (μM)	Average of 3 Days
F1	3.2 ± 0.45	5.15 ± 0.17	4.34 ± 0.18	4.2
F2	10.8 ± 1.3	-	3.09 ± 0.05	6.9
F3	4.14 ± 0.04	7.82 ± 0.28	2.15 ± 0.35	4.7
F4	11.0 ± 0.1	-	11.3 ± 0.5	11.2
F5	4.20 ± 0.30	-	8.59 ± 0.44	6.4
F6	3.187 ± 0.005	5.74 ± 0.37	-	4.5
F7	2.68	4.31 ± 0.41	-	3.5
F8	6.74 ± 0.09	15.2	-	11.0
F9	-	-	9.82 ± 0.5	9.8
F10	-	-	-	-
M1	3.72 ± 0.21	4.43	2.40 ± 0.13	3.5
M2	3.80 ± 0.07	8.27	9.35 ± 0.84	7.1
M3	9.32 ± 0.37	4.02	11.3	8.2
M4	6.92 ± 0.51	5.09 ± 0.88	5.65 ± 0.43	5.9
M5	9.991 ± 0.002	-	-	10.0
M6	4.29	7.24 ± 0.47	-	5.8
M7	4.30	4.76	-	4.5
M9	4.96 ± 0.30	4.05	-	4.5
M9	7.84 ± 0.13	10.6	-	9.2
M10	-	11.9	-	11.9
			Average of Female	**6.91**
			Average of Male	**7.07**
			Average of Female and Male	**6.99**

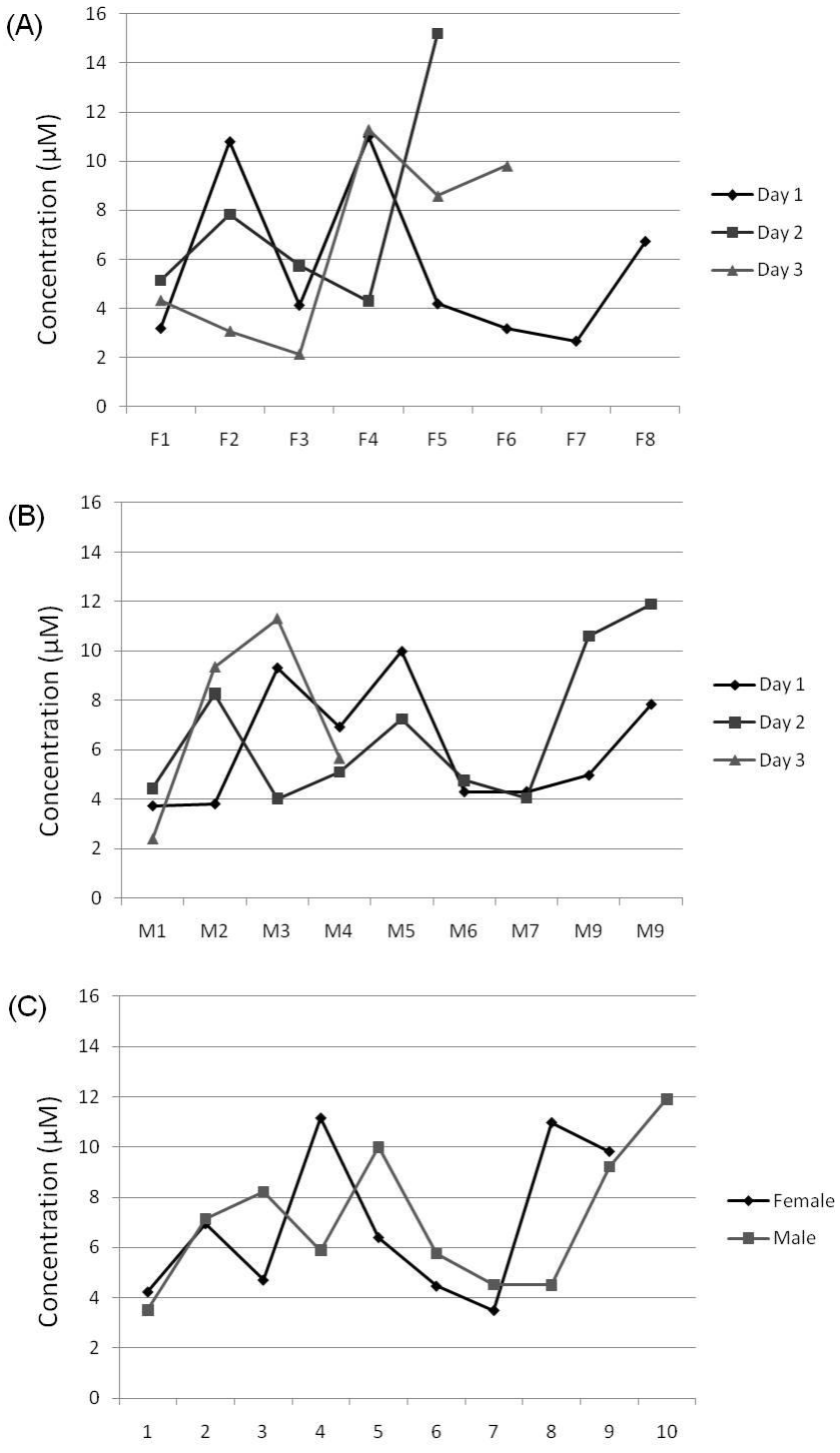

Figure 3.22. (A) Day 1, 2, and 3 arabinose concentrations found for the ten female volunteers. (B) Day 1, 2, and 3 arabinose concentrations found for the ten male volunteers. (C) The average arabinose concentration over the three days for each of the ten female and ten male volunteers.

Table 3.15. List of fucose concentrations determined for the ten female and ten male human urine samples obtained over a three day period by relative quantitation with a three day pooled urine sample using the differential $^{15}N_2$-/$^{14}N_2$-DH labeling strategy with analysis by capLC-ESI FT-ICR-MS.

Gender Sample #	Day 1 Conc (μM)	Day 2 Conc (μM)	Day 3 Conc (μM)	Average of 3 Days
F1	11.6 ± 0.7	15.0 ± 0.0	9.55 ± 0.2	12.1
F2	2.37 ± 0.18	4.76 ± 0.05	4.11 ± 0.03	3.7
F3	10.8 ± 1.3	-	3.09 ± 0.35	6.9
F4	4.14 ± 0.04	7.82 ± 0.28	2.15 ± 0.35	4.7
F5	11.2 ± 0.5	14.6	11.0 ± 1.5	12.3
F6	3.20 ± 0.15	-	5.95 ± 0.67	4.6
F7	4.44 ± 0.15	11.2 ± 0.1	-	7.8
F8	2.91	4.66 ± 0.26	-	3.8
F9	10.2	-	-	10.2
F10	-	3.01 ± 0.04	-	3.0
M1	4.19 ± 0.42	4.76 ± 0.02	2.44	3.8
M2	3.86 ± 0.02	6.32	5.74 ± 0.12	5.3
M3	15.8 ± 0.8	4.47	11.6	10.6
M4	7.08 ± 0.09	5.22 ± 0.17	6.45 ± 0.49	6.3
M5	9.56 ± 0.06	5.78	-	7.7
M6	6.07 ± 1.07	11.2 ± 0.4	-	8.6
M7	2.37	3.24 ± 0.35	-	2.8
M9	6.77 ± 0.66	6.64 ± 0.05	-	6.7
M9	9.50 ± 0.25	23.1 ± 9.8	-	16.3
M10	-	13.0 ± 1.3	-	13.0
			Average of Female	**6.91**
			Average of Male	**8.11**
			Average of Female and Male	**7.51**

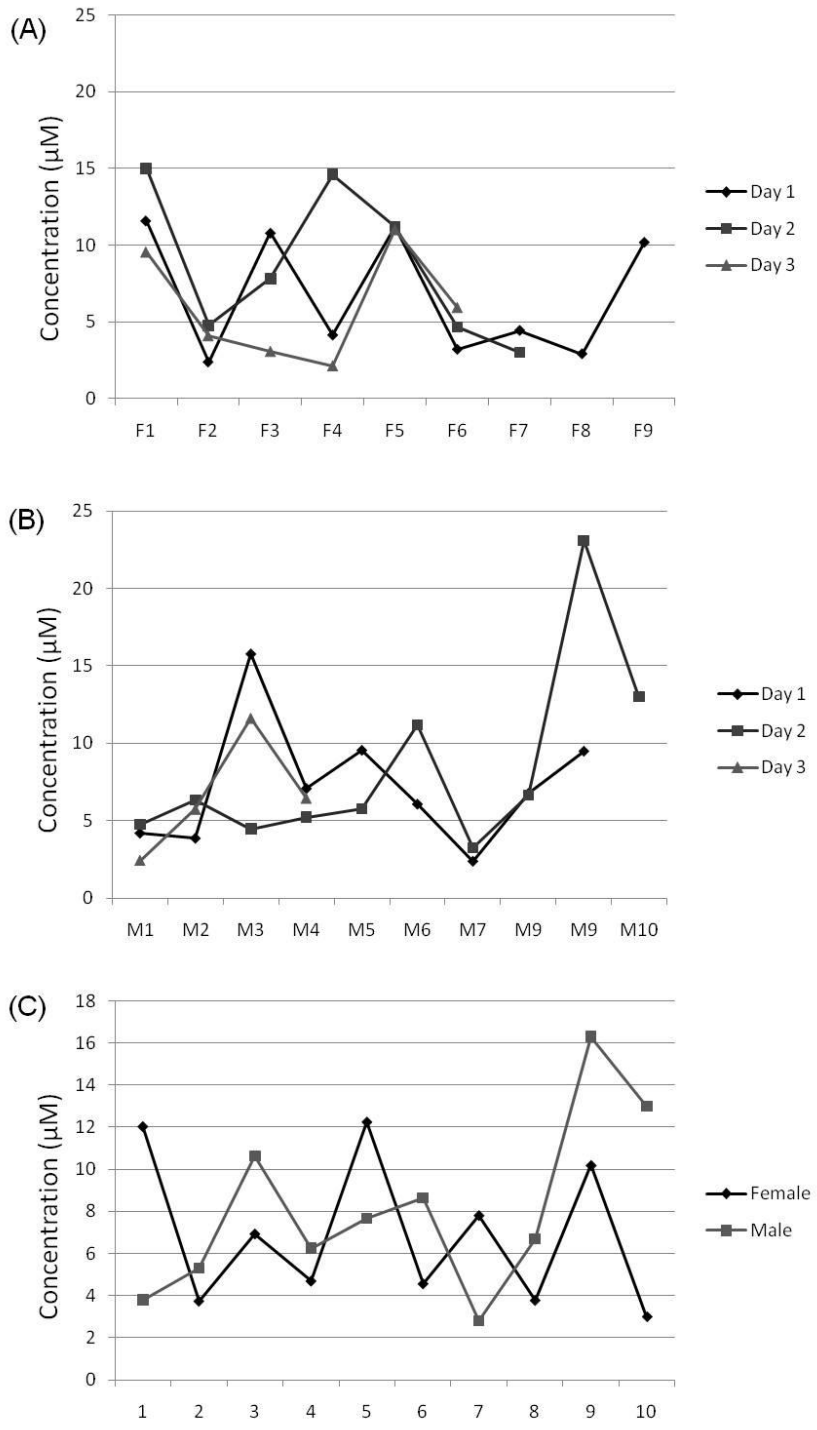

Figure 3.23. (A) Day 1, 2, and 3 fucose concentrations found for the ten female volunteers. (B) Day 1, 2, and 3 fucose concentrations found for the ten male volunteers. (C) The average fucose concentration over the three days for each of the ten female and ten male volunteers.

With further method optimization for larger scale studies of biofluids, specifically for sample pre-treatment, a more complete profile of the baseline concentrations of the healthy human urinary carbonyl metabolome can be achieved. From this study, applications of the differential $^{15}N_2$-/$^{14}N_2$-DH labeling strategy to potential disease biomarker discovery for compromised biological states such as diabetes and cancer can be performed. Such studies would be conducted in a similar manner performing absolute quantitation on a pooled biofluid sample and then relative quantitation on the individual biofluid samples, where carbonyls present in concentrations outside the baseline amounts may be indicative of a disease state.

3.4. Conclusions

In this chapter, the development and application of the new differential $^{15}N_2$-/$^{14}N_2$-isotope DH labeling technique for the identification and quantification of carbonyl metabolites using LC FT-ICR-MS was presented. The scheme developed for the synthesis of $^{15}N_2$-isotope dansylhydrazine *via* a one-step reaction was described. Absolute quantitation using the $^{15}N_2$-/$^{14}N_2$-DH labeling method with analysis by nLC-nESI FT-ICR-MS was described and presented for the carbonyl metabolomes of human urine and plasma. The DH labeling method was also described for the identification and quantification of sugar metabolites and applied to the absolute quantitation of simple carbohydrates in a human urine and plasma sample. Relative quantitation using the differential $^{15}N_2$-/$^{14}N_2$-DH labeling method was demonstrated for a urinary metabolome profiling study to determine the baseline concentrations of urinary carbonyls present in the urine provided by a study group of ten female and ten male healthy volunteers over a three day period. The presented differential $^{15}N_2$-/$^{14}N_2$-isotope DH labeling strategy with analysis by LC-MS was found to be a robust, quantitative carbonyl metabolome profiling technique allowing for reliable, absolute and relative quantitation of human metabolites. It is envisaged that this labeling method, combined with other high-performance isotope labeling methods such as dansyl chloride for amines and phenols and DmPA for carboxylic acids, will allow our

laboratory to profile a greater number of metabolites for metabolomics studies of biosystems.

3.5. Literature Cited

(1) Fiehn, O. *Plant Mol.Biol.* **2002**, *48*, 155-171.
(2) Fiehn, O. *Compar. Funct. Genom.* **2001**, *2*, 155-168.
(3) Villas-Boas, S. G.; Mas, S.; Akesson, M.; Smedsgaard, J.; Nielsen, J. *Mass Spectrom. Rev.* **2005**, *24*, 613-646.
(4) Kim, Y. S.; Maruvada, P.; Milner, J. A. *Future Oncol.* **2008**, *4*, 93-102.
(5) Dettmer, K.; Aronov, P. A.; Hammock, B. D. *Mass Spectrom. Rev.* **2007**, *26*, 51-78.
(6) Want, E. J.; Nordstrom, A.; Morita, H.; Siuzdak, G. *J. Proteome Res.* **2007**, *6*, 459-468.
(7) Fernie, A. R.; Trethewey, R. N.; Krotzky, A. J.; Willmitzer, L. *Nat. Rev. Mol. Cell Biol.* **2004**, *5*, 763-769.
(8) Lu, W.; Bennett, B. D.; Rabinowitz, J. D. *J. Chromatogr. B* **2008**, *871*, 236-242.
(9) Guo, K.; Ji, C.; Li, L. *Anal. Chem.* **2007**, *79*, 8631-8638.
(10) Guo, K.; Li, L. *Anal. Chem.* **2009**, *81*, 3919-3932.
(11) Guo, K.; Li, L. *Anal. Chem.* **2010**, *82*, 8789-8793.
(12) Avigad, G. *J. Chromatogr.* **1977**, *139*, 343-347.
(13) Mopper, K.; Johnson, L. *J. Chromatogr.* **1983**, *256*, 27-38.
(14) Alpenfels, W. F. *Anal. Biochem.* **1981**, *114*, 153-157.
(15) Turowski, M.; Yamakawa, N.; Meller, J.; Kimata, K.; Ikegami, T.; Hosoya, K.; Tanaka, N.; Thornton, E. R. *J. Am. Chem. Soc.* **2003**, *125*, 13836-13849.
(16) Shestakov, A. D.; Nikitina, V. N. *Izobreteniya.* **1994**, *(12)*, *196*; Office, E. P., Ed.: U.S.S.R., 1994; Vol. SU 1213713.
(17) Perez, S. A.; Colon, L. A. *Electrophoresis.* **1996**, *17*, 352-358.

Chapter 4: Conclusions and Future Work

This work described a mass spectrometry based approach for the comprehensive profiling of the human carbonyl metabolome. The development and application of the new differential $^{15}N_2$-/$^{14}N_2$-isotope DH labeling technique for the quantitation of carbonyl and sugar metabolites in human urine and plasma using LC FT-ICR-MS was presented. This isotope labeling strategy greatly facilitates high confidence identification of carbonyls and sugars in the complex matrices of biofluids and allows for high precision absolute and relative quantitation of these targeted metabolites.

In Chapter 2, an optimized method for the determination of carbonyl-containing metabolites in human biofluids using DH labeling was described. The detection of ketones, aldehydes, and keto-acids in biofluids has been considered in the past to be a challenging task as these analytes are poorly ionized by ESI. The conversion of these carbonyls to their dansylhydrazone derivatives was shown to improve the ESI surface activity of the analyte by at least four orders of magnitude through the introduction of the easily ionized dimethyl amino moiety which makes it amenable for detection by mass spectrometry. Derivatization with DH was also shown to significantly improve the chromatographic properties by increasing the hydrophobicity of the analyte and hence retention on the reversed phase column. Furthermore, derivatization increases the mass of the analyte (+247.07793 Da), bringing it out of the low mass region where solvent peaks often interfere, giving it an improved signal to noise ratio. The enhanced analyte signal with labeling allows for significant reduction of sample size. To this end, nano-flow LC methods appropriate for the analysis of derivatized biological samples were developed which were suitable for the interface with nESI-MS using a 9.4 Tesla FT-ICR-MS allowing for increased sensitivity. With the mass accuracy offered by FT-ICR-MS in combination with the analysis of DH labeled standards, it was possible to compose a carbonyl metabolite library consisting of eighty-one standards for use in profiling DH labeled biofluids. The development of protocols for the collection, treatment, and DH labeling of human urine and

plasma for carbonyl metabolite profiling were outlined. Qualitative profiling of labeled human urine and plasma allowed for the putative identification of twenty-seven carbonyl metabolites using the DH standard library.

In Chapter 3, the differential $^{15}N_2$-/$^{14}N_2$-isotope dansylhydrazine labeling strategy with analysis by LC FT-ICR-MS for improved qualitative and accurate quantitative profiling of the human carbonyl metabolome was presented. The scheme for the novel synthesis of $^{15}N_2$-isotope dansylhydrazine *via* a one-step reaction of DnsCl and $^{15}N_2$-hydrazine sulfate salt was described. Absolute quantitation using the differential $^{15}N_2$-/$^{14}N_2$-DH labeling method with analysis by nLC-nESI FT-ICR-MS was described and presented for human urine and plasma carbonyl metabolomes. This labeling strategy can be used to generate a $^{15}N_2$-stable isotope labeled internal standard for each corresponding $^{14}N_2$-labeled analyte. The DH isoforms are co-eluted and simultaneously detected and hence no isotopic effect is observed allowing for reliable, absolute quantitation of metabolites. The characteristic mass difference obtained between the heavy and light dansylhydrazones (1.99407 Da) provides additional information which facilitates confident peak and compound identification as well as quantification. Using this labeling strategy in combination with the DH standard library, the absolute quantity of thirty-six metabolites in human urine ranging from 0.4 nM – 5.5 μM and thirty-six metabolites in human plasma ranging from 0.3 nM – 3.09 μM was determined. Qualitative profiling using this technique revealed a total of ninety-nine carbonyl metabolites present in a human urine sample and sixty-one carbonyl metabolites present in a human plasma sample demonstrating the complexity of carbonyl compounds present in these biofluids and identifying carbonyls as an important class of human metabolites. Further expansion of the DH standard library will aid in the identification and quantitation of the unknown peak pairs.

In Chapter 3, the optimization of the labeling technique for the identification and quantification of sugars present in human biofluids was also described. Qualitative profiling and absolute quantitation of sugar metabolites in urine and plasma was performed using the differential isotope labeling method.

Five sugar metabolites were positively identified and quantified in a human urine sample, ranging from 14 – 289 nM, and two sugar metabolites were positively identified and quantified in a human plasma sample, ranging from 0.2 – 1.9 μM. The results of a larger carbonyl metabolome profiling study carried out to determine baseline concentrations of urinary carbonyls present in the urine provided by a study group of ten female and ten male healthy volunteers over a three day period was presented. This was performed by relative quantitation using the differential $^{15}N_2$-/$^{14}N_2$-DH labeling method with analysis by capLC-ESI FT-ICR-MS. Future studies can include a larger study group and more comprehensive coverage of the baselines concentrations of carbonyls present in the biofluids of healthy individuals such that studies of carbonyl disease biomarkers for different conditions such as diabetes and cancer can be performed.

Future expansion of the DH standard library will increase the coverage and understanding of the human carbonyl metabolome. The labeling chemistry and methodology developed here is expected to be transferable to other human biofluids such as CSF (and other biological systems such as mouse, rat, plants, etc.), and future experiments can be performed to validate the method for other biofluids such that more complete coverage of the full human carbonyl metabolome can be achieved. If targeted analyses of certain carbonyl metabolites is required for disease biomarker studies or further profiling experiments are desired, tandem MS experiments which retain the isotope label in the fragmentation are believed to be possible and could be investigated in the future. MS/MS studies would also aid in the positive identification of the unknown peak pairs found in the biofluids. The synthesis of a multiplex isotope DH labeling reagent based on a similar reaction scheme as presented is possible in the future and would add increased confidence to the peak pair picking.

The developed differential $^{15}N_2$-/$^{14}N_2$-isotope DH labeling strategy with analysis by LC-MS was found to be a robust, qualitative and quantitative carbonyl metabolome profiling technique allowing for reliable, absolute and relative identification and quantification of human metabolites. It is envisaged that this labeling method, combined with other high-performance isotope labeling methods

developed within our laboratory, including $^{13}C_2$-/$^{12}C_2$-DnsCl for amines and phenols and $^{13}C_2$-/$^{12}C_2$-DmPA for carboxylic acids, will allow us to profile a greater number of metabolites for metabolomics studies of biosystems. With the ability for comprehensive profiling of the majority of the human metabolome the technique can now be applied to disease biomarker discovery and biological studies.